LEANDRO COELHO DALVI

DEPOSIÇÃO DE XILANA SOBRE CELULOSE KRAFT DE EUCALIPTO

Tese apresentada à Universidade Federal de Viçosa, como parte das exigências do Programa de Pós-Graduação em Agroquímica, para obtenção do título de *Doctor Scientiae*.

Orientador: Antônio Jacinto Demuner

Coorientador: Rubens Chaves de Oliveira

VIÇOSA – MINAS GERAIS
2019

Ficha catalográfica preparada pela Biblioteca Central da Universidade Federal de Viçosa - Câmpus Viçosa

T
D152d
2019

Dalvi, Leandro Coelho, 1978-
Deposição de xilana sobre celulose kraft de eucalipto / Leandro Coelho Dalvi. – Viçosa, MG, 2019.
109f. : il. (algumas color.) ; 29 cm.

Texto em inglês.
Inclui anexos.
Orientador: Antônio Jacinto Demuner.
Tese (doutorado) - Universidade Federal de Viçosa.
Inclui bibliografia.

1. Celulose. 2. Deposição. I. Universidade Federal de Viçosa. Departamento de Química. Programa de Pós-Graduação em Agroquímica. II. Título.

CDD 22 ed. 676.4

LEANDRO COELHO DALVI

DEPOSIÇÃO DE XILANA SOBRE CELULOSE KRAFT DE EUCALIPTO

Tese apresentada à Universidade Federal de Viçosa, como parte das exigências do Programa de Pós-Graduação em Agroquímica, para obtenção do título de *Doctor Scientiae*.

APROVADA: 14 de novembro de 2019.

Assentimento:

Leandro Coelho Dalvi
Autor

Antônio Jacinto Demuner
Orientador

A Deus.

A meus pais e à minha irmã.

À minha amada esposa.

A meus filhos...

AGRADECIMENTOS

Após cinco anos de estudos e trabalhos confesso que é difícil organizar os pensamentos, acalmar o coração e escrever os agradecimentos sem me emocionar.

Em 2015 recebi um convite, quase uma intimação, para retornar à Universidade Federal de Viçosa após quatorze anos. Já era um profissional experiente, casado e com três filhos. Teoricamente não havia necessidade de passar horas em sala de aula, mais horas na estrada em madrugadas frias e outras tantas estudando e escrevendo esta tese. Mas o desafio era grande demais e os resultados muito promissores para negar o convite.

Este desafio era mais que especial. Não deveria ser aceito somente por mim, mas por minha família. Por isso agradeço aos meus pais, Pedro e Regina, que sempre me amaram incondicionalmente. Apesar de perceber a preocupação em seus olhos sabia que encontraria apoio. Amo vocês.

À minha amada irmã Juliana. Sempre por perto, mesmo à distância. Eu não seria nada sem você.

À minha esposa, companheira, amiga, confidente, um anjo que Deus colocou em minha vida. Agradeço imensamente pela sabedoria, paciência e pelo amor tranquilo onde, finalmente, encontrei a minha paz.

A meus filhos Cecília, João Pedro e Daniel. Não há palavras para definir este amor. Eu simplesmente daria a vocês todo o ar que há para eu respirar e assim o farei enquanto houver ar.

Aos meus queridos amigos da CENIBRA Léo, Cleide, Walaston, Cleuber, Silvano, Marcus, Marília, Daniel, Flávio Paoliello e Ronaldo Ribeiro que me ajudaram neste trabalho. Obrigado! Ainda agradeço à inestimável equipe do Departamento de Fabricação pelo companheirismo e dedicação. Vocês me inspiram e me instigam a seguir em frente.

À CENIBRA, nas pessoas de meus Diretores Róbinson Félix e Júlio Ribeiro, por todo o apoio e compreensão.

Ao meu estimado orientador, de longa data, Antônio Jacinto Demuner, que de surpresa aceitou este desafio junto comigo. Isso não seria possível sem você. Incomparável!

Finalmente, agradeço ao meu admirável orientador Jorge Luiz Colodette pelo convite, que foi aceito. Espero que este trabalho esteja a sua altura.

O presente trabalho foi realizado com apoio da Coordenação de Aperfeiçoamento de Pessoal de Nível Superior – Brasil (CAPES) – Código de Financiamento 001.

RESUMO

DALVI, Leandro Coelho, D.Sc., Universidade Federal de Viçosa, novembro de 2019. **Deposição de xilana sobre celulose kraft de eucalipto.** Orientador: Antônio Jacinto Demuner. Coorientador: Rubens Chaves de Oliveira

O desenvolvimento de propriedades físicas de polpa de eucalipto kraft branqueada é tipicamente baseado em processos de refino. Entretanto, muitos trabalhos relatam a viabilidade da deposição de xilana sobre as fibras de celulose. Como os mecanismos de deposição ainda não são claros, o principal objetivo deste trabalho foi buscar um melhor entendimento destas interações. Considerando a complexidade de uma matriz de celulose com deposição de xilana, alguns modelos foram utilizados. Nanofilmes de celulose foram preparados através das técnicas de *spincoating* e do método Langmuir-Schaefer (LS) com trimetilsililcelulose. As interações foram monitoradas através de Microbalança de Quartzo com Monitoramento por Dissipação (QCM-D). As alterações topográficas foram estudadas com Microscopia de Força Atômica (AFM). Para os estudos de RMN em Estado Sólido de ^{13}C, foram preparadas amostras com celulose microcristalina comercial (MCC) e xilana, que foi obtida através de extração alcalina a frio (CCE) de polpa kraft branqueada de bétula. Também foi avaliada a deposição de xilana sobre a celulose em condições industriais nos estágios de deslignificação e branqueamento, bem como sua estabilidade através do processo industrial além do estudo dos efeitos da deposição de xilana sobre as propriedades da polpa e sobre o processo de reciclagem das fibras e os efeitos da carga de NaOH e temperatura sobre as eficiências de extração de xilana de polpa kraft branqueada de eucalipto. O monitoramento por QCM-D mostrou deposição somente com soluções mais concentradas de xilana (1 mg L^{-1}) nos experimentos com o método LS. As imagens de AFM mostraram que a xilana deposita na forma de aglomerados sobre a superfície da celulose e os experimentos de RMN indicaram que há interações entre xilana e celulose nas regiões cristalinas e amorfas da celulose. A deposição de xilana no estágio de deslignificação se mostrou tecnicamente viável apesar do elevado

consumo de NaOH devido às condições ácidas do extrato de xilana. Entretanto, os experimentos de branqueamento indicam a redução do conteúdo de xilana através da sequência testada, em que a xilana depositada continua acessível para reações de oxidação e hidrólise. Os experimentos de deposição nos estágios do branqueamento demonstraram viabilidade principalmente no primeiro estágio com dióxido de cloro (D1), apesar da elevação dos consumos de NaOH e ClO_2. Os melhores resultados de deposição e evolução das propriedades da polpa foram obtidos no estágio de deslignificação. Foram observadas melhorias de rendimento e propriedades físicas da polpa e, principalmente, redução do consumo de energia no processo de refino em todos os estágios testados. Finalmente, foi possível observar os efeitos da deposição da xilana sobre a histerese, melhorando a reciclabilidade das fibras. A carga de 240 g de NaOH nos testes de extração alcalina atingem as máximas eficiências. Cargas mais elevadas não mostraram diferenças significativas em relação ao teor de pentosanas. As extrações a 25 ºC mostraram melhores resultados. Entretanto, a extração a 60 ºC, que é uma condição mais adequada ao processo de produção de celulose, mostrou resultados similares aos obtidos com temperaturas mais baixas.

Palavras-chave: AFM. Branqueamento. Celulose. Deslignificação. Deposição. RMN. QCM-D. Xilana.

ABSTRACT

DALVI, Leandro Coelho, D.Sc., Universidade Federal de Viçosa, November, 2019. **Xylan deposition on eucalytus kraft pulp.** Advisor: Antônio Jacinto Demuner. Co-advisor: Rubens Chaves de Oliveira.

The development of physical properties of bleached eucalyptus kraft pulp is typically based on the refining process. However, many works reported that xylan deposition is a viable alternative. Since the mechanisms of the xylan and cellulose interactions are not clear, the main goal of this work was to achieve a better understanding of these interactions. Considering that a sample of pulp enriched with xylan is a very complex matrix, a model system was developed. Cellulosic thin films were prepared by spincoating and Langmuir-Schaefer (LS) method from trimethylsilylcellulose. Their interactions with xylan were analysed by Quartz Crystal Microbalance with Dissipation Monitoring (QCM-D) technique. The topological changes on cellulose were studied by Atomic Force Microscopy (AFM). For the ^{13}C Solid-State NMR studies, samples were prepared using commercial microcrystalline cellulose (MCC) and xylan. The xylan was extracted from bleached birch kraft pulp using a cold caustic extraction (CCE) method. Other objectives of this work were: to evaluate xylan deposition on eucalyptus kraft pulp under industrial conditions in oxygen delignification and bleaching stages, as well as its stability along the production process; to study the effects of xylan deposition on the pulp properties and on the recycling process; to study the effect of NaOH load and temperature on the xylan extraction efficiency from bleached eucalyptus kraft pulp. The QCM-D monitoring showed deposition only with higher concentration of xylan solution (1 mg L^{-1}) for the LS method. The AFM images showed that xylan deposits as agglomerates on the cellulose surface and the NMR experiments showed that there are interactions for the more ordered region of cellulose fiber and for the less ordered region. Xylan deposition in oxygen delignification stage showed to be technically viable, despite the higher sodium hydroxide consumption due to the acidic conditions of the cold extraction liquor. However, bleaching experiments indicate a xylan content decreasing

throughout the bleaching sequence, meaning that the deposited xylan is still accessible for oxidation or hydrolysis reactions. Although a reduced drainability was observed, there was an increasing in yield and improvement the physical properties. The hornification phenomena was reduced by xylan deposition only in the first recycling cycle. The 240g NaOH load, in the alkaline extractions trials, showed similar results of pentosan reported for previous studies, achieving the maximum extraction efficiency. The higher loads did not show significant differences for pentosan content. The extraction trial at 25 ºC showed a better result. However, the extraction at 60 ºC, which is a more realistic condition for pulp mills, showed results similar to that at lower temperature.

Keywords: AFM. Bleaching. Cellulose. Oxygen delignification. Deposition, NMR. QCM-D. Xylan.

SUMÁRIO

INTRODUÇÃO GERAL

A celulose é o composto orgânico mais abundante do planeta e o principal componente estrutural das células vegetais. É um polissacarídeo linear formado por unidades de β-D-glicopiranose unidas por ligações covalentes β-1,4-glicosídicas (Sjöström 1981). A celulose nativa é formada por dois alomorfos cristalinos, Iα e Iβ, demonstrados por técnicas de RMN CPMAS^{13}C. Os dois alomorfos são diferentes em relação à estrutura cristalina, ligações de hidrogênio e conformação molecular (Atalla & Vanderhart 1984).

As hemiceluloses, juntamente com celulose e pectina, são polissacarídeos que formam a parede celular de vegetais superiores (Sjöström 1981). Podem ser encontradas nas paredes primária e secundária e, em menores quantidades, na lamela média. As hemiceluloses são heteropolímeros ramificados, amorfos, constituídos por diferentes monossacarídeos com formas de furanoses ou piranoses em diferentes proporções (Srndovic 2011; Timell 1967) e proporcionam flexibilidade às paredes das fibras (Atalla et al. 1993).

Simulações moleculares dinâmicas sugerem que múltiplas camadas de xilanas podem envelopar as microfibrilas (Li et al. 2015a) e são capazes de fazer ligações cruzadas entre elas (Mikkelsen et al. 2015). Foi proposto recentemente que as xilanas são capazes de formar ligações de hidrogênio com superfícies hidrofílicas da celulose através de uma forma helicoidal de dupla dobra (Busse-Wicher et al. 2014; Busse-Wicher et al. 2016a; Bromley et al. 2013) enquanto apresenta uma forma helicoidal de dobra tripla em solução (Simmons et al. 2016).

Xilanas são facilmente removidas por soluções alcalinas devido à sua estrutura amorfa e aos resíduos de ácidos urônicos presentes em suas cadeias laterais (Pedrazzi 2009).

Os principais pontos para extração de xilanas na indústria de polpa kraft são os cavacos de madeira, os licores de cozimento e a polpa branqueada (Axelsson et al. 1962; Simonson 1963; Dahlman et al. 2008; Sjöström & Enström 1967; Janzon et al. 2006; Krogerus & Furhmann 2009).

O interesse da indústria papeleira sobre o conteúdo de xilana em polpas é baseado nos grupos carboxílicos que são introduzidos nas fibras de celulose pela xilana (Kleppe 1970). Fibras com elevados teores de xilana incham facilmente, aumentando a área superficial, os sítios ativos para as reações das fibras e as ligações interfibras (Eriksson & Sjöström 1968; Mobarak et al. 1973). Tem sido demonstrado que xilanas adsorvidas na polpa aumentam as propriedades de resistência dos papéis (Sihtola & Blomberg 1975; Schömberg et al. 2001) e reduzem o consumo de energia durante os processos de refino (Aurell 1965; Mobarak et al. 1973; Vaaler et al. 2002). Além disso, reduzem os efeitos de histerese durante a secagem dos papéis (Köhnke & Gatenholm 2007).

O aumento do teor de hemiceluloses na parede da fibra pode ser conseguido de duas diferentes formas: melhorando sua retenção durante a etapa de deslignificação (Kleppe 1970) ou realizando a deposição de hemiceluloses dissolvidas sobre as fibras (Yllner & Enström 1956; Aurell 1965; Dahlman et al. 2003).

Assim, devido ao interesse sobre o teor de xilanas das polpas demonstrado pelos fabricantes de celulose e papel, torna-se importante o conhecimento dos mecanismos envolvidos no seu processo de deposição. Devido à elevada complexidade das amostras de polpa industriais, foram realizados experimentos de deposição utilizando celulose microcristalina e xilana pura para os ensaios de RMN (Ressonância Magnética Nuclear) de ^{13}C. Além disso, foram criados modelos nanofilmes de celulose e xilana, monitorados através de QCM-D (Quartz Crystal Microbalance with Dissipation Monitoring (QCM-D) e AFM (Atomic Force Microscopy) para um entendimento mais aprofundado de suas interações.

Ainda foi avaliada a deposição de xilanas sobre a celulose em condições industriais nos estágios de deslignificação com oxigênio, bem como nos estágios de branqueamento com dióxido de cloro (D1) e extração alcalina com oxigênio e peróxido de hidrogênio (EP).

Após as etapas de deposição foram verificados os efeitos da xilana sobre propriedades físicas da polpa e sobre o processo de reciclagem das fibras.

Finalmente, considerando o fluxograma das fábricas contemporâneas de celulose foram realizados experimentos de extração alcalina em condições mais próximas daquelas praticadas na indústria.

REFERÊNCIAS

Atalla, R. H., Vanderhart, D. L. (1984) Native cellulose: A composite of 2 distinct crystalline forms. Science. 223:283−285.

Atalla, R.H., Hackney, J.M., Uhlin, I., Thompson, N.S. (1993) Hemicelluloses as structure regulators in the aggregation of native cellulose. Int. J. Biol. Macromol. 15:109-112.

Aurell, R. (1965) Increasing kraft pulp yield by redeposition of hemicelluloses. Tappi. 48:80-84.

Axelsson, S., Croon, I., Enström, B. (1962) Dissolution of hemicelluloses during sulphate pulping. Svensk Papperstidning. 65:693-697.

Bromley, J.R., Busse-Wicher, M., Tryfona, T., Mortimer, J.C., Zhang, Z., Brown, D.M., Dupree, P. (2013) GUX1 and GUX2 glucuronyltransferases decorate distinct domains of glucuronoxylan with different substitution patterns. Plant J. 74:423-434.

Busse-Wicher, M., Gomes, T.C.F., Tryfona, T., Nikolovski, N., Stott, K., Grantham, N.J., Bolam, D.N., Skaf, M.S., Dupree, P. (2014) The pattern of xylan acetylation suggests xylan may interact with cellulose microfibrils as a twofold helical screw in the secondary plant cell wall of *Arabidopsis thaliana*. Plant J. 79:492-506.

Busse-Wicher, M., Li, A., Silveira, R.L., Pereira, C.S., Tryfona, T., Gomes, T.C.F., Skaf, M.S., Dupree, P. (2016b) Evolution of xylan substitution patterns in gymnosperms and angiosperms: implications for xylan interaction with cellulose. Plant Physiol. 171:2418-2431.

Dahlman, O., Jensen, A., Tormund, D., Östlund, J. (2008) Processing of xylan from hardwood spent cooking liquors. In: Conference proceedings from the Nordic Wood Biorefinery Conference, Sweden, pp 114-119.

Dahlman, O., Sjöberg, J., Jansson, U.B., Larsson, P.O. (2003) Effects of surface hardwood xylan on the quality of softwood pulps. Nordic Pulp Paper Res. J. 18:310-315.

Eriksson, E., Sjöström, E. (1968) Influence of acidic groups on the physical properties of high-yield pulps. Tappi. 51:56-59.

Janzon, R., Puls, J., Saake, B. (2006) Upgrading of paper-grade pulps to dissolving pulps by nitren extraction: optimization of extraction parameters and application to different pulps. Holzforschung. 60:347-354.

Kleppe, P. (1970) Kraft pulping. Tappi. 53:35-47.

Köhnke, T., and Gatenholm, P. (2007) The effect of controlled glucuronoxylan adsorption on drying-induced strength loss of bleached softwood pulp. Nordic Pulp Paper Res. J. 22:508-515.

Krogerus, B., Fuhrmann, A. (2009) Isolation of xylan and use as wet end- and binder chemical. In: Conference proceedings from the 15th International Symposium on Wood, Fibre and Pulping Chemistry, Norway. pp-110.

Li, L., Perre, P., Frank, X., Mazeau, K. (2015a) A coarse-grain force-field for xylan and its interaction with cellulose. Carbohydr. Polym. 127:438-450.

Mikkelsen, D., Flanagan, B.M., Wilson, S.M., Bacic, A., Gidley, M.J. (2015) Interactions of arabinoxylan and (1,3)(1,4)-β-glucan with cellulose networks. Biomacromolecules. 16:1232-1239.

Mobarak, F., El-Ashawy, A.E., Fahmy, Y. (1973) Hemicelluloses as additive in papermaking. Part 2. The role of added hemicellulose in situ on paper properties. Cellulose Chem. Technol. 7:325-335.

Pedrazzi, C. Influência das xilanas na produção e nas propriedades de polpas de eucalipto para papéis. Universidade Federal de Viçosa, Brazil, 2009.

Schömberg, C., Oksanem, T., Suurnäkki, A., Kettunem, H., Bucghert, J. (2001) The importance of xylan for the strength properties of spruce kraft fibres. Holzforscung. 55:639-644.

Sihtola, H., Blomberg, L. (1975) Hemicelluloses precipitated from steeping liquor in the viscose process as additives in papermaking. Cellul. Chem. and Technol. 9:555-560.

Simmons, T.J., Mortimer, J.C., Bernardinelli, O.D., Pöppler, A., Brown, S.P., Azevedo, E.R., Dupree, R., Dupree, P. (2016) Folding of xylan onto cellulose fibrils in plant cell walls revealed by solid-state NMR. Nat. Commun. 7:1-9.

Simonson, R. (1963) The hemicellulose in the sulphate pulping process. I. Isolation of hemicellulose fractions from sulphate cooking liquors. Svensk Papperstidning. 66:839-845.

Sjöström, E. Wood chemistry, fundamentals and applications. Academic Press, New York, 1981.

Sjöström, E., Enström, B. (1967) Characterization of acidic polysaccharides isolated from different pulps. Tappi. 50:32-36.

Srndovic, J.S. Interactions between wood polymers in wood cell walls and celulose/hemicellulose biocomposites. Chalmers University of Technology. Sweden, 2011.

Timell, T.E. (1967) Recent progress in the chemistry of wood hemicelluloses. Wood Sci. Technol. 1:45-70.

Vaaler, D., Ljones, S., Ribe, E., Toven, K., Moe, S. (2002) Effects of hemicellulose stabilisation and raw material on the beatability of softwood kraft pulps. In: 7th EWLP, Finland. pp 147-150.

Yllner, S., Enström, B. (1956) Studies of the adsorption of xylan on cellulose fibers during the sulphate cook. Part 1. Svensk Papperstidning. 59:229-232.

PAPER 1: STUDY OF XYLAN AND CELLULOSE INTERACTIONS MONITORED BY SOLID-STATE NMR AND QCM-D

Aceito para publicação em: **Holzforschung**

ABSTRACT

The development of physical properties of bleached eucalyptus kraft pulp is typically based on the refining process. However, many works reported that xylan deposition is a viable alternative. Since the mechanisms of the xylan and cellulose interactions are not clear, the main goal of this work was to achieve a better understanding of these interactions. Considering that a sample of pulp enriched with xylan is a very complex matrix, a model system was developed. Cellulosic thin films were prepared by spincoating and Langmuir-Schaefer (LS) method from trimethylsilylcellulose. Their interactions with xylan were analysed with Quartz Crystal Microbalance with Dissipation Monitoring (QCM-D) technique. The topological changes on cellulose were studied with Atomic Force Microscopy (AFM). For the ^{13}C Solid-State NMR studies, samples were prepared using commercial microcrystalline cellulose (MCC) and xylan. The xylan was extracted from bleached birch kraft pulp using a cold caustic extraction (CCE) method. The QCM-D monitoring showed deposition only with higher concentration of xylan solution (1 mg L^{-1}) for the LS method. The AFM images showed that xylan deposits as agglomerates on the cellulose surface and the NMR experiments showed that there are interactions for the more ordered region of cellulose fiber and for the less ordered region.

Keywords: AFM, cellulose, deposition, NMR, QCM-D, xylan

1. INTRODUCTION

Cellulose is the most abundant organic compound of the planet and the main structural component of the plant cells. It is a linear polysaccharide formed by β-D-glucopyranose units linked by β-1,4-glycosidic covalent bonds (Sjöström 1981). The native cellulose is formed by two crystalline allomorphs, Iα and Iβ, demonstrated by CPMAS ^{13}C NMR techniques. Those two allomorphs are different regarding crystalline structure, hydrogen bonds and molecular conformation (Atalla & Vanderhart 1984).

Hemicelluloses, along cellulose and pectin, are polysaccharides that form the cell wall of higher plants (Sjöström 1981). The hemicelluloses can be found both in the primary and secondary walls and, in a small amount, in the middle lamella. Hemicelluloses are branched heteropolymers constituted by different monosaccharides in pyranose or furanose forms in different proportions (Srndovic 2011; Timell 1967).

The hemicelluloses are amorphous polymers, without the tendency to form crystalline regions in their native forms on the fiber walls, providing flexibility (Atalla et al. 1993).

It has recently been proposed that xylan might be able to hydrogen bond to the hydrophilic surfaces of cellulose through folding as a twofold helical screw (Busse-Wicher 2014; Busse-Wicher et al. 2016b; Bromley et al. 2013) while it adapts a threefold helical screw xylan in solution (Simmons et al. 2016).

Xylans are hemicelluloses easily removed by alkali solutions, due to their amorphous structure and high amount of acid groups typically present as side groups in xylans (Aurell 1965).

The main sources for xylan extraction in a kraft pulp mill are wood chips, cooking liquors and bleached pulp (Axelsson et al. 1962; Simonson 1963; Dahlman et al. 2008; Sjöström & Enström 1967; Janzon et al. 2006; Krogerus & Furhmann 2009).

An increase in the amount of hemicelluloses in the fiber wall can be achieved in two different ways: improving the retention of hemicelluloses in the fibers during the oxygen delignification process (Kleppe 1970) and conducting a deposition process of dissolved hemicellulose polymers onto the fiber (Yllner & Enström 1956; Aurell 1965; Dahlman et al. 2003).

Earlier studies of xylan sorption onto cellulose surfaces have reported first order kinetics. This indicates a physical process, with Van der Waals or hydrogen bonds between the sorbed xylan and the cellulose substrate (Clayton & Phelps 1965; Mitikka-Eklund, 1996; Hansson 1970; Danielsson & Lindström 2005; Ribe et al. 2009; Mora et al. 1986). Other studies have reported the adsorption of xylan on the cellulose fibers as a relatively slow process, probably due to the molecular diffusion in the porous fiber wall (Clayton & Phelps 1965; Hansson 1970).

Hydrogen bonds have been demonstrated to be involved in the xylan retention during sorption-desorption experiments with hydrogen bond disruptor reagents (Mora et al. 1986). However, the hydrogen bonds formation between xylan and cellulose has been questioned. Previous studies affirm that if hydrogen bonds formation does occur, the xylan layer on the cellulose surface should be flat, according to the models for free energy between flat surfaces (Derjaguin, 1934), and not swollen with water as observed in experiments using techniques like QCM-D (Quartz Crystal Microbalance with Dissipation). They suggest, then, that the driving force is a combination of entropy increasing, associated to the release of solvent molecules during the polymer adsorption, and the weak Van der Waals attraction, rather than formation of hydrogen bonds as has been cited before (Tammelin et al. 2009; Mora et al. 1986). Despite that, hydrogen bonds may be important for dried systems (Paananen et al. 2004).

Other studies suggested that xylan exists both as single molecules in aqueous solution and as aggregates in the colloidal state. The aggregates formation is provided by the interaction of unsubstituted regions of the xylan chain and by the hydrophobic interaction due to lignin residues covalently bonded to xylan. Consequently, the adsorption on the cellulose surface happens through single molecules and aggregates. This mechanism is, probably, more relevant for systems where the xylan solubility is lower (Linder et al. 2003; Mora et al. 1986).

The xylan adsorption is considered as irreversible and only small amounts are removed by dilution (Paananen et al. 2004) or water washing (Eriksson et al. 1963). The exposure to alkaline conditions under high temperatures increases the desorption rate (Hansson & Hartler 1969). It is

easy to understand since the solubility of hemicelluloses is higher under alkaline conditions (Miao et al. 2014; Li et al. 2015b).

However, it has been reported that adsorbed xylan from cold caustic extraction liquors is kept in the cellulose surface even after oxygen delignification process or bleaching sequences (Dahlman et al. 2003; Soares 2009).

The interest of the pulp and paper industry over the xylan content of cellulose pulps is based on the carboxylic groups which are introduced in the cellulose fibers by xylan (Kleppe 1970). Fibers with high xylan content get swollen easily, exposing a higher superficial area, increasing the active sites for the fiber reactions (Eriksson & Sjöström 1968; Mobarak et al. 1973). It has been reported that adsorbed xylan on pulp increases tensile properties of the paper (Sihtola & Blomberg 1975; Schömberg et al. 2001) and decreases the energy consumption during the refining process (Aurell 1965; Mobarak et al. 1973; Vaaler et al. 2002).

Nuclear magnetic resonance has been used as an extensive spectroscopic method to determine organic compounds structure. The developments of high-resolution solid-state NMR of organic materials over the last 30 years have been deeply established (Dybowski & Bai 2006). The materials that are investigated can be natural, synthetic and even biological systems, and the ^{13}C is undoubtedly the most feasible nucleus that can be studied with high-resolution NMR in the solid phase. It can be easily observed and the interpretation of ^{13}C spectra is almost a direct reading of the carbon skeleton of molecules (Lambert et al. 2000; Ghisalberti & Godfrey 1998; Alesiani et al. 2005; Pournou 2008; Santonia et al. 2015; Dupree et al. 2015).

The structures of cellulose in wood and pulp have been extensively studied employing CPMAS ^{13}C NMR spectroscopy (Van der Hart & Atalla 1984; Newman & Hemmingson 1990; Newman 1992; Newman et al. 1993; Lindgren et al. 1995; Larsson et al. 1997; Newman 1998; Wickholm et al. 1998; Larsson et al. 1999; Hult et al. 2000; Maunu et al. 2000).

Other advanced techniques, such as atomic force microscopy (AFM) and quartz crystal microbalance with dissipation monitoring (QCM-D) have been used as support for a better knowledge of xylan and cellulose interactions

(Binnig et al. 1986; Ducker et al. 1991; Korolkov et al. 2019; Fatisson et al. 2009; Thio et al. 2011; Chen et al. 2016; Mocchiuttia et al. 2016).

Since there is a great interest in the xylan content from pulp and paper producers, knowledge of the mechanisms of xylan adsorption on cellulose surface is desirable. Therefore, the main goal of this work was to study the interactions of xylan and cellulose using techniques such as ^{13}C Solid-State NMR, AFM and QCM-D associated to nanofilms samples to achieve a purer model than the industrial pulp samples.

2. MATERIALS AND METHODS

2.1. Xylan samples

Xylan has been extracted from commercial bleached birch kraft pulp using 1 M NaOH solution at room temperature followed by ultra and diafiltration as described earlier (Laine et al. 2015) and shown in Figure 1.

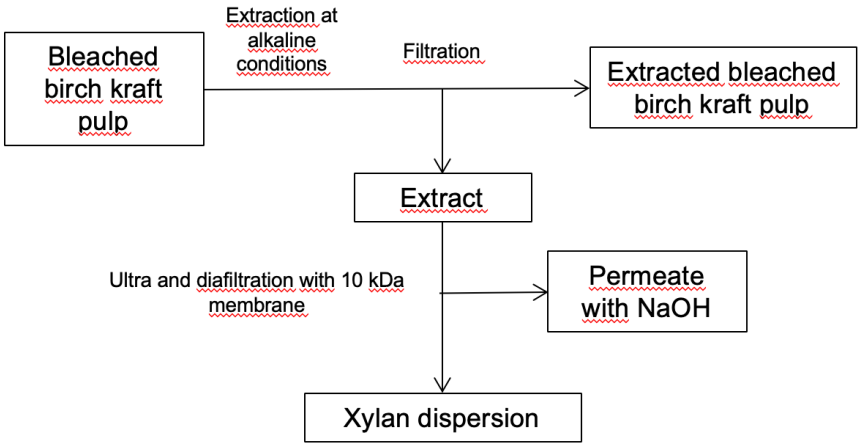

Figure 1. Schematic flow to obtain xylan dispersion according to Laine et al. 2015.

Saturated solutions/dispersions of xylan were prepared, at different pH, from a xylan slurry of dry matter content (DMC) by adding deionized water and 1 M NaOH solution and regulating the pH several times during stirring for 48h at room temperature. After centrifugation, the supernatants were the samples used for the adsorption trials, according to Figure 2.

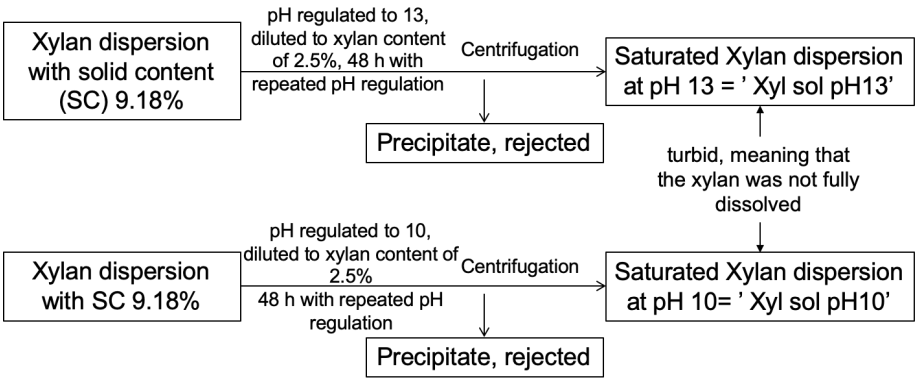

Figure 2. Schematic flow to obtain saturated xylan dispersion samples.

The carbohydrate content of the saturated xylan solutions and the DMC were determined (Table 1).

Table 1. Xylan and dry matter content of the xylan solutions/dispersions for the adsorption trial.

Sample	Xylan content (g L^{-1})	Dry matter content (wt.-%)
Xyl sol pH 13	9.22	2.20*
Xyl sol pH 10	11.19	1.27

* The sample contains significant amounts of sodium hydroxide from the pH regulation.

2.2. Preparation of cellulose samples with adsorbed xylan

Microcrystalline cellulose (Sigmacell Type 50) (MCC) was selected as cellulose model. Xylan isolated from bleached birch Kraft pulp was added to the cellulose suspension at selected pH values, 13 (represents a high pH during pulp processing) and 10 (where xylan precipitation in practice may take place at the final phase of pulping). Adsorption experiments were performed by mixing soluble/dispersed xylan and MCC at defined conditions.

The dry matter contents (DMC) were 95.1% for MCC and 9.18% for the original xylan dispersion.

The soluble part of the xylan dispersion was isolated by regulating the pH of 1.2 L of xylan dispersion to pH 13 and pH 10 and a final xylan content of 2.5 %wt. After stirring at room temperature for 48 h and pH adjustment as necessary, the dispersion/solution was centrifuged with 4,750 rpm for 1 h at room temperature with an Allegra X-15R centrifuge and the supernatant was

collected. The resulting samples were saturated xylan solution at pH 13 (Xyl sol pH 13) and saturated xylan solution pH10 (Xyl sol pH 10).

10 g of MCC (as bone dry) and 990 g of Xyl sol pH 13 or Xyl sol pH 10 were stirred at room temperature for 7 days. The pH was recorded several times during this period.

After the adsorption, both samples were divided into two equal parts for further analysis.

A. Half of the sample was centrifuged resulting in the solid sample MCC+Xyl pH 13 unwashed and the supernatant (Sup Xyl pH 13). The same procedure was used for the samples at pH 10. The solid sample was air-dried except for a small portion (20% of the original sample).

B. The other half was centrifuged and redispersed into 990 mL pH 13 water and centrifuged. This was repeated once more resulting into MCC+Xyl pH 13 washed. The same procedure was performed at pH 10. The solid sample was air-dried except a small portion (20% of the original sample).

The carbohydrate analysis of MCC, freeze-dried xylan and the four solid MCC+Xyl samples were determined after prehydrolysis with 72% (w/w) sulphuric acid for 60 min at 30 °C and autoclaving at 4% (w/w) sulphuric acid concentration for 60 min at 120 ºC. The resulting monosaccharides were determined by HPAEC with pulse amperometric detection (Dionex ICS 3000 equipped with CarboPac PA1 column or Dionex ICS 5000 equipped with CarboPac PA20 column, Dionex, USA) according to NREL method (National Renewable Energy Laboratory). The carbohydrate analysis of Xyl sol pH 13 and Xyl sol pH 10 was performed after neutralization using the same protocol but without prehydrolysis.

The carbohydrate composition, including neutral and acidic sugars, was determined according to Sundberg et al. (1996) with two parallel determinations.

2.3. Solid-state NMR experiments

The ^{13}C cross polarization (CP) magic angle spinning (MAS) NMR measurements were performed using an Agilent DD2 600 NMR spectrometer with magnetic flux density of 14.1 T, equipped with a 3.2 mm T3 MAS NMR probe operating in a double resonance mode. MAS rate in experiments was

set to 10 kHz. For the CPMAS spectra of the reference materials 8,000 scans were accumulated using a 1.3 ms contact time and a 6.0 s delay between successive scans. The relaxation time constants $T_{1\rho}(H)$ for pure xylan and MCC were determined with a delayed contact pulse sequence to be 9.2 ms (xylan) and 18.5 ms (MCC). The clear difference in $T_{1\rho}(H)$ values indicates that the PSRE spectral edition for ordered MCC and amorphous xylan components can be carried out. The delayed contact pulse sequence was used also for the PSRE experiments with a duration for the spinlock pulse set as 8.0 ms for the partially relaxed spectra. 4,000 scans were collected for both relaxed and non-relaxed spectra. Protons were decoupled during acquisition using SPINAL-64 proton decoupling with a field strength of 80 kHz. 90-degree pulse durations and Hartmann-Hahn match for cross polarization were calibrated using α-glycine. The spectra were processed using TopSpin 3.5 software.

2.4. Adsorption of xylan on cellulose analyzed by QCM-D and AFM

Adsorption and desorption of xylan on cellulose was investigated using the E4 QCM-D instrument (Q-sense AB, Gothenburg, Sweden). QCM-D allows the simultaneous monitoring of changes in frequency and dissipation at solid/liquid interface at the fundamental frequency of (5 MHz) and its six overtones. These changes are further translated to mass changes and changes in viscoelastic properties taking place during the adsorption/desorption process. The interpretation is described in detail in Rodahl et al. (1995). Briefly, when the adsorbed mass is evenly distributed, rigidly attached and fully elastic, the areal mass can be calculated according to the Sauerbrey equation (Sauerbrey 1959) where Δm is the adsorbed mass per unit surface, $\Delta f = f - f_0$ is the frequency change, n is the overtone number (n = 1, 3, 5, 7, 9, 11, 13) and C is the sensitivity constant of the device. In the present case C = 0.177 mg m^{-2} Hz^{-1} as reported by the supplier (Q-sense AB).

$$\Delta m = -\frac{C\Delta f}{n}$$

If the material on the QCM-D sensor surface is not fully elastic, unevenly distributed or relatively thick, frictional losses occur that lead to a damping of the oscillation with the decay rate of amplitude that depends on the viscoelastic

properties of the material. This is monitored by following the changes in dissipation energy, *D*, which is defined by

$$D = \frac{E_{dissipation}}{2\pi E_{storage}}$$

where $E_{dissipation}$ is the total dissipated energy during one oscillating cycle and $E_{storage}$ is the total energy stored in the oscillation.

Cellulose coated thin films were deposited on gold QCM-D crystals by spincoating or by Langmuir-Schaefer (LS) method using trimethylsilylcellulose (TMSC) (Kontturi at al. 2003; Tammelin et al. 2006). LS surfaces were prepared on gold QDM-D sensors with polystyrene coating. Polystyrene (0.1 w-%, Mw 280,000 g mol^{-1}) in toluene was first spincoated on the sensor (4,000 rpm, 30 s) and dried in oven (60 °C for 10 minutes). TMSC was dissolved in chloroform (0.4 mg mL^{-1}) and the 30 TMSC layers were deposited on the sensor using LS method.

TMSC surfaces were regenerated to cellulose via desilylation in 10% HCl vapour in vacuum for 5 min (Schaub et al. 1993).

TMSC was prepared from microcrystalline cellulose powder (Fluka) by first dissolving in DMAc/LiCl followed by silylation with hexamethyl silazane (Greber & Paschinger 1981; Cooper et al. 1981). The successful silylation was evidenced by ^{1}H NMR in chloroform.

Prior to the adsorption studies the cellulose surfaces were swollen in water over night. The QCM-D sensors with cellulose thin films were placed in the QCM-D measurement cells, and the surfaces were allowed to stabilize in the appropriate buffer solution until a stable baseline was attained. The xylan dispersions were allowed to adsorb on the cellulose surfaces in the selected conditions which are shown in Table 2. After the measurement the sample surfaces were rinsed with the given buffer solutions and dried by using nitrogen gas.

Table 2. Sample set points (all sample points are at least duplicated).

Samples	Xylan concentration (mg mL^{-1})
r1. pH 13 NaOH solution with 1 mM NaCl (reference)	0
r2. pH 10 NaOH solution with 1 mM NaCl (reference)	0
a1. pH 13 NaOH solution with 1 mM NaCl	0.01
a2. pH 13 NaOH solution with 1 mM NaCl	0.1
a3. pH 13 NaOH solution with 1 mM NaCl	1
b1. pH 10 NaOH solution with 1 mM NaCl	0.01
b2. pH 10 NaOH solution with 1 mM NaCl	0.1
b3. pH 10 NaOH solution with 1 mM NaCl	1

2.5. AFM microscopy

The changes in the topography of the cellulose surfaces before and after the xylan adsorption were monitored by AFM microscopy (ANASYS AFM+® (ANASYS Instruments Inc., Santa Barbara, CA USA)). The AFM characterization was carried out in dry conditions directly after the QCM-D measurement. The images were taken in tapping mode in air using aluminum coated n-type silicon cantilevers (HQ:NSC15/Al BS, Micromasch, Tallinn, Estonia) with typical probe radius of 8 nm, force constant of 40 N m^{-1} and nominal resonance frequencies between 265 and 410 kHz. The images were not processed in any way except for flattening.

3. RESULTS AND DISCUSSION

3.1. Preparation and characterization of the samples

The xylan content was 9.22 and 11.19 g L^{-1} for Xyl sol pH 13 and Xyl sol pH 10, respectively. This could not be calculated directly from the DMC content and pH because the NaOH addition was not literally the amount necessary for adjusting aqueous solutions due to the buffering capacity of the xylan. It is interesting that more xylan remained dissolved or dispersed at pH 10 compared to pH 13. This phenomenon could not be studied in more detail in this work.

Adsorption experiments were performed using 10 g MCC (as bone dry) with 990 g of the Xyl sol pH13 and Xyl sol pH10, respectively. This means that approximately equal amounts of xylan and MCC were present in the experiments (xylan content of 9.13 g at pH 13 and 11.08 g at pH 10). The pH was not adjusted after addition of the xylan dispersions/solutions and mixing at room temperature for 7 days. For the experiment with Xyl sol pH 13, the final pH was 10.71 while for that with Xyl sol pH 10, the final pH was 8.60. Most probably, the MCC was also buffering the pH together with the xylan. After 7 days, the samples were separated into two equal parts and centrifuged.

The solids from one-half was collected as such ‘unwashed sample’ and the wet yield and DMC were determined. The solids of the other half were washed with pH-adjusted water and centrifuged again and this was repeated one more time. After that, the solids were collected (‘washed sample’). Again, wet yield and DMC were determined. Part of all samples was dried for carbohydrate analysis and NMR analysis and the rest was stored wet.

The list of obtained samples with the yields and carbohydrate contents are shown in Table 3. The xylan content was high in the MCC samples after adsorption at pH 13 accounting for even 60% of the unwashed sample and 28% of the washed samples. This indicates strong adsorption tendency that was only partly reversible during washing. During the adsorption trial, the pH decreased which either enhanced the adsorption or was a consequence of it. At pH 10, the xylan content was moderate with 7.6% in the unwashed sample and 2.5% in the washed sample, respectively.

Table 3. Yield of MCC samples with adsorbed xylan and polysaccharide contents.

Sample	Wet yield (g)	DMC (%)	Dry yield (g)	Cellulose (g)	Xylan (g)	Mannan (g)
MCC+Xyl pH 13 unwashed	115.7*	14.95	17.30	6.7	10.4	0.1
MCC+Xyl pH 13 washed	34.0	8.89	3.02	2.14	0.85	0.04
MCC+Xyl pH 10 unwashed	19.27**	30.92	5.96	5.46	0.45	0.09
MCC+Xyl pH 10 washed	14.76	27.54	4.06	3.89	0.10	0.06

*50.8% of wet sample

**51.5% of the wet sample

The ratio of xylose to 4-methyl glucuronic acid was calculated based on analysis of the data for the xylan sample used for the fractionation as well as for the xylan dispersed at pH 10. The ratios were 19 and 22, respectively. As the difference is only minor, uronic acid substitution is not expected to have a significant effect on solubility or dispersibility under these conditions.

3.2. Adsorption of xylan on cellulose analyzed by NMR

The solid-state NMR spectra for the reference materials, pure MCC and xylan, are shown in Figure 3.

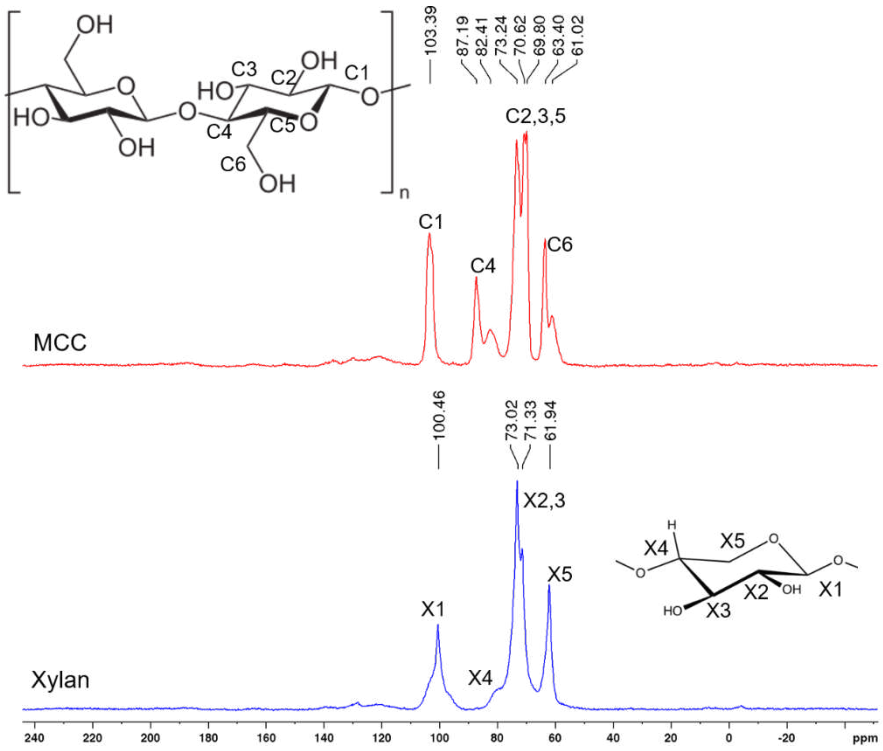

Figure 3. ^{13}C CPMAS NMR spectra of MCC and amorphous xylan reference samples.

Each carbon atom in cellulose and xylan produces distinctive signals in the solid-state NMR spectrum according to their chemical environment in the molecule and to the level of molecular ordering. Due to similarity in chemical structure of MCC and xylan, most of their solid-state ^{13}C NMR signals overlap. However, the signals from xylan carbon X1 at 100.46 ppm, and C4 carbon in ordered cellulose from crystalline interiors of MCC at 87.19 ppm, appear in the spectral regions with only partial overlap. These signals were chosen for spectral editing purposes to distinguish the ordered and less ordered components into subspectra, as described later. The cellulose C4 signal at 82.2 ppm is known to originate from somewhat less ordered fibril surfaces.

The NMR spectra for MCC samples with adsorbed xylan, before and after washing step, are shown in Figure 4. It can be seen that in MCC+Xyl pH 10 there are no visible signals from xylan present. In contrast to this, there is a strong signal from xylan X1 observed close to cellulose C1 in MCC+Xyl pH 13. The washing step decreases the intensity of the X1 signal, but it can still be observed in the spectrum as a shoulder on the cellulose C1 signal.

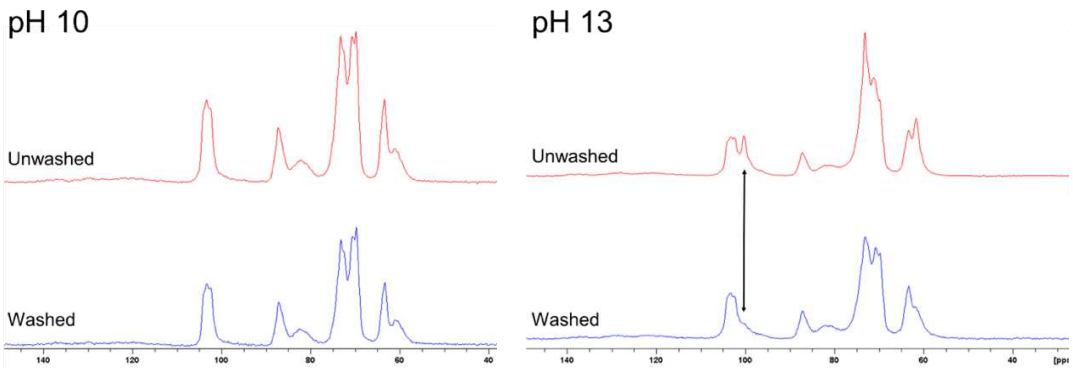

Figure 4. Solid-state ^{13}C NMR spectra of MCC+xylan samples prepared at different pH before and after the sample washing step. The arrow on the right-hand side figure marks the xylan X1 signal.

Figure 5 shows the result of PSRE in the case of MCC+Xyl pH 13 unwashed. The xylan subspectrum correlates well with the reference xylan spectrum. This suggests that xylan is precipitated mainly in unordered form. There is also a clear xylan signal left at MCC subspectrum at 100.4 ppm, representing a fraction closely associated with the ordered cellulose fibrils.

In the PSRE spectra of MCC+Xyl pH 13 washed (Figure 6), the remaining xylan does not contribute to the MCC subspectrum, which is assumed to represent the crystalline cellulose from the interiors of the crystallites. Xylan is observed in the subspectrum of less ordered material, together with some cellulose signals, which most likely originate from the somewhat less ordered cellulose on the fibril surfaces, which apparently show similar relaxation behavior with xylan.

In the case of MCC+Xyl pH 10 unwashed (Figure 7), the only effect of PSRE appears to be a separation of cellulose signals into highly crystalline and less ordered parts, the latter originating from the fibril surfaces. The same result is obtained from the MCC+Xyl pH 10 washed (spectra not shown here).

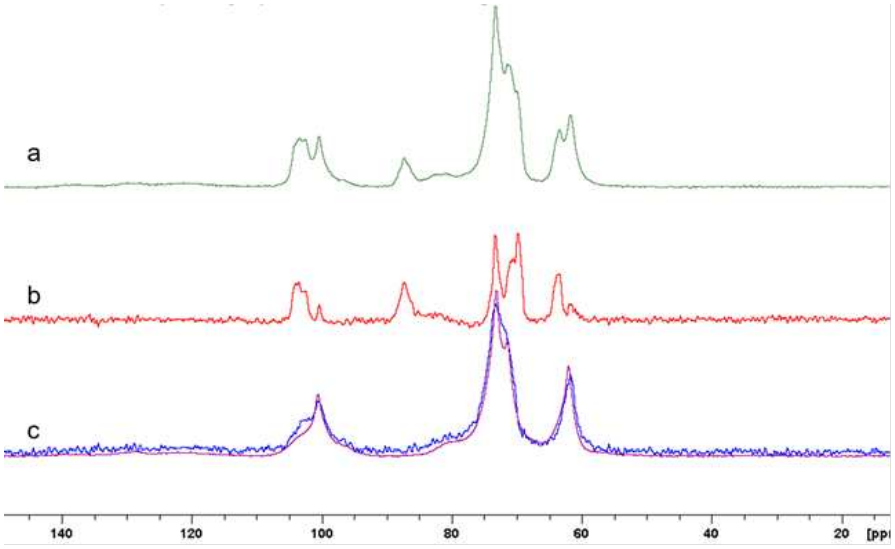

Figure 5. PSRE spectra of MCC+Xyl pH 13 unwashed. (a) Original spectrum. (b) MCC sub spectrum. (c) Xylan subspectrum, together with the overlayed xylan reference spectrum (in purple).

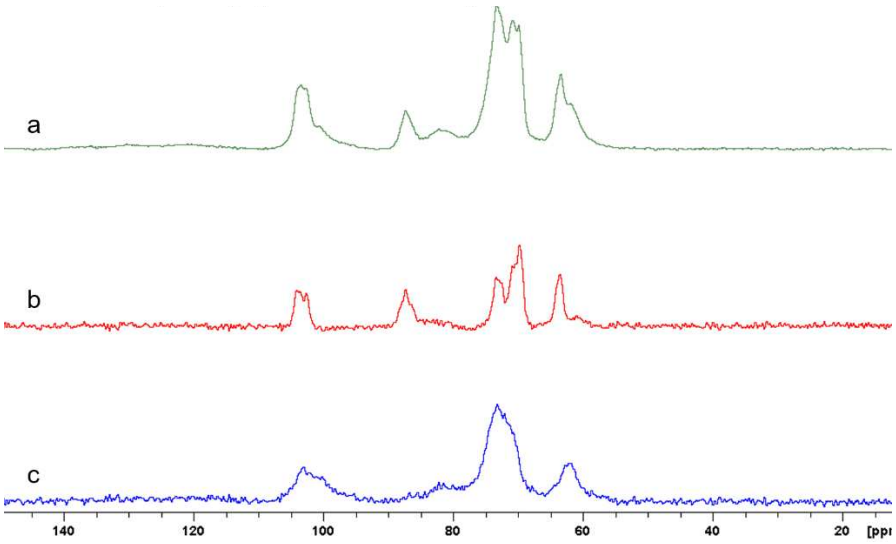

Figure 6. PSRE spectra of MCC+Xyl pH 13 washed. (a) Original spectrum. (b) MCC sub spectrum. (c) Xylan subspectrum.

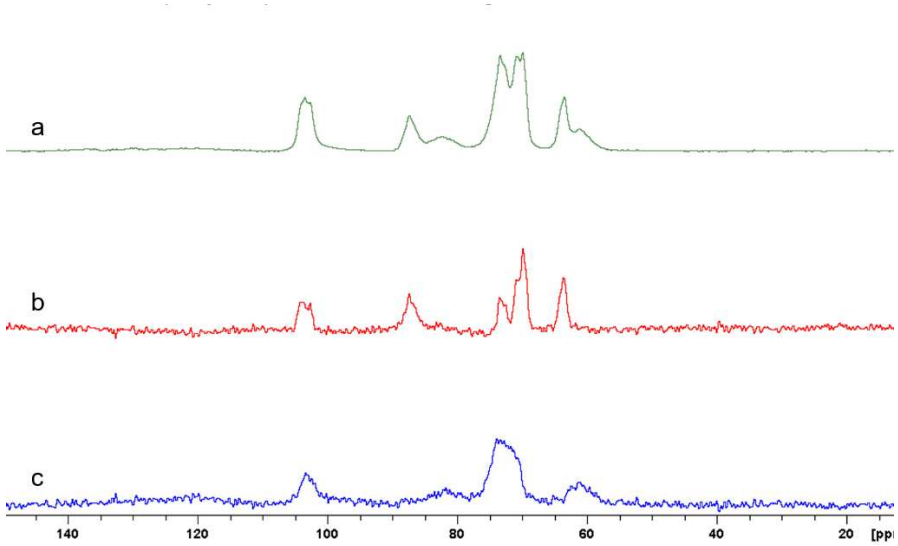

Figure 7. PSRE spectra of MCC+Xyl pH 10 unwashed. (a) Original spectrum. (b) MCC subspectrum. (c) Xylan or less-ordered MCC subspectrum.

According to CPMAS ^{13}C spectra the amount of xylan in MCC+Xyl pH 10 is below the detection limit of the experiment. In the MCC+Xyl pH 13 most of the xylan is in amorphous form, and not closely associated with cellulose. However, part of the xylan that could not be removed by washing is closely associated to MCC, and follows into the subspectrum of cellulose at fibril surfaces. Even though the fibril surfaces are less ordered than cellulose in the interior of cellulose crystallites, it is more ordered compared to the amorphous isolated xylan, suggesting that the xylan associated on the fibril surfaces might also have ordered conformation.

3.3. Adsorption of xylan on cellulose analyzed by QCM-D and AFM

Adsorption behavior of xylan on cellulose at high pH was investigated using surface sensitive methods (QCM-D and AFM) to reveal the interactions taking place directly at the cellulose surface. At highly alkaline conditions (pH 10 and pH 13), it is essential to follow and ensure the durability of the cellulose thin films which are deposited on the QCM-D sensor surfaces. Based on the preliminary tests it was found that only highly crystalline cellulose surfaces prepared via the Langmuir-Schaefer method were able to tolerate high alkaline conditions. More amorphous ultrathin films of cellulose produced via spincoating instantaneously dissolved when contacted with alkaline buffer solutions (results not shown). Furthermore, the most reliable adsorption

experiments were produced at pH 10 (LS-cellulose surfaces), and are therefore presented in the following.

Prior to the xylan adsorption experiments, the QCM-D sensors with cellulose thin films were first allowed to swell and stabilize overnight in milliQ water. Subsequently, the cellulose thin films were contacted with buffer solution (1 mM NaCl at pH 10) until no changes in frequency and dissipation were detected indicating that no changes due to swelling and/or cellulose dissolution occur, see Figure 8. As shown by Figure 8 the plateau level was attained after 150 minutes in contact with the buffer. A minor positive change in frequency indicates a corresponding loss of cellulose from the sensor surface. Such a small change in frequency (<4Hz corresponds a mass change of <0.7 mg m^{-2} calculated using Sauerbrey equation) can be considered as a negligible mass loss and does not interfere in the following xylan adsorption experiments.

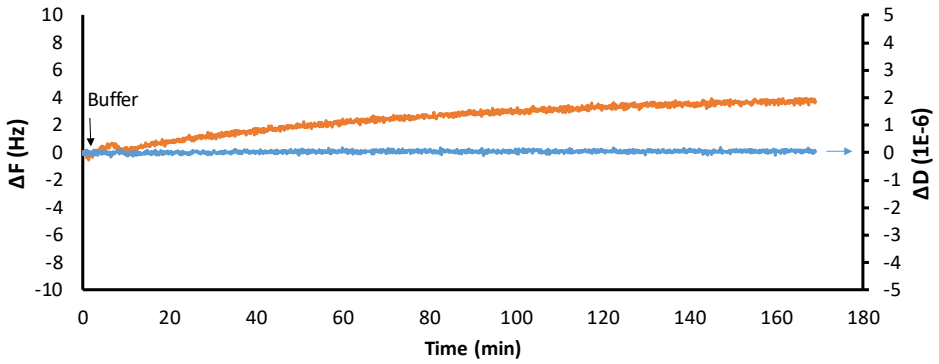

Figure 8. Changes in frequency (orange curve) and dissipation (blue curve) as a function of time recorded for LS-cellulose ultrathin films when stabilized and in contact with buffer solution of pH 10 and 1 mM NaCl. (f_0 = 5 MHz n/3).

Figure 9 shows the adsorption isotherm of dissolved xylan on cellulose surface using three concentration levels of xylan (0.01 mg mL^{-1}, 0.1 mg mL^{-1} and 1 mg mL^{1}) at pH 10. Again, the changes in frequency and dissipation as a function of time were followed in order to estimate the mass change due to xylan adsorption and to evaluate the physical properties of the formed xylan layers. Figure 9 clearly illustrates that significant xylan adsorption takes place only at the highest solution concentration of 1 mg mL^{-1} showing that xylan concentration has an important role in the deposition kinetics. Simultaneously

the dissipation change at the end of the adsorption is relatively high (~6.5 × 10^{-6}) although the frequency change is as low as -11 Hz. This suggest that the formed xylan layer is not uniformly attached on the cellulose surface.

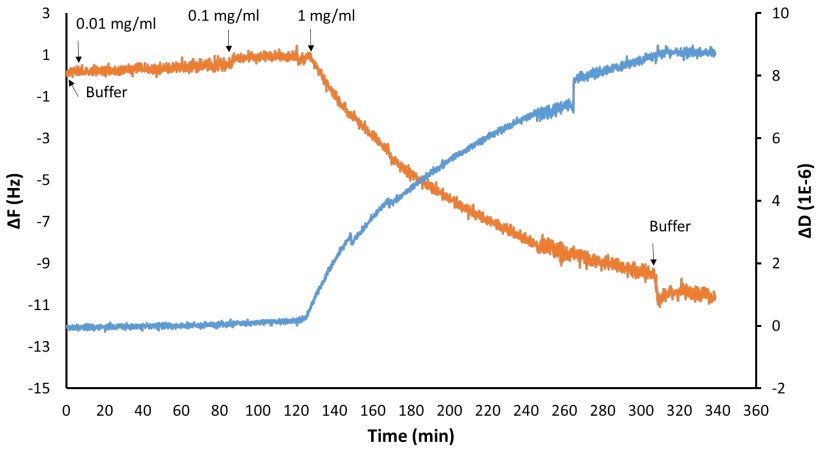

Figure 9. Adsorption isotherm of xylan from solutions containing 0.01 mg mL^{-1}, 0.1 mg mL^{-1} and 1 mg mL^{-1} of xylan at pH 10 and 1 mM NaCl. Δf and ΔD versus time for n=3.

Evenly distributed thin and rigidly attached polymer layer normally generates a dissipation change lower than 1 × 10^{-6} with the similar levels of frequency change. These findings are fully consistent with our previous results and are also supported by the AFM imaging, see Figure 10. After adsorbing xylan on cellulose, the clear changes can be seen in both AFM height and phase contrast images, see Figure 10. Spherical xylan particles (Figure 10 b and 10 d) with the diameters varying within 0.01-0.1 μm. The height image of the reference cellulose surface in Figure 10a. Our system here behaves exactly in the similar way as earlier discussed in (Paananen et al. 2004; Tammelin et al. 2009). The main driving force for xylan to adhere on cellulose surface seems to be the poor solubility of xylan in aqueous solutions. High xylan concentration in solution restricts the solubility of the xylan chains and favors the formation of agglomerates. Attachments on the cellulose surface begins only when the concentration is relatively high, probably close to the limit of precipitation. In solution polymer-polymer contacts dominates over polymer-solvent contacts, which promotes adsorption since xylan chains tend to escape from poor solvent. Chains either form agglomerates, adsorb on surfaces or even precipitate to avoid polymer-solvent contacts. Here any precipitation was

observed and care was taken to utilize freshly prepared xylan dispersions in all QCM-D experiments.

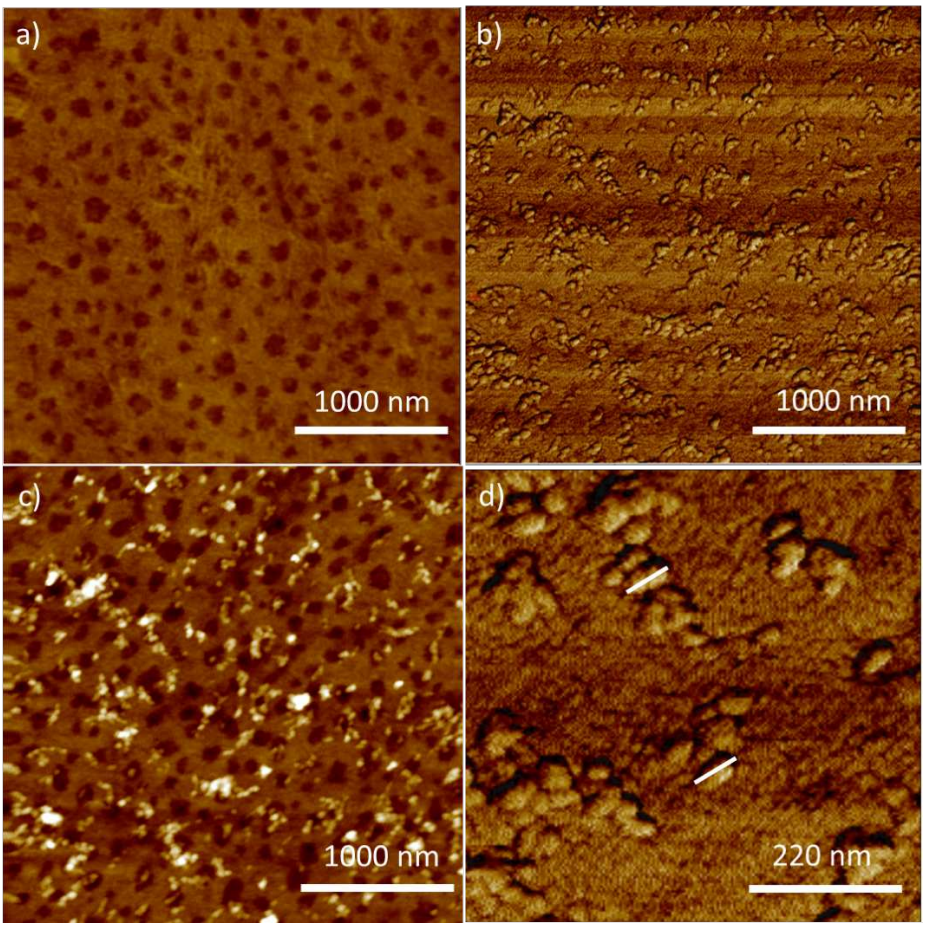

Figure 10. AFM height images of the cellulose surface before a) and after c) xylan adsorption. AFM phase image of the cellulose surface after xylan adsorption with two magnifications b) and d).

4. CONCLUSIONS

Adsorption of xylan from saturated solution on MCC particles was successful, when starting from pH 13. Significant amount of xylan was strongly adsorbed and could not be removed by washing. Only minor irreversible enrichment of xylan was detected when the starting pH was 10. The pH dropped during the 7 days adsorption time, indicating a buffering effect by the cellulose.

The xylan-adsorbed MCC samples before and after washing were analyzed by solid-state NMR. The amount of xylan in the MCC+Xyl pH 10 samples was below the detection limit of the experiment. In the MCC+Xyl pH 13 sample, the xylan was closely associated to MCC as it could not be

completely separated from the MCC subspectrum. However, the washing step removed the xylan signal from the MCC subspectrum, while the remaining xylan signals were observed in the xylan subspectrum together with less ordered cellulose signals, which are known to originate from the accessible fibril surfaces. This may indicate that the xylan fraction that remains after washing step is closely associated with the surface of MCC. Therefore, through the use of NMR techniques two distinct regions of xylan adsorption on cellulose fibers were possible to be seen. It suggests that there may be different adsorption mechanisms for each region, probably related to the size of xylan fragment.

QCM-D experiments showed that xylan was irreversibly deposited on cellulose surface, when the xylan concentration was high enough (1 mg mL^{-1}). The AFM image of the formed surface indicated that xylan had deposited as oval particles with diameters around 0.01-0.1 μm, while most of the cellulose surface seems to be uncovered.

Aknowledgements: The authors thank to Celulose Nipo-Brasileira S.A – CENIBRA, for the supporting to this research and to CNPq, CAPES and FAPEMIG. Atte Mikkelson (VTT) is thanked for the composition analyses. This work was a part of the Academy of Finland's Flagship Programme under Projects No. 318890 and 318891 (Competence Center for Materials Bioeconomy, FinnCERES).

5. REFERENCES

Alesiani, M., Proietti, F., Capuani, S., Paci, M., Fioravanti, M., Maraviglia, B. (2005) ^{13}C CPMAS NMR spectroscopic analysis applied to wood characterization. Appl. Magn. Reson. 29:177-185.

Atalla, R. H., Vanderhart, D. L. (1984) Native cellulose: A composite of 2 distinct crystalline forms. Science. 223:283−285.

Atalla, R.H., Hackney, J.M., Uhlin, I., Thompson, N.S. (1993) Hemicelluloses as structure regulators in the aggregation of native cellulose. Int. J. Biol. Macromol. 15:109-112.

Aurell, R. (1965) Increasing kraft pulp yield by redeposition of hemicelluloses. Tappi. 48:80-84.

Aurell, R., Hartler, N. (1965) Kraft pulping of pine. Part 1. The changes in the composition of the wood residue during the cooking process. Sven. Papperstidn. 68:59-68.

Axelsson, S., Croon, I., Enström, B. (1962) Dissolution of hemicelluloses during sulphate pulping. Sven. Papperstidn. 65:693-697.

Binnig, G., Quate, C.F., Gerber, C. (1986) Atomic force microscope. Phys. Rev. Lett. 56:930-933.

Bromley, J.R., Busse-Wicher, M., Tryfona, T., Mortimer, J.C., Zhang, Z., Brown, D.M., Dupree, P. (2013) GUX1 and GUX2 glucuronyltransferases decorate distinct domains of glucuronoxylan with different substitution patterns. Plant J. 74:423-434.

Busse-Wicher, M., Gomes, T.C.F., Tryfona, T., Nikolovski, N., Stott, K., Grantham, N.J., Bolam, D.N., Skaf, M.S., Dupree, P. (2014) The pattern of xylan acetylation suggests xylan may interact with cellulose microfibrils as a twofold helical screw in the secondary plant cell wall of *Arabidopsis thaliana*. Plant J. 79:492-506.

Busse-Wicher, M., Grantham, N.J., Lyczakowski, J.J., Nikolovski, N., Dupree, P. (2016a) Xylan decoration patterns and the plant secondary cell wall molecular architecture. Biochem. Soc. Trans. 44:74-78.

Busse-Wicher, M., Li, A., Silveira, R.L., Pereira, C.S., Tryfona, T., Gomes, T.C.F., Skaf, M.S., Dupree, P. (2016b) Evolution of xylan substitution patterns in gymnosperms and angiosperms: implications for xylan interaction with cellulose. Plant. Physiol. 171:2418-243.

Chen, Q., Xu, S., Liu, Q., Masliyah, J., Xu, Z. (2016) QCM-D study of nanoparticle interactions. Adv. Colloid Interface Sci. 233:94-114.

Clayton, D.W., Phelps, G.R. (1965) The sorption of glucomannan and xylan on α-cellulose wood fibres. J. Polym. Sci. 11:197-220.

Cooper G.K., Sandberg K.R., Hinck J.F. (1981) Trimetylsilyl cellulose as precursor to regenerated cellulose fiber. J. Appl. Polym. Sci. 26:3827-3836

Dahlman, O., Sjöberg, J., Jansson, U.B., Larsson, P.O. (2003) Effects of surface hardwood xylan on the quality of softwood pulps. Nordic Pulp Paper Res. J. 18:310-315.

Dahlman, O., Jensen, A., Tormund, D., Östlund, J. (2008) Processing of xylan from hardwood spent cooking liquors. In: Conference proceedings from the Nordic Wood Biorefinery Conference, Sweden, pp 114-119.

Danielsson, S., Lindström, M.E. (2005) Influence of birch xylan adsorption during kraft cooking on softwood pulp strength. Nordic Pulp Paper Res. J. 20:436-441.

Derjaguin, B. (1934) Friction and adhesion. IV. The theory of adhesion of small particles. Kolloid-Zeit. 69:155-164.

Ducker, W.A., Senden, T.J., Pashley, R.M. (1991) Direct measurement of colloidal forces using an atomic force microscope. Nature. 353:239-241.

Dupree, R., Simmons, T.J., Mortimer, J.C., Patel, D., Iuga, D., Brown, S.P., Dupree, P. (2015) Probing the molecular architecture of *Arabidopsis thaliana* secondary cell walls using two- and three-dimensional ^{13}C solid-state nuclear magnetic resonance spectroscopy. Biochemistry. 54:2335-2345.

Dybowski, C., Bai, S. (2006) Solid-state nuclear magnetic resonance. Anal. Chem. 78:3853-3858.

Eriksson, E., Samuelson, O., Viale, A. (1963) Adsorption of hemicellulose isolated from sulfite cooking liquors by cellulose fibers. Sven. Papperstidn. 66:403-406.

Fatisson, J., Domingos, R.F., Wilkinson, K.J., Tufenkji, N. (2009) Deposition of TiO_2 nanoparticles onto silica measured using a quartz crystal microbalance with dissipation monitoring. Langmuir. 25:6062-6069.

Ghisalberti, E.L., Godfrey, I.M. (1998) Application of nuclear magnetic resonance spectroscopy to the analysis of organic archaeological materials. Stud. Conserv. 43:215-230.

Greber G., Paschinger O. (1981) Silylderivate der cellulose. Das Papier 35:547-554.

Hansson, J-Å., Hartler, N. (1969) Sorption of hemicelluloses on cellulose fibres. Part 1. Sorption of xylans. Sven. Papperstidn. 72:521-530.

Hansson, J-Å. (1970) Sorption of hemicelluloses on cellulose fibres. Part 3. The temperature dependence on sorption of birch xylan and pine glucomannan at kraft pulping conditions. Sven. Papperstidn. 73:49-53.

Hult, E-L., Larsson, P.T., Iversen, T. (2000) A comparative CP/MAS ^{13}CNMR study of cellulose structure in spruce wood and kraft pulp. Cellulose. 7:35-55.

Janzon, R., Puls, J., Saake, B. (2006) Upgrading of paper-grade pulps to dissolving pulps by nitren extraction: optimization of extraction parameters and application to different pulps. Holzforschung. 60:347-354.

Kleppe, P. (1970) Kraft pulping. Tappi. 53:35-47.

Kontturi, E., Thune, P.C., Niemantsverdriet, J.W. (2005) Trimethylsilylcellulose/polystyrene blends as a means to construct cellulose domains on cellulose. Macromolecules. 38:10712-10720.

Kontturi, K.S., Tammelin,T., Johansson, L.-S. Stenius, P. (2008) Adsorption of cationic starch on cellulose studied by QCM-D. Langmuir. 24:4743-4749.

Kontturi, E., Suchy, M., Penttilä, P., Jean, B., Pirkkalainen, K., Torkkeli, M., Serimaa, R. (2011) Amorphous characteristics of an ultrathin cellulose film. Biomacromolecules. 12:770-777.

Korolkov, V.V., Summerfield, A., Murphy, A., Amabilino, D.B., Watanabe, K., Taniguchi, T., Beton, P. (2019) Ultra-high resolution imaging of thin films and single strands of polythiophene using atomic force microscopy. Nat Commun. 10:1537-1545.

Krogerus, B., Fuhrmann, A. (2009) Isolation of xylan and use as wet end- and binder chemical. In: Conference proceedings from the 15th International Symposium on Wood, Fibre and Pulping Chemistry, Norway. pp-110.

Laine, C., Kemppainen, K., Kuutti, L., Varhimo, A., Asikainen, S., Grönroos, A., Määttänen, M., Buchert, J., Harlin, A. (2015) Extraction of xylan from wood pulp and brewer's spent grain, Ind. Crop. Prod. 70:231-237.

Lambert, J.B., Shawl, C.E., Stearns, J.A. (2000) Nuclear magnetic resonance in archaeology. Chem. Soc. Rev. 29:175-182.

Larsson, P.T., Wickholm, K., Iversen, T. (1997) A CP/MAS ^{13}C NMR investigation of molecular ordering in celluloses. Carbohydr. Res. 302:19-25.

Larsson, P.T., Hult, E-L., Wickholm, K., Pettersson, E., Iversen, T. (1999) CP/MAS ^{13}C-NMR spectroscopy applied to structure and interaction studies on cellulose I. Solid State Nucl. Magnet. Resonan. 15:31-40.

Li, J., Zhang, H., Duan, C., Liu, Y., Ni, Y. (2015) Enhancing hemicelluloses removal from a softwood sulfite pulp. Bioresour. Technol. 192:11-16.

Linder, A., Bergman, R., Bodin, A., Gatenholm, P. (2003) Mechanism of assembly of xylan onto cellulose surfaces. Langmuir. 19:5072-5077.

Lindgren, T., Edlund, U., Iversen, T. (1995) A multivariate characterization of crystal transformations of cellulose. Cellulose. 2:273-288.

Maunu, S., Liitiä, T., Kauliomäki, S., Hortling, B., Sundquist, J. (2000) ^{13}C CPMAS NMR investigations of cellulose polymorphs in different pulps. Cellulose. 7:147-159.

Miao, Q., Chen, L., Huang, L., Tian, C., Zheng, L., Ni, Y., (2014) A process for enhancing the accessibility and reactivity of hardwood kraft-based dissolving pulp for viscose rayon production by cellulase treatment. Bioresour. Technol. 154:109-113.

Mitikka-Eklund, M. Sorption of xylans on cellulose fibers. University of Jyväskylä, Finland, 1996.

Mobarak, F., El-Ashawy, A.E., Fahmy, Y. (1973) Hemicelluloses as additive in papermaking. Part 2. The role of added hemicellulose in situ on paper properties. Cellulose Chem. Technol. 7:325-335.

Mocchiuttia, P., Galvána, M.V., Peresinb, M.S., Schnella, C.N., Zanuttinia, M.A. (2015) Complexes of xylan and synthetic polyelectrolytes. Characterization and adsorption onto high quality unbleached fibres. Carbohydr. Polym. 116:131-139.

Mocchiuttia, P., Schnella, C.N., Rossia, G.D., Peresinb, M.S., Zanuttinia, M.A., Galvána, M.V. (2016) Cationic and anionic polyelectrolyte complexes of xylan and chitosan. Interaction with lignocellulosic surfaces. Carbohydr. Polym. 150:89-98.

Mora, F., Ruel, K., Comtat, J., Joseleau, J.P. (1986) Aspects of native and redeposited xylans at the surface of cellulose microfibrils. Holzforschung. 40:85-91.

Newman, R.H., Hemmingson, J.A. (1990) Determination of the degree of cellulose crystallinity in wood by carbon-13 nuclear magnetic resonance spectroscopy. Holzforschung. 44:351-355.

Newman, R.H. (1992) Nuclear magnetic resonance study of spatial relationships between chemical components in wood cell walls. Holzforschung. 46:205-210.

Newman, R.H., Hemmingson, J.A., Suckling, I.D. (1993) Carbon-13 nuclear magnetic resonance studies of kraft pulping. Holzforschung. 47:234-238.

Newman, R.H. (1998) Evidence for assignment of ^{13}C NMR signals to cellulose crystallite surfaces in wood, pulp and isolated celluloses. Holzforschung. 52:157-159.

Paananen, A., Österberg, M., Rutland, M., Tammelin, T., Saarinen, T., Tappura, K., Stenius, P. (2004) Interaction between cellulose and xylan: an atomic force microscope and quartz crystal microbalance study. In: Hemicelluloses: Science and technology. ACS Symposium Series 864. Eds. Gatenholm P., Tenkanen M. pp. 269-290.

Pournou, A. (2008) Deterioration assessment of waterlogged archaeological lignocellulosic material via ^{13}C CP/MAS NMR. Archaeometry. 50:129-141.

Ribe, E., Wernersson, F., Theliander, H. (2009) Optimal industrial birch black liquor for xylan sorption. In: Tappi Engineering, Pulping and Environmental Conference, USA. 19.3

Rodahl, M., Höök, F., Krozer, A., Brzezinski, P., Kasemo, B. (1995) Quartz crystal microbalance setup for frequency and Q-factor measurements in gaseous and liquid environments. Rev. Sci. Instrum. 66:3924-3930.

Santonia, I., Calloneb, E., Sandaka, A., Sandaka, J., Dirèb, S. (2015) Solid-state NMR and IR characterization of wood polymer structure in relation to tree provenance. Carbohydr. Polym. 117:710-721.

Sauerbrey, G.Z. (1959) Verwendung von Schwingquarzen zur Wägung dünner Schichten und zur Mikrowägung. Physik. 155: 206.

Schaub M., Wenz G., Wegner G., Stein A., Klemm D. (1993) Ultrathin films of cellulose on silicon wafers. Adv. Mater. 5:919-922.

Schönberg, C., Oksanen, T., Suurnäkki, A., Kettunen, H., Buchert, J. (2001) The importance of xylan for the strength properties of spruce kraft fibres. Holzforscung. 55:639-644.

Sihtola, H., Blomberg, L. (1975) Hemicelluloses precipitated from steeping liquor in the viscose process as additives in papermaking. Cellul. Chem. and Technol. 9:555-560.

Simonson, R. (1963) The hemicellulose in the sulphate pulping process. I. Isolation of hemicellulose fractions from sulphate cooking liquors. Sven. Papperstidn. 66:839-845.

Simmons, T.J., Mortimer, J.C., Bernardinelli, O.D., Pöppler, A., Brown, S.P., Azevedo, E.R., Dupree, R., Dupree, P. (2016) Folding of xylan onto cellulose fibrils in plant cell walls revealed by solid-state NMR. Nat. Commun. 7:1-9.

Sjöström, E. Wood chemistry, fundamentals and applications. Academic Press, New York, 1981.

Sjöström, E., Enström, B. (1967) Characterization of acidic polysaccharides isolated from different pulps. Tappi. 50:32-36.

Soares, M.C.D.S.M. Métodos alternativos para deposição de xilanas em polpas de eucalipto. Universidade Federal de Viçosa, Brazil, 2009.

Srndovic, J.S. Interactions between wood polymers in wood cell walls and celulose/hemicellulose biocomposites. Chalmers University of Technology. Sweden, 2011.

Sundberg A., Sundberg K., Lillandt C., Holmbom B.R. (1996) Determination of hemicelluloses and pectins in wood and pulp fibres by acid methanolysis and gas chromatography, Nord Pulp Pap Res J. 11:216-219.

Tammelin, T., Saarinen, T., Österberg, M., Laine, J. (2006) Preparation of Langmuir/Blodgett-cellulose surfaces by using horizontal dipping procedure. Application for polyelectrolyte adsorption studies performed with QCM-D. Cellulose. 13:519-535.

Tammelin, T., Paananen, A. and Österberg, M. (2009) Hemicelluloses at interfaces: Some aspects on the interactions In: The Nanoscience and Technology of Renewable Biomaterials, Lucia, A. L. and Rojas, O.J. (Eds), Wiley- Blackwell Publishing Ltd, West Sussex, UK, 149-172.

Thio, B.J.R., Zhou, D., Keller, A.A. (2011) Influence of natural organic matter on the aggregation and deposition of titanium dioxide nanoparticles. J. Hazard. Mater. 189:556-563.

Timell, T.E. (1967) Recent progress in the chemistry of wood hemicelluloses. Wood Sci. Technol. 1:45-70.

Vaaler, D., Ljones, S., Ribe, E., Toven, K., Moe, S. (2002) Effects of hemicellulose stabilisation and raw material on the beatability of softwood kraft pulps. In: 7th EWLP, Finland. pp 147-150.

Van der Hart, D.L., Atalla, R.H. (1984) Studies of microstructures in native celluloses using solid-state ^{13}C NMR. Macromolecules. 17:1465-1472.

Wickholm, K., Larsson, P.T., Iversen, T. (1998) Assignment of noncrystalline forms in cellulose I by CP/MAS ^{13}C NMR spectroscopy. Carbohydr. Res. 312:123-129.

Yllner, S., Enström, B. (1956) Studies of the adsorption of xylan on cellulose fibers during the sulphate cook. Part 1. Sven. Papperstidn. 59:229-232.

PAPER 2: STUDY OF XYLAN ADSORPTION UNDER INDUSTRIAL CONDITIONS

Submetido para: **Nordic Pulp & Paper Research Journal**

ABSTRACT

The development of physical properties of bleached eucalyptus kraft pulp is typically based on refining process. However, many works have reported that chemical treatments are viable alternatives, as the xylan deposition. Among the chemical characteristics of eucalyptus pulp the hemicellulose content influences the development of physical properties. Specifically, xylan content shows potential to increase tensile index, reduce energy consumption in the refining process and decrease the drainability. Therefore, the purposes of this work are (a) to evaluate xylan deposition on eucalyptus kraft pulp under industrial conditions in oxygen delignification, as well as its stability along the production process; (b) to study the effects of xylan deposition on the pulp properties and on the fiber recycling process. Xylan deposition in the oxygen delignification stage showed to be technically viable, despite the higher sodium hydroxide consumption due to the acidic conditions of the cold extraction liquor. However, bleaching experiments indicated a xylan content decreasing throughout the bleaching sequence, meaning that the deposited xylan was still accessible for oxidation or hydrolysis reactions. Although a reduction on the drainability, an increasing in yield and improvement of physical properties were observed. The hornification phenomena were reduced by xylan deposition only in the first recycling cycle.

Keywords: bleachability, cellulose, deposition, oxygen delignification, xylan.

1. INTRODUCTION

Cellulose is the most abundant organic compound of the planet and the main structural component of the plant cells. It's a linear polysaccharide formed by β-D-glucopyranose units linked by β-1,4-glycosidic covalent bonds (Sjöström 1981). The native cellulose is formed by two crystalline allomorphs, Iα e Iβ, demonstrated by CPMAS ^{13}C NMR techniques. Those two allomorphs are different regarding crystalline structure, hydrogen bonds and molecular conformation (Atalla & Vanderhart 1984).

Hemicellulose, together with cellulose and pectin, are polysaccharides that form the cell wall of higher plants (Sjöström 1981). The hemicelluloses can be found both on the primary and secondary walls and, in a small amount, on the lamella. They are big groups of branched heteropolymers constituted by different monomers of pyranose and furanose in different proportions (Srndovic 2011; Timell 1967).

The hemicelluloses are amorphous polymers, without the tendency to form crystalline regions in their native forms on the fiber walls, providing fiber flexibility (Atalla et al. 1993).

Molecular dynamics simulations suggest multiple layers of xylan could envelop microfibrils (Li et al. 2015a), and reconstitution studies have revealed that xylan is able to crosslink microfibrils (Mikkelsen et al. 2015). It has been proposed that xylan might be able to hydrogen bond to the hydrophilic surfaces of cellulose through folding as a twofold helical screw (Busse-Wicher 2014; Busse-Wicher et al. 2016a; Bromley et al. 2013) and a threefold helical screw xylan in solution forms (Simmons et al. 2016).

Xylans are hemicelluloses easily removed by alkali solutions, due to its amorphous structure, with high amount of acid groups (Pedrazzi 2009).

The main sources to xylan extraction in a kraft pulp mill are wood chips, cooking liquors and bleached pulp (Axelsson et al. 1962; Simonson 1963; Dahlman et al. 2008; Sjöström & Enström 1967; Janzon et al. 2006; Krogerus & Furhmann 2009).

An increase in hemicelluloses content in the fiber wall can be achieved in two different ways: improving the retention of hemicelluloses in the fibers during the oxygen delignification process (Kleppe 1970) and conducting a

deposition process of dissolved hemicelluloses polymers onto the fiber (Yllner & Enström 1956; Aurell 1965; Dahlman et al. 2003).

Earlier studies of xylan sorption onto cellulose surfaces have reported first order kinetics. This indicates a physical process, with Van der Waals or hydrogen bonds interactions between the sorbed xylan and the cellulose substrate (Clayton & Phelps 1965; Mitikka-Eklund, 1996; Hansson 1970; Danielsson & Lindström 2005; Ribe et al. 2009; Mora et al. 1986). Others studies have reported the adsorption of xylan on the cellulose fibers as a relatively slow process, probably due to the molecular diffusion in the porous fiber wall (Clayton & Phelps 1965; Hansson 1970).

It has been demonstrated that strong hydrogen bonds are involved in the xylan retention during sorption-desorption experiments with hydrogen bond disruptors reagents (Mora et al. 1986). However, the hydrogen bonds formation between xylan and cellulose has been questioned. Previous studies affirm that if hydrogen bonds formation does occur the xylan layer on the cellulose surface should be flat and not swollen with water as observed in experiments using techniques as QCM-D (Quartz Crystal Microbalance with Dissipation). Besides that, it has been proposed that the driving force is a combination of entropy increasing, associated to the release of solvent molecules during the polymer adsorption, and the weak Van der Waals attraction. Since the xylan solubility in water is relatively low, even weak forces could promote substantial adsorption. Despite that, hydrogen bonds may be important for dried systems such as paper and market pulp (Paananen et al. 2004).

Others studies suggested that xylan exists both as single molecules in aqueous solution and as aggregates in the colloidal size. The aggregates formation is provided by the interaction of unsubstituted regions of the xylan chain and by the hydrophobic interaction due to lignin residues covalently bonded to xylan. Consequently, the adsorption on the cellulose surface happens through single molecules and aggregates. This mechanism is, probably, more relevant for systems where the xylan solubility is lower (Linder et al. 2003; Mora et al. 1986). The aggregation of xylan into clusters reduces its solubility, and aggregates are reported to be preferably sorbed even though molecular xylan also adsorbs to cellulose surfaces. This might be due to strong

self-association between xylan molecules in solution (Henriksson & Gatenholm 2001; Linder et al. 2003)

The xylan adsorption is considered irreversible and only small amounts are removed by dilution (Paananen et al. 2004) or water washing (Eriksson et al. 1963). The exposure to alkaline conditions under high temperatures increases the desorption rate (Hansson & Hartler 1969).

However, it has been reported that adsorbed xylan from cold caustic extraction liquors is kept on the cellulose surface even after the oxygen delignification process or bleaching sequences (Dahlman et al. 2003; Soares 2009).

The interest of the paper industry over the xylan content of cellulose pulps is based on the carboxylic groups which are introduced in the cellulose fibers by xylan (Kleppe 1970). Xylan have carboxylic acid groups that increase the amount of negatively charged fibrils, thereby increasing the number and quality of hydrogen bonds between them (Laine & Stenius 1997; Winuprasith & Suphantharika 2013). Low pKa values of carboxylic acids are present in xylan-like hemicelluloses, around 3.13 for 4-O-methylglycuronic acid and 3.03 for hexenuronic acids (Teleman et al. 1995), compared to hydroxyl groups of cellulose and hemicelluloses, pKa 13.0-14.0 (Saric & Schofield 1946; Rydholm 1965; Burkinshaw 2016), greatly favor hydrogen bonds and water retention by fibers. Therefore, fibers with high xylan content get swollen easily, exposing a higher superficial area, increasing the active sites for the fiber reactions (Eriksson & Sjöström 1968; Mobarak et al. 1973), which provides to pulp the tensile properties increasing (Sihtola & Blomberg 1975; Schömberg et al. 2001) and the energy consumption decreasing during the refining process (Aurell 1965; Mobarak et al. 1973; Vaaler et al. 2002).

It has also been found that an increase in hemicelluloses content in the fibers decreases hornification during pulp drying (Köhnke & Gatenholm 2007; Köhnke et al. 2010). On the other hand, a negative effect in the tear index is often observed as the amount of xylan increases.

The purposes of this work were (a) to evaluate xylan deposition on eucalyptus kraft pulp under industrial conditions in oxygen delignification stage, as well as its stability along the production process; (b) to study the effects of xylan deposition on the pulp properties and on the recycling process.

2. MATERIAL AND METHODS

For the cooking experiments 150 kg of eucalyptus chip samples were collected after the screening system. The samples were classified in 4 and 6 mm sieves.

The chip samples were kept in controlled conditions of moisture (50 ± 2%) and temperature (23 ± 1 ºC) for 24 hours.

Cooking curves were performed to determine alkali charge required for the different target kappa numbers. Those conditions were used for further cooking experiments, as shown in Table 1.

Table 1. Laboratory cooking conditions.

Temperature	160 °C
White liquor/chips	3:1
Total time	170 min
Sulfidity	30%

For the xylan extraction it was used a Cold Caustic Extraction (CCE) method (Soares 2009) from eucalypt bleached kraft pulp using 240 g of NaOH for 300 g of oven dried pulp with 10% of consistency, for 30 minutes at 25 ºC. The suspension was centrifuged and the liquid phase stored as “xylan liquor”.

After the caustic extraction, the xylan content in the pulp samples was reduced from 14.8% to 3.9%.

Xylan was deposited onto pulp samples during the oxygen delignification process in a laboratory equipment simulating the industrial process conditions, showed in Table 2. A sample of 1500 mL of xylan liquor was used after pH adjustment to 5.0 using concentrated sulfuric acid.

Table 2. Laboratory oxygen delignification conditions.

Pressure reactor	4.16 kgf cm^{-2}
O_2 charge	20 kg t^{-1}
Alkaly charge	10, 20 and 30 kg t^{-1}
Time	30 and 60 minutes
Temperature	85, 95 and 105 ºC

The bleaching study was divided in two steps: oxygen delignification and bleaching sequence of the samples with xylan deposition and samples without xylan deposition, according to the conditions shown in Table 3.

Table 3. Bleaching conditions in laboratory.

Stages	OO		D0	(EP)	D1	P
Time (min)	23	31	113	105	222	120
Temperature (ºC)	95	100	75	80	80	80
Consistency (%)	10		10	10	10	10
pH	10.5		3.5	10.8	5.5	10.2

The bleaching sequence was run out in steam bath after tests to find sulfuric acid and sodium hydroxide consumptions required to reach the target pH in the end of each stage.

The chemicals load used to reach 89% ISO brightness are shown in Table 4 for each bleaching stage.

Table 4. Chemical loads in bleaching trials.

Sample/Kappa		Chemical Load (Kg Adt^{-1})									
		OO		D0		(EP)		D1		P	
		NaOH	O_2	NaOH	ClO_2	NaOH	H_2O_2	NaOH	ClO_2	NaOH	H_2O_2
Reference	14	10.1	15.4	2.8	17.2	11.1	3.0	2.1	4.0	2.1	3.0
	16	11.0	17.7	2.8	19.7	11.5	3.0	2.1	4.1	2.3	3.0
	18	12.0	19.7	2.8	21.3	11.5	3.0	2.1	4.1	2.2	3.0
Xylan	14	19.3	15.4	2.7	17.6	6.9	3.0	1.9	2.9	2.4	3.0
	16	19.9	17.7	2.6	20.2	6.9	3.0	1.9	3.7	2.6	3.0
	18	20.8	19.7	2.3	20.8	8.3	3.0	2.0	4.1	2.2	3.0

After each bleaching stage pulp samples were analyzed in brightness, brightness reversion after P, viscosity, ash content, pentosan content, drainability (Freeness and Schopper Riegler), refinability and pulp strength, optical and anatomical properties.

In order to simulate the hornification effect, caused by recycling process, pulp samples, “reference” (without any treatment), “deposition” (after xylan deposition) and “extracted” (samples from which the xylan were extracted), were dried in an oven for 60 minutes at 60 ºC, then were dampened and disintegrated five times. After each cycle, pulp drainability was evaluated (Freeness).

The experiments results were statistically evaluated for the 95% confidence interval in ANOVA Factorial design, and the means were compared using TUKEY orthogonal contrast also at 95% confidence.

3. RESULTS AND DISCUSSION

The results for pulp properties and bleaching showed a high similarity among the different conditions for kappa value, temperature and retention time after the statistics analyzes of cooking and oxygen delignification trials, in a 95% confidence interval. Therefore, all the results were discussed based on “reference samples” and “deposition samples”, representing the samples before and after the xylan deposition, respectively.

The effect of oxygen delignification stage on the pulp viscosity, showed in Figure 1b, was expected. This stage has a low selectivity, decreasing the polymerization degree due to cleavage reaction during the oxidation of hydroxyl groups to carbonyl (Colodette & Martino 2015). It was also noticed that the lower kappa value, the lower is the viscosity loss due to the milder conditions of oxygen delignification required for a lower lignin content.

Due to the acidic characteristic of the xylan liquor, a higher consumption of alkali was demanded to reach the desired final pH, 70 to 90% higher than the reference, shown in Figure 1a, causing a significant viscosity drop for all kappa conditions. Besides, is possible to notice the kappa effect on the NaOH consumption due to the higher lignin content for the higher kappa conditions, as expected.

The oxygen delignification results indicated an increase in yield (Figure 1d) and in pentosans content (Figure 1c) after the xylan deposition process, confirming the adsorption of xylan onto cellulose fiber, independently of the alkali charge, since the yield results did not present statistically significant

differences for a confidence interval of 95% and pentosan results were similar for all the kappa conditions.

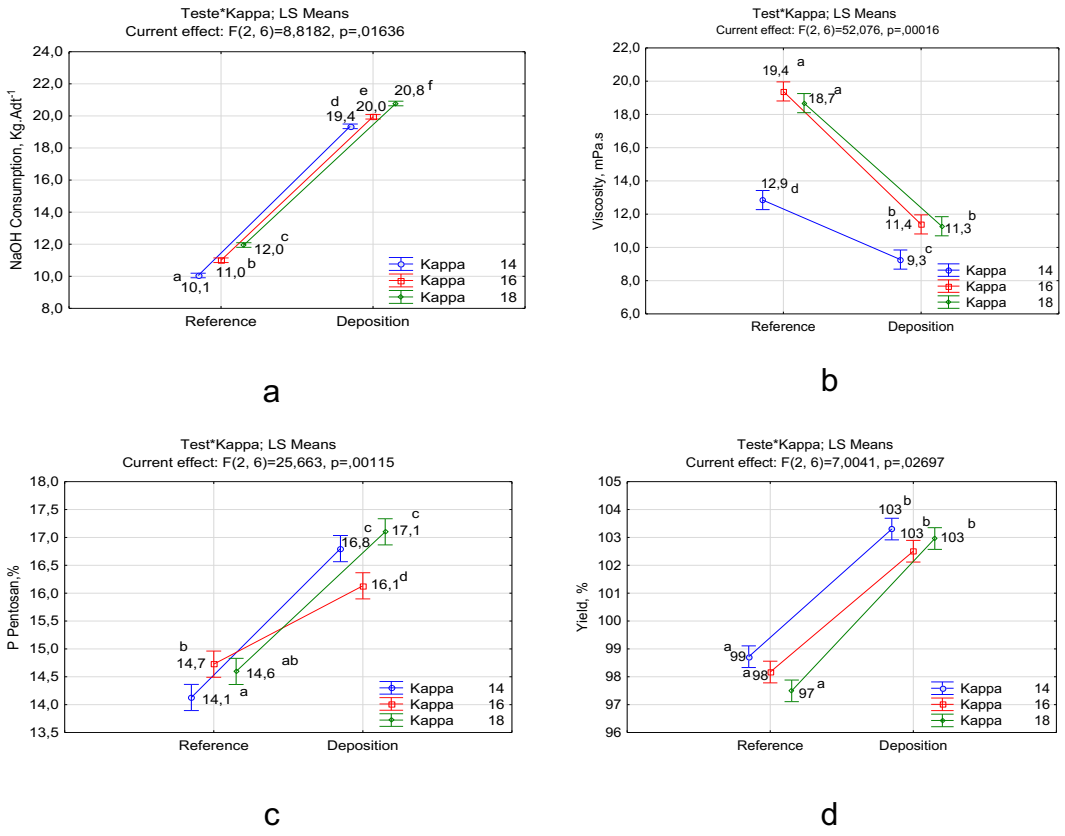

Figure 1. Oxygen delignification experiments. Vertical bars denote 0.95 confidence intervals. Same letters denote groups without statistically significant differences.

The results of the bleaching experiments, Figure 2b, indicated a xylan decrease throughout the bleaching sequence, which means that the deposited xylan is still accessible for oxidation or hydrolysis reactions, contradicting previous studies (Dahlman et al. 2003; Soares 2009). Since the extraction method uses a high load of NaOH, comparing to the mass of pulp, it is expected that the xylan solution will be formed by a large range of xylan fragments and other carbohydrates, with different molecular masses and solubilities, which might explain this behavior.

Pulps with xylan deposition showed no significant difference ($p>0.05$) for chlorine dioxide consumption (Figure 2a). The kappa value had a stronger effect on the chlorine dioxide consumption than the xylan content.

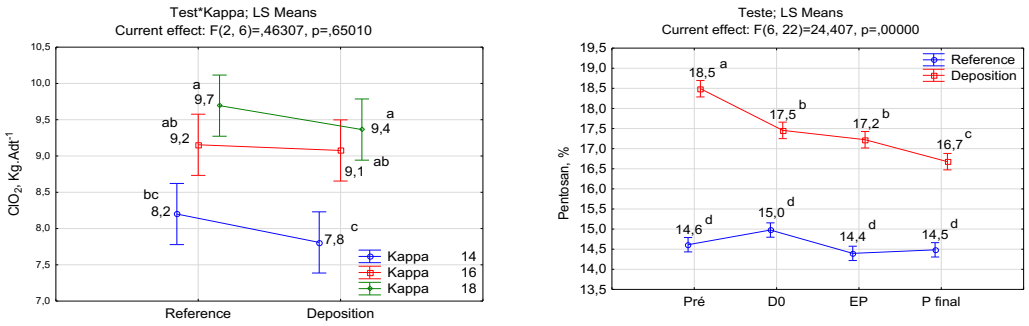

a b

Figure 2. Bleaching experiments. Vertical bars denote 0.95 confidence intervals. Same letters denote groups without statistically significant differences.

The increase in xylan content affected significantly the pulp properties such as drainability, tensile index, tear index and, specially, energy consumption, confirming the results obtained in previous studies (Sihtola & Blomberg 1975; Schömberg et al. 2001; Aurell 1965; Mobarak et al. 1973; Vaaler et al. 2002). No effects on the light scattering and opacity were observed, not showed in this paper, which was expected, since the improvement in the physical properties caused by fiber swollen do not provide optical changes. The tendency of tensile index improvement is clear (Figure 3c) due to the stronger interactions between fibers promoted by xylan. This effect was previously shown by many researchers.

Pulps with high xylan content showed higher water interactions, since it is a hydrophilic compound, as can be observed in Schopper results of Figure 3b. Therefore, the steam consumption in the drying process in the pulp mill should be higher for the xylan enriched pulps.

The tear index results (Figure 3d) showed a tendency to decrease the resistance, which might be explained by the lower fiber content, comparing to a pulp sample with lower xylan content. Since the analytical method uses the same amount of pulp sample to make the sheets, the fiber content, responsible for tear resistance, is lower in the xylan enriched samples.

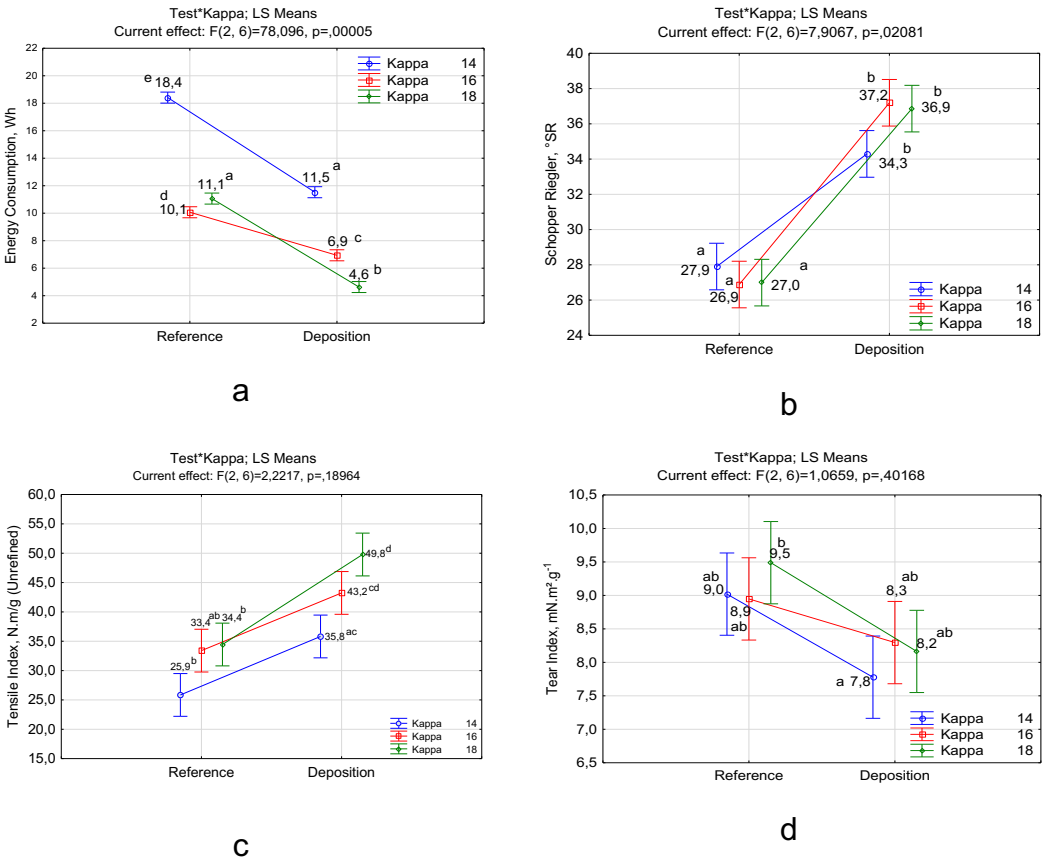

Figure 3. Properties of non-refined pulps. Vertical bars denote 0.95 confidence intervals. Same letters denote groups without statistically significant differences.

The relationship between the hemicellulose content and pulp refinability is positive, the higher is the hemicellulose content the higher is the fibers flexibility and the better is the bond among them. The fibers walls become more plastic and flexible, the interaction with water molecules is improved and the microfibrils become exposed to the refining process (Eriksson & Sjöström 1968; Mobarak et al. 1973). Therefore, pulps with higher hemicellulose contents will reach the refining level faster and can be associated with lower energy consumption (Figure 3a).

The results of the refining experiments confirmed the better refinability of xylan enriched pulps (Figure 4a). The refining level of 35 ºSR is important for printing & writing paper grade and 20 ºSR is commonly used for tissue paper producers.

The results showed an energy consumption from 60 to 90% lower for the xylan enriched samples compared to reference samples (Figure 4a). However, the samples with xylan deposition showed a lower tensile (Figure 4b) and air

resistance (Figure 4c) indexes than the samples without xylan, due to the lower refining exposure, since the refining process was set up to 35 ºSR, i.e. the intensity of refining was sufficient to achieve the desired drainability but not to cause the fibrillation required for an increase of resistance. In general, kappa value conditions showed a weak influence on the discussed properties, except for energy consumption of kappa 14 samples, which had the highest xylan content.

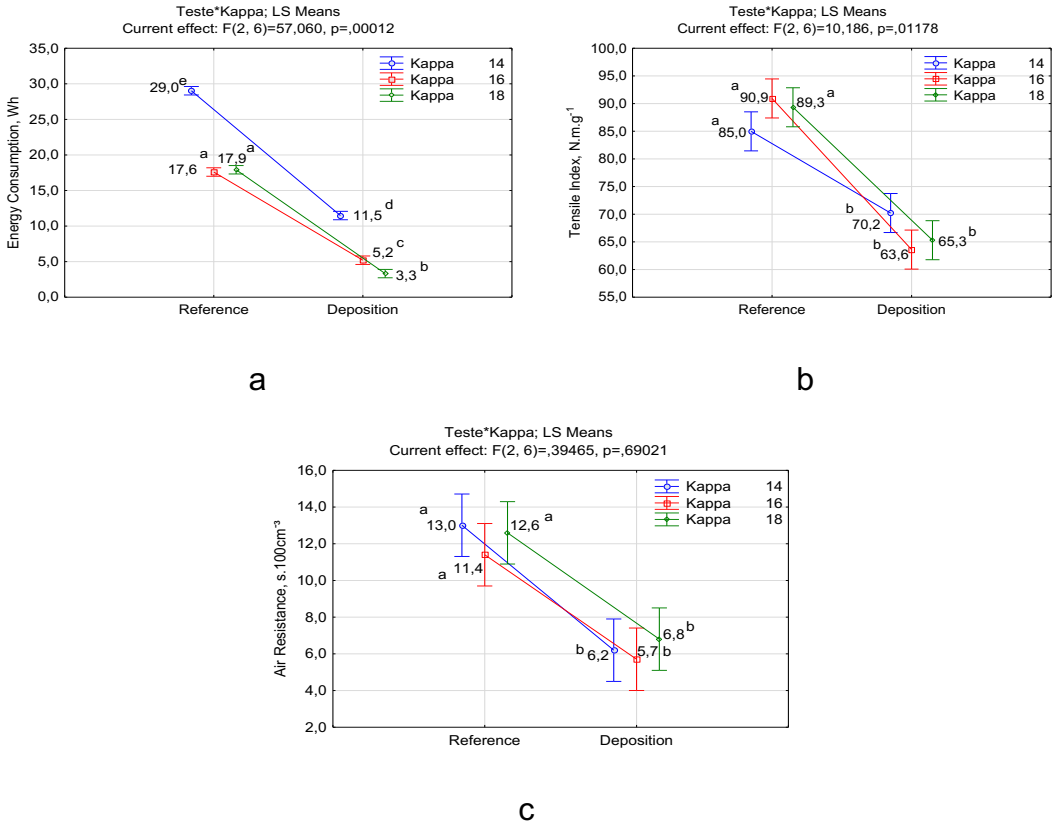

Figure 4. Pulp properties refined to 35 ºSR. Vertical bars denote 0.95 confidence intervals. Same letters denote groups without statistically significant differences.

Figure 5 shows the results of refining for Tensile Index 70 N m g^{-1}. The same behavior of the xylan enriched samples was observed, providing an energy consumption from 30 to 50% lower than the reference samples (Figure 5a) and lower drainability (Figure 5b). No effects on air resistance were observed (Figure 5c), probably due to the lower refining exposure. The same effect was observed on the energy consumption for kappa 14 samples.

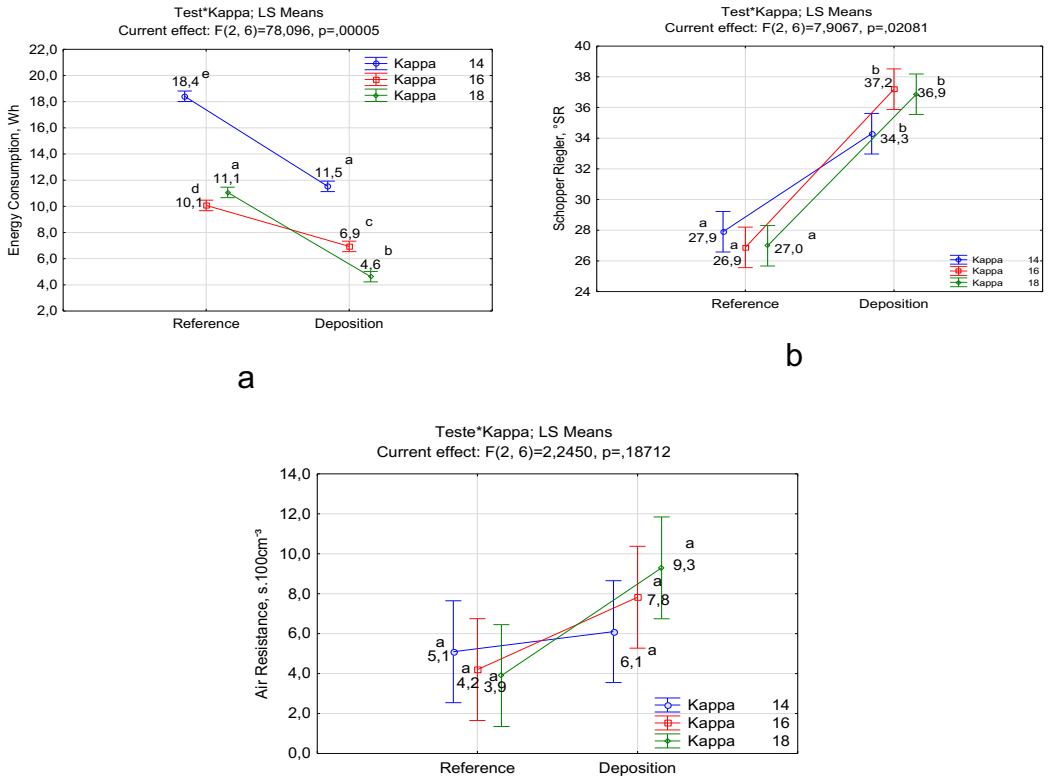

Figure 5. Pulp properties refined to tensile index 70 N m g^{-1}. Vertical bars denote 0.95 confidence intervals. Same letters denote groups without statistically significant differences.

Drying generates inter-fibrillar bonding, which closes pore spaces and decreases the elasticity of the fiber wall, both resulting in a lower fiber swelling (Köhnke et al. 2010). It has also been found that an increase in hemicelluloses content in the fibers decreases hornification during drying (Köhnke & Gatenholm 2007).

A strong relationship between xylan content and pulp drainability can be observed in Figure 6, since the extracted samples (ES) showed the highest CSF results compared to the reference (REF) and deposition (DEP) samples, which had natural xylan and enriched xylan respectively.

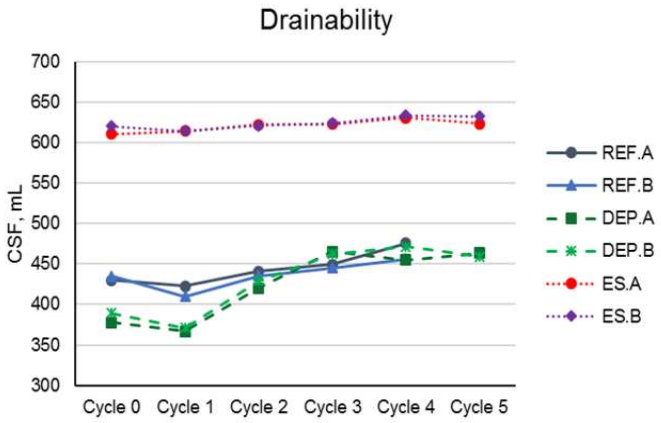

Figure 6. Pulp drainability during recycling simulation trial.

A low drainability showed by the deposition samples in the first cycle, suggested a higher water content linked with xylan. However, it was possible to observe, a tendency to drainability stabilization, getting close to the reference samples, after the second cycle. It probably indicates a xylan solubility after the second cycle.

4. CONCLUSIONS

Xylan deposition in the oxygen delignification stage proved to be technically viable for pulp mills. However, bleaching experiments indicated a xylan content decrease throughout the bleaching sequence, meaning that the deposited xylan was still accessible for oxidation or hydrolysis reactions. An increase in yield and improvements in physical properties, such as tensile index and energy consumption were observed. Optical properties were not affected by the xylan content of the pulp.

The use of xylan liquor in acid conditions increased significantly the sodium hydroxide consumption of the oxygen delignification stage.

It was possible to observe a strong relationship between xylan content and pulp drainability during the recycling and hornification simulation. However, there was a tendency to drainability stabilization after the second cycle. It probably indicates a xylan solubility.

Aknowledgements: The authors thank to Celulose Nipo-Brasileira S.A – CENIBRA, for the supporting to this research and to CNPq, CAPES and FAPEMIG.

5. REFERENCES

Atalla, R. H., Vanderhart, D. L. (1984) Native cellulose: A composite of 2 distinct crystalline forms. Science. 223:283−285.

Atalla, R.H., Hackney, J.M., Uhlin, I., Thompson, N.S. (1993) Hemicelluloses as structure regulators in the aggregation of native cellulose. Int. J. Biol. Macromol. 15:109-112.

Aurell, R. (1965) Increasing kraft pulp yield by redeposition of hemicelluloses. Tappi. 48:80-84.

Axelsson, S., Croon, I., Enström, B. (1962) Dissolution of hemicelluloses during sulphate pulping. Svensk Papperstidning. 65:693-697.

Bromley, J.R., Busse-Wicher, M., Tryfona, T., Mortimer, J.C., Zhang, Z., Brown, D.M., Dupree, P. (2013) GUX1 and GUX2 glucuronyltransferases decorate distinct domains of glucuronoxylan with different substitution patterns. Plant J. 74:423-434.

Burkinshaw, S.M. (2016) Physico-chemical Aspects of Textile Coloration. West Yorkshire: John Wiley & Sons. v. 53.

Busse-Wicher, M., Gomes, T.C.F., Tryfona, T., Nikolovski, N., Stott, K., Grantham, N.J., Bolam, D.N., Skaf, M.S., Dupree, P. (2014) The pattern of xylan acetylation suggests xylan may interact with cellulose microfibrils as a twofold helical screw in the secondary plant cell wall of *Arabidopsis thaliana*. Plant J. 79:492-506.

Busse-Wicher, M., Li, A., Silveira, R.L., Pereira, C.S., Tryfona, T., Gomes, T.C.F., Skaf, M.S., Dupree, P. (2016a) Evolution of xylan substitution patterns in gymnosperms and angiosperms: implications for xylan interaction with cellulose. Plant Physiol. 171:2418-2431.

Clayton, D.W., Phelps, G.R. (1965) The sorption of glucomannan and xylan on α-cellulose wood fibres. J. Polym. Sci. 11:197-220.

Colodette, J.L., Martino, D.C. (2015) Oxygen Delignification. In: Pulp Bleaching. Eds. Colodette, J.L., Gomes, F.J.B. Editora UFV, Viçosa, pp. 269-312.

Dahlman, O., Jensen, A., Tormund, D., Östlund, J. (2008) Processing of xylan from hardwood spent cooking liquors. In: Conference proceedings from the Nordic Wood Biorefinery Conference, Sweden, pp 114-119.

Dahlman, O., Sjöberg, J., Jansson, U.B., Larsson, P.O. (2003) Effects of surface hardwood xylan on the quality of softwood pulps. Nordic Pulp Paper Res. J. 18:310-315.

Danielsson, S., Lindström, M.E. (2005) Influence of birch xylan adsorption during kraft cooking on softwood pulp strength. Nordic Pulp Paper Res. J. 20:436-441.

Eriksson, E., Sjöström, E. (1968) Influence of acidic groups on the physical properties of high-yield pulps. Tappi. 51:56-59.

Hansson, J-Å., Hartler, N. (1969) Sorption of hemicelluloses on cellulose fibres. Part 1. Sorption of xylans. Svensk Pappertidning. 72:521-530.

Hansson, J-Å. (1970) Sorption of hemicelluloses on cellulose fibres. Part 3. The temperature dependence on sorption of birch xylan and pine glucomannan at kraft pulping conditions. Svensk Papperstidning. 73:49-53.

Henriksson, A., Gatenholm, P. (2001) Controlled assembly of glucuronoxylans onto cellulose fibers. Holzforschung. 55:494-502.

Janzon, R., Puls, J., Saake, B. (2006) Upgrading of paper-grade pulps to dissolving pulps by nitren extraction: optimization of extraction parameters and application to different pulps. Holzforschung. 60:347-354.

Kleppe, P. (1970) Kraft pulping. Tappi. 53:35-47.

Köhnke, T., and Gatenholm, P. (2007) The effect of controlled glucuronoxylan adsorption on drying-induced strength loss of bleached softwood pulp. Nordic Pulp Paper Res. J. 22:508-515.

Köhnke, T., Lund, K., Brelid, H., and Westmannd, G. (2010) Kraft pulp hornification: A closer look at the preventive effect gained by glucuronoxylan adsorption. Carbohydr. Polym. 81:226-233.

Krogerus, B., Fuhrmann, A. (2009) Isolation of xylan and use as wet end- and binder chemical. In: Conference proceedings from the 15th International Symposium on Wood, Fibre and Pulping Chemistry, Norway. pp-110.

Laine, J., Stenius, P. (1997) Effect of charge on the fibre and paper properties of bleached industrial kraft pulps. Pap. Puu-Pap. Tim. 70:257-266.

Li, L., Perre, P., Frank, X., Mazeau, K. (2015a) A coarse-grain force-field for xylan and its interaction with cellulose. Carbohydr. Polym. 127:438-450.

Linder, A., Bergman, R., Bodin, A., Gatenholm, P. (2003) Mechanism of assembly of xylan onto cellulose surfaces. Langmuir. 19:5072-5077.

Mikkelsen, D., Flanagan, B.M., Wilson, S.M., Bacic, A., Gidley, M.J. (2015) Interactions of arabinoxylan and (1,3)(1,4)-β-glucan with cellulose networks. Biomacromolecules. 16:1232-1239.

Mitikka-Eklund, M. Sorption of xylans on cellulose fibers. University of Jyväskylä, Finland, 1996.

Mobarak, F., El-Ashawy, A.E., Fahmy, Y. (1973) Hemicelluloses as additive in papermaking. Part 2. The role of added hemicellulose in situ on paper properties. Cellulose Chem. Technol. 7:325-335.

Mora, F., Ruel, K., Comtat, J., Joseleau, J.P. (1986) Aspects of native and redeposited xylans at the surface of cellulose microfibrils. Holzforschung. 40:85-91.

Paananen, A., Österberg, M., Rutland, M., Tammelin, T., Saarinen, T., Tappura, K., Stenius, P. (2004) Interaction between cellulose and xylan: an atomic force microscope and quartz crystal microbalance study. In: Hemicelluloses: Science and technology. ACS Symposium Series 864. Eds. Gatenholm P., Tenkanen M. pp. 269-290.

Pedrazzi, C. Influência das xilanas na produção e nas propriedades de polpas de eucalipto para papéis. Universidade Federal de Viçosa, Brazil, 2009.

Ribe, E., Wernersson, F., Theliander, H. (2009) Optimal industrial birch black liquor for xylan sorption. In: Tappi Engineering, Pulping and Environmental Conference, USA. 19.3.

Rydholm, S.A. (1965) Pulping processes. London: Interscience. 1269 p.

Saric, S.P., Schofield, R.K. (1946) The dissociation constants of the carboxyl and hydroxyl groups in some insoluble and sol-forming polysaccharides. Proc. R. Soc. Lon. Ser-A. 1003:431-447.

Schömberg, C., Oksanem, T., Suurnäkki, A., Kettunem, H., Bucghert, J. (2001) The importance of xylan for the strength properties of spruce kraft fibres. Holzforscung. 55:639-644.

Sihtola, H., Blomberg, L. (1975) Hemicelluloses precipitated from steeping liquor in the viscose process as additives in papermaking. Cellul. Chem. and Technol. 9:555-560.

Simmons, T.J., Mortimer, J.C., Bernardinelli, O.D., Pöppler, A., Brown, S.P., Azevedo, E.R., Dupree, R., Dupree, P. (2016) Folding of xylan onto cellulose fibrils in plant cell walls revealed by solid-state NMR. Nat. Commun. 7:1-9.

Simonson, R. (1963) The hemicellulose in the sulphate pulping process. I. Isolation of hemicellulose fractions from sulphate cooking liquors. Svensk Papperstidning. 66:839-845.

Sjöström, E. Wood chemistry, fundamentals and applications. Academic Press, New York, 1981.

Sjöström, E., Enström, B. (1967) Characterization of acidic polysaccharides isolated from different pulps. Tappi. 50:32-36.

Soares, M.C.D.S.M. Métodos alternativos para deposição de xilanas em polpas de eucalipto. Universidade Federal de Viçosa, Brazil, 2009.

Srndovic, J.S. Interactions between wood polymers in wood cell walls and celulose/hemicellulose biocomposites. Chalmers University of Technology. Sweden, 2011.

Teleman, A., Harjunpää, V., Tenkanen, M., Buchert, J., Hausalo, T., Drakenberg, T., Vuorinen, T. (1995) Characterisation of 4-deoxy-β-L-enopyranosyluronic acid attached to xylan in pine Kraft pulp and pulping liquor by 1H and 13C NMR spectroscopy. Carbohydr. Res. 272:55-71, (1995)

Timell, T.E. (1967) Recent progress in the chemistry of wood hemicelluloses. Wood Sci. Technol. 1:45-70.

Vaaler, D., Ljones, S., Ribe, E., Toven, K., Moe, S. (2002) Effects of hemicellulose stabilisation and raw material on the beatability of softwood kraft pulps. In: 7th EWLP, Finland. pp 147-150.

Yllner, S., Enström, B. (1956) Studies of the adsorption of xylan on cellulose fibers during the sulphate cook. Part 1. Svensk Papperstidning. 59:229-232.

Winuprasitha, T., Suphantharik, M. (2013) Microfibrillated cellulose from mangosteen (Garcinia mangostana L.) rind: Preparation, characterization, and evaluation as an emulsion stabilizer. Food Hydrocoll. 32:383-394.

PAPER 3: ALTERNATIVES FOR XYLAN DEPOSITION UNDER INDUSTRIAL CONDITIONS

Será submetido para: **Journal of Wood Chemistry and Technology**

ABSTRACT

The development of physical properties of bleached eucalyptus kraft pulp is typically based on the refining process. However, several works reported that chemical treatments are viable alternatives, as the xylan deposition. Specifically, xylan content shows potential to increase tensile index, reduce refining energy consumption and decrease drainability. This work studied the effect of NaOH load and temperature on the xylan extraction efficiency of bleached eucalyptus kraft pulp and evaluated the effects of xylan deposition under industrial conditions in the oxygen delignification and bleaching stages. Xylan deposition showed to be technically viable, despite the high sodium hydroxide consumption in all the stages and ClO_2 consumption increase in D1 stage. The best results for tensile index and energy consumption were obtained in oxygen delignification stage. The experiments in D1 and EP stages confirmed the tendency to decrease the energy consumption after xylan deposition.

Keywords: bleaching, cellulose, deposition, xylan.

1. INTRODUCTION

Cellulose is the most abundant organic compound of the planet and the main structural component of the plant cells. It is a linear polysaccharide formed by β-D-glucopyranose units linked by β-1,4-glycosidic covalent bonds (Sjöström 1981). The native cellulose is formed by two crystalline allomorphs, Iα e Iβ, demonstrated by CPMAS ^{13}C NMR techniques. Those two allomorphs are different regarding crystalline structure, hydrogen bonds and molecular conformation (Atalla et al. 1984).

Hemicellulose, together with cellulose and pectin, are polysaccharides that forms the cell wall of higher plants (Sjöström 1981). The hemicelluloses can be found both on the primary and secondary cell walls and, in a small amount, on the lamella. There are big groups of branched heteropolymers constituted by different monomers of pyranose and furanose in different proportions (Srndovic 2011; Timell 1967).

The hemicelluloses are amorphous polymers, without showing the tendency to form crystalline regions in their native forms on the fiber walls, providing a higher flexibility (Atalla et al. 1993).

Molecular dynamics simulations suggest multiple layers of xylan could envelop microfibrils (Li et al. 2015a), and reconstitution studies have revealed that xylan is able to crosslink microfibrils (Mikkelsen et al. 2015). It has been proposed that xylan might be able to hydrogen bond to the hydrophilic surfaces of cellulose through folding as a twofold helical screw (Busse-Wicher 2014; Busse-Wicher et al. 2016a; Bromley et al. 2013) and a threefold helical screw xylan in solution forms (Simmons et al. 2016).

Xylans are hemicelluloses easily removed by alkali solutions, due to their amorphous structure, containing high amount of acid groups (Pedrazzi 2009).

Several methods have been reported in the literature for the hemicelluloses removal from the pulp such as hot and cold caustic extractions (David et al. 2010; Li et al. 2015b; Panthapulakkal et al. 2015, Panthapulakkal et al. 2013) and enzymatic hydrolysis. Mechanical pre-treatments are also proposed combined with other techniques (Gehmayr et al. 2011; Hakala et al. 2013; Panthapulakkal et al. 2015).

The hemicellulose alkaline extraction stage can be carried out either as a cold or a hot stage (Rydholm 1965). Cold Caustic Extraction (CCE), usually

takes place at a low pulp consistency, 3%, temperature below 40 ºC, retention time between 10 and 20 minutes and high sodium hydroxide concentration. Xylan can be removed almost completely from the pulp by an alkaline extraction at 25 ºC (Gomes 2011).

In the hot caustic extraction (HCE the NaOH concentration is not as high as in a cold alkali treatment, but the temperature is higher, usually between 80 ºC and 120 ºC. The retention time is in the range of 1 to 2 hours. Typical pulp consistencies are in the range of 10% and 15% (Syed et al. 2013).

A hot alkaline extraction stage can be assumed to be especially suitable for sulfite pulps due to the fact that the carbohydrates are not stabilized via peeling reactions during cooking at low pH. In a prehydrolyzed kraft pulp on the other hand, the carbohydrates are stabilized during the cooking and a further hot alkaline treatment is therefore not efficient (Syed et al. 2013).

The hemicellulose extraction process can be divided in three removal phases: bulk, transition and residual. In the bulk removal phase, the low-Mw hemicellulose fraction is removed from all the regions of the fiber wall. In the transition phase, the residual hemicelluloses are transferred from the inner region to the outer region. In the residual removal phase, the high-Mw hemicelluloses continue to be gradually removed (Li et al. 2017).

The cold caustic extraction (CCE) presents an industrial advantage over the other methods since the sodium hydroxide can be recovered or the liquor, product of the extraction processes, can be used in other steps of the pulp production (Li et al. 2017).

The main sources to xylan extraction in a kraft pulp mill are the wood chips, cooking liquors and the bleached pulp (Axelsson et al. 1962; Simonson 1963; Dahlman et al. 2008; Sjöström & Enström 1967; Janzon et al. 2006; Krogerus & Furhmann 2009).

An increase in the hemicellulose content in the fiber wall can be achieved in two different ways: improving the retention of hemicelluloses in the fibers during the oxygen delignification process (Kleppe 1970) or conducting a deposition process of dissolved hemicelluloses polymers onto the fiber (Yllner & Enström 1956; Aurell 1965; Dahlman et al. 2003).

Previous studies suggested that xylan exists both as single molecules in aqueous solution and as colloidal size aggregates. The aggregates formation

is provided by the interaction of unsubstituted regions of the xylan chain and by the hydrophobic interaction due to lignin residues covalently bonded to xylan. Consequently, the adsorption on the cellulose surface happens through single molecules and aggregates. This mechanism is, probably, more relevant for systems where the xylan solubility is lower (Linder et al. 2003; Mora et al. 1986).

The xylan adsorption is considered as irreversible and only small amounts are removed by dilution (Paananen et al. 2004) or water washing (Eriksson et al. 1963). Neverthless, it is well known that the exposure to alkaline conditions under high temperatures increases the desorption rate (Hansson & Hartler 1969). However, has been reported that adsorbed xylan from cold caustic extraction liquors is kept on the cellulose surface even after oxygen delignification process or bleaching sequences (Dahlman et al. 2003; Soares 2009).

The interest of the paper industry over the xylan content of cellulose pulps is based on the carboxylic groups which are introduced in the cellulose fibers by xylan (Kleppe 1970). Xylan has carboxylic acid groups that increase the amount of negatively charged fibrils, thereby increasing the number and quality of hydrogen bonds among them (Laine & Stenius 1997; Winuprasith & Suphantharika 2013). The low pKa values of carboxylic acids in xylan-like hemicelluloses, around 3.13 for 4-O-methylglycuronic acid and 3.03 for hexenuronic acids (Teleman et al. 1995), compared to hydroxyl groups of cellulose and hemicelluloses, pKa 13.0-14.0 (Saric & Schofield 1946; Rydholm 1965; Burkinshaw 2016), greatly favors hydrogen bonds and water retention by fibers. Therefore, fibers with high xylan content get swollen easily, exposing a higher superficial area, increasing the active sites for the fiber reactions (Eriksson & Sjöström 1968; Mobarak et al. 1973).

It has been reported that adsorbed xylan on pulp increases tensile properties of the paper (Sihtola & Blomberg 1975; Schömberg et al. 2001) and decreases the energy consumption during the refining process (Aurell 1965; Mobarak et al. 1973; Vaaler et al. 2002, Muguet et al. 2011). They may also prevent aggregation and hornification (Köhnke & Gatenholm 2007; Köhnke et al. 2010).

Several studies have been carried out to increase xylan content in pulp fibers, especially during the cooking process (Yllner & Enström 1956; Aurell 1965; Hansson & Hartler 1969; Danielsson & Lindström 2009). The dissolved xylan in the black liquor is thought to be precipitated onto the fibers (Yllner & Enström 1956) and this process improves both yield and tensile strength (Dahlman et al. 2003; Danielsson & Lindström 2005). Other workers have tried to increase pulp xylan content on a laboratory scale through xylan addition on bleached pulp (Köhnke & Gatenholm 2007). Xylan is deposited onto bleached pulps on both external surfaces and inner layers of the fiber (Mitikka-Eklund 1996; Schönberg et al. 2001).

Considering that the modern kraft pulping and bleaching processes are performed at high temperatures and in a large range of pH, it is really desirable to achieve alkaline extraction and xylan deposition in similar conditions of the industrial process.

This work study the effect of NaOH load and temperature on the xylan extraction efficiency from bleached eucalyptus kraft pulp and evaluate the effects of xylan deposition under industrial conditions in oxygen delignification and bleaching stages.

2. MATERIALS AND METHODS

2.1. Xylan extraction

Pulp samples from the final P (89% ISO) stage of a four-stages industrial bleaching sequence: D(EP)DP were used. Those samples were oven dried and consistency was measured.

Dried 300 g pulp samples, were transferred to a 4,000 mL becker and NaOH solutions with different concentrations were added to achieve 10% consistency pulp suspension which were stirred for 30 minutes at 25 ºC.

The same bleached pulp samples and the same stirring method were used in the temperature variation tests. However, the NaOH load was fixed in 240 g and temperature used were 25 and 60 ºC.

2.2. Xylan deposition in oxygen delignification and bleaching stages

For the xylan deposition experiments in the oxygen delignification stage was used a laboratory equipment simulating the industrial process conditions, according to Table 1. A sample of 1,500 mL of xylan extract was used, after pH adjustment to 5.0 using concentrated sulfuric acid, with 250 g of dried pulp.

Table 1. Laboratory oxygen delignification conditions.

Pressure	4.16 kgf cm^{-2}
O_2 charge	20 kg t^{-1}
Alkaly charge	10, 20 e 30 kg t^{-1}
Time	30 e 60 minutes
Temperature	85, 95 e 105 ºC

Pulp samples from an industrial (EP) (80% ISO) bleaching stage were used in the xylan deposition experiments. All the samples were bleached to 89% ISO at 10% consistency and 80 ºC using the same bleaching sequence as the industrial plant (DEPDP). The retention times were 222 and 120 minutes for D and P stages, respectively. The oxygen delignification and bleaching experiments were performed twice, including the reference samples without xylan deposition.

A sample of 1,500 mL of xylan extract was used, after pH adjustment to 5.0 using concentrated sulfuric acid, with 250 g of dried pulp for oxygen delignification and bleaching trials.

2.3. Refining experiments

The pulp samples, after oxygen delignification bleaching and xylan deposition were refined in a PFI mill at zero gap and 0, 750, 1,500 and 2,250 revolutions. Laboratory sheets (60 $g.m^{-2}$) were made for the physical tests for each refining level.

The following analysis were carried out: ºSR (Schopper Riegler), tensile index, #permanganate, pentosan, and viscosity for different pulp samples, accordingly to the reference methods showed in Table 2.

Table 2. Reference methods.

Analysis	Methods
ºSR	NBR 14031:2004
Tensile index	NBR NM ISO 1924-2:2012
#Permanganate	TAPPI UM 251-2013
Pentosan	NBR 6968:1998
Viscosity	NBR 7730:1998
Laboratory refining PFI	NBR 5264-2:2012

2.4. Statistics

The experiments results were statistically evaluated for the 95% confidence interval in ANOVA Factorial design, and the means were compared using TUKEY orthogonal contrast also at 95% confidence.

3. RESULTS AND DISCUSSION

3.1. Study of xylan extraction

Since the modern bleaching sequences end with hydrogen peroxide alkaline stages (P), an adequate point to install a xylan extraction stage would be right after it, before the dryer, due to the pulp quality, pH and pulp consistency. Besides that, in this point of the process, it is possible to avoid the undesirable effects on the brightness caused by xylan deposited with high lignin content, which is the case for the xylan extracted from black liquor.

Production cost is always a concern for pulp mills and sodium hydroxide represents one of the biggest costs. Considering that the xylan extraction methodology runs under high alkaline conditions, optimization is required to achieve the lower NaOH consumption. Several extractions were carried out under different NaOH loads and the pentosan content in the extracted pulp was analyzed. The results are showed in Figure 1

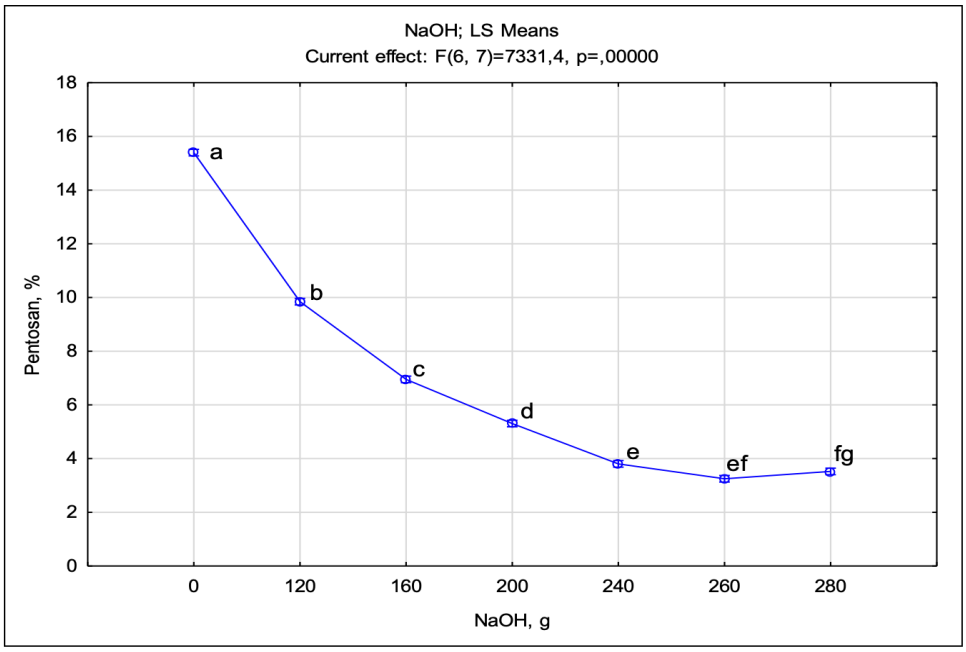

Figure 1. Pentosan of extracted pulp samples at different NaOH loads.

The 240g NaOH load showed similar results of pentosan reported for previous studies (Muguet 2011), achieving an optimum extraction efficiency. Higher loads from 240 g did not show significant differences for pentosan content. On the other hand, depending on the xylan content requirements, lower NaOH loads might be used in order to decrease the costs of the extraction process.

Considering that the bleaching reactions occur, typically, in temperatures around 80 ºC, it would be desirable that the xylan extraction was performed at higher temperatures than the cold caustic extraction methodology, 25 ºC. It is well known that xylan can be removed almost completely from the pulp by an alkaline extraction at 25 ºC (Wayman 1963; Gomes 2011). However, hot extraction would avoid chilling and heating of pulp current and steam consumption as well.

Therefore, two extraction trials were performed at different temperature conditions using the same NaOH load of 240 g per 300 g of pulp. The pentosan content was measured in the extracted pulps as showed in Figure 2.

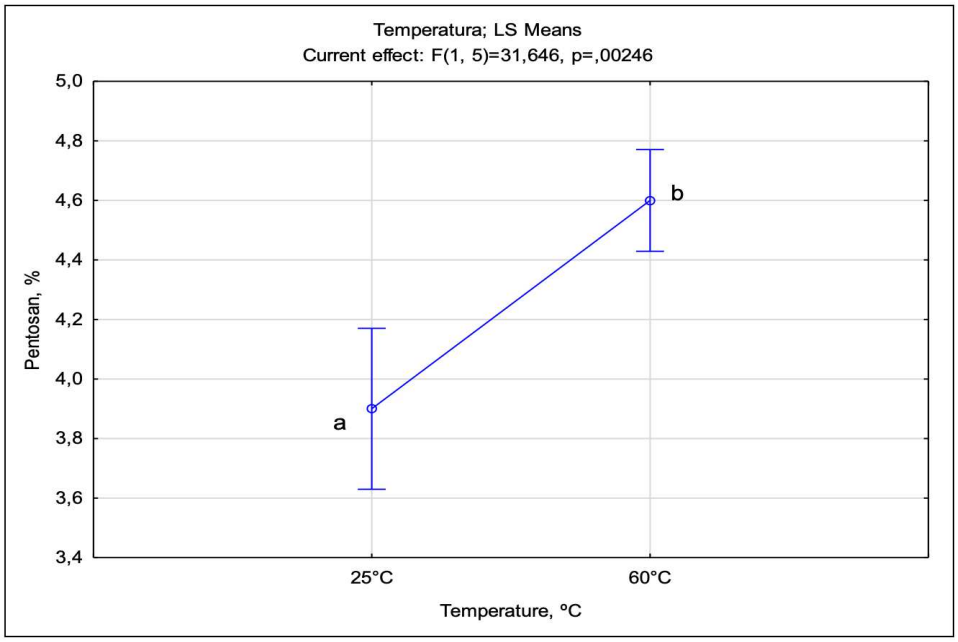

Figure 2. Pentosan of extracted pulp samples at different temperatures.

The extraction trial at 25 ºC showed a better result regarding xylan extraction efficiency. However, the extraction at 60 ºC, which is a more realistic condition for pulp mills, showed results similar to that at lower temperature. It means that hot extraction is a more economical alternative.

3.2. Xylan deposition in oxygen delignification and bleaching stages

The NaOH load has a strong influence to keep xylan in solution or in suspension (Syed 2013). However, the pH of xylan extract during the deposition trials is about 5.0, which probably induces the xylan deposition on the cellulose fibers due to the solubility reduction. The experiments of xylan deposition in the oxygen delignification stage showed promising results regarding xylan content increase and physical properties of the xylan enriched pulps. At this pH variation an increase in the NaOH of 81.3% was observed, showed in Table 3.

Table 3. Results of deposition in oxygen delignification stage.

Pulp Sample	NaOH (Kg Adt^{-1})	Viscosity (mPa s)	Pentosan (%)
Reference	11.1^{a}	27.9^{c}	14.6^{e}
Deposition	20.1^{b}	14.9^{d}	18.5^{f}

It was observed a pulp viscosity decrease after xylan deposition of 46.5%, which was expected, due to the higher NaOH consumption and lower polymerization degree of the xylan compared to cellulose.

The increasing in pentosan content was 26.6% and 4.9% in the yield, confirming the adsorption of xylan on cellulose pulp.

Since the increasing in NaOH consumption is a concern, deposition trials were performed simulating D1 and EP stages conditions in order to minimize costs.

However, it was observed an increase in the NaOH and ClO_2 demand by 208% and 95%, respectively, comparing deposition samples to reference samples, as showed in Table 4.

On the other hand, pentosan content increased with deposition in 10.3%, lower than deposition in oxygen delignification stage, but it is still significant.

Table 4. Results of deposition in D1 stage.

Sample	NaOH (Kg Adt^{-1})	ClO_2 (Kg Adt^{-1})	Pentosan (%)	Permanganate number
Reference	2.4^{a}	4.0^{c}	15.5^{e}	1.1^{g}
Deposition	7.4^{b}	7.8^{d}	17.1^{f}	1.4^{h}

The increase in ClO_2 consumption was not expected to be that high. It might be explained by the lignin residual bonded to xylan, since it was observed that deposition samples showed higher results for permanganate number. Another explanation for the ClO_2 consumption is the expected increase in the hexenuronic acid content which is a side group in the xylan chain and is hydrolyzed in acidic conditions.

The deposition trials in the EP stage did not show significant differences between reference and deposition samples, as showed in Table 5, except in NaOH consumption for the deposition sample which is related to the low pH of

the xylan extract. The fibers swelling caused by pH conditions in the oxygen delignification stage is, probably, important for a better xylan deposition.

Table 5. Results of deposition in EP stage.

Sample	NaOH (Kg Adt^{-1})	ClO_2 (Kg Adt^{-1})	Pentosan (%)	Permanganate number
Reference	11.9^{a}	6.8^{c}	15.4^{d}	1.1^{e}
Deposition	18.2^{b}	6.8^{c}	15.6^{d}	1.4^{e}

3.3. Refining experiments

Pulp properties are strongly affected by xylan deposition in oxygen delignification stage, showed in Table 6.

Table 6. Properties of reference and deposition pulp samples in oxygen delignification stage. Unrefined samples and refining adjustment for 35 ºSR (Schopper Riegler) and TI70 (Tensile Index 70 N m g^{-1}).

Refining adjustment	Sample	ºSR	Tensile Index (N m g^{-1})	Energy Consumption (Wh)
Zero	Reference	19.0^{a}	31.2^{c}	-
	Depposition	26.2^{b}	42.9^{d}	-
35ºSR	Reference	35.0	88.4^{e}	21.5^{g}
	Deposition	35.0	66.4^{f}	6.7^{h}
TI70	Reference	27.3^{i}	70.0	12.8^{k}
	Deposition	36.8^{j}	70.0	7.7^{l}

The tensile index increased 37.4% even for unrefined pulp samples. The effects observed in tensile index for 35ºSR were expected since the refining adjustment favored drainability. A similar conclusion is valid for TI70 adjustment regarding drainability. However, it is clear that the xylan deposition improved the tensile index of the pulp.

A significant result for the oxygen delignification trials was the energy consumption decrease observed for 35 ºSR (69.0%) and TI70 (39.8%) which is a desirable effect for highly refined paper grades.

In the trials of xylan deposition in D1 stage, similar effects were obtained as showed in Table 7. The ºSR of unrefined pulp decreased, but there were

no statistically significant differences for tensile index results, as showed in Table 7.

Table 7. Properties of reference and deposition pulp samples in D1 stage. Unrefined samples and refining adjustment for 35 ºSR (Schopper Riegler) and TI70 (Tensile Index 70 N m g^{-1}).

Refining adjustment	Sample	ºSR	Tensile Index (N m g^{-1})	Energy Consumption (Wh)
Zero	Reference	21.0[a]	30.4[c]	-
	Deposition	25.3[b]	32.8[c]	-
35ºSR	Reference	35.0	71.8[d]	16.8[e]
	Deposition	35.0	61.3[d]	11.6[f]
TI70	Reference	34.0[g]	70.0	15.7[h]
	Deposition	42.7[g]	70.0	19.8[h]

The energy consumption obtained in 35ºSR trials was lower (30.9%) after xylan deposition. However, no statistically significant difference was observed for IT70 trials.

In the deposition trials of EP stage there were no statistically significant differences for ºSR and tensile index in any refining adjustment, as shown in Table 8, which validates the results of pentosan showed in Table 5. However, were observed energy consumption decreasing for 35ºSR (21.1%) and IT70 (27.1%) trials. These are the lowest reduction results observed for all deposition experiments, but are still significant.

Table 8. Properties of reference and deposition pulp samples in EP stage. Unrefined samples and refining adjustment for 35 ºSR (Schopper Riegler) and TI70 (Tensile Index 70 N m g^{-1}).

Refining adjustment	Sample	ºSR	Tensile Index (N m g^{-1})	Energy Consumption (Wh)
Zero	Reference	26.5[a]	38.0[b]	-
	Deposition	27.0[a]	37.4[b]	-
35ºSR	Reference	35.0	66.0[c]	9.0[d]
	Deposition	35.0	67.3[c]	7.1[e]
TI70	Reference	37.0[f]	70.0	10.7[g]
	Deposition	36.1[f]	70.0	7.8[h]

4. CONCLUSIONS

Xylan deposition showed to be technically viable, despite the high sodium hydroxide consumption in all the stages and the increasing of ClO_2 consumption in D1 stage. It was observed an increase in pentosan content only in oxygen delignification and D1 stages. The best results for tensile index and energy consumption were obtained from the trials in oxygen delignification stage. However, the experiments in D1 and EP stages confirmed the tendency to decrease the energy consumption after xylan deposition.

Aknowledgements: The authors thank to Celulose Nipo-Brasileira S.A – CENIBRA, for the supporting to this research and to CNPq, CAPES and FAPEMIG.

5. REFERENCES

Alesiani, M., Proietti, F., Capuani, S., Paci, M., Fioravanti, M., Maraviglia, B. (2005) ^{13}C CPMAS NMR spectroscopic analysis applied to wood characterization. Appl. Magn. Reson. 29:177-185.

Atalla, R. H., Vanderhart, D. L. (1984) Native cellulose: A composite of 2 distinct crystalline forms. Science. 223:283−285.

Atalla, R.H., Hackney, J.M., Uhlin, I., Thompson, N.S. (1993) Hemicelluloses as structure regulators in the aggregation of native cellulose. Int. J. Biol. Macromol. 15:109-112.

Aurell, R. (1965) Increasing kraft pulp yield by redeposition of hemicelluloses. Tappi. 48:80-84.

Aurell, R., Hartler, N. (1965) Kraft pulping of pine. Part 1. The changes in the composition of the wood residue during the cooking process. Svensk Papperstidning. 68:59-68.

Axelsson, S., Croon, I., Enström, B. (1962) Dissolution of hemicelluloses during sulphate pulping. Svensk Papperstidning. 65:693-697.

Bardet, M., Gerbaud, G., Giffard, M., Doan, C., Hediger, S., Le Pape, L. (2009) ^{13}C high-resolution solid-state NMR for structural elucidation of archaeological woods. Prog. Nucl. Magn. Reson. Spectrosc. 55:199-214.

Binnig, G., Quate, C.F., Gerber, C. (1986) Atomic force microscope. Phys. Rev. Lett. 56:930-933.

Blodgett, K.B. (1934) Monomolecular films of fatty acids on glass. J. Am. Chem. S. 56:495-495.

Blodgett, K.B. (1935) Films built by depositing successive monomolecular layers on a solid surface. J. Am. Chem. S. 57:1007-1022.

Bromley, J.R., Busse-Wicher, M., Tryfona, T., Mortimer, J.C., Zhang, Z., Brown, D.M., Dupree, P. (2013) GUX1 and GUX2 glucuronyltransferases decorate distinct domains of glucuronoxylan with different substitution patterns. Plant J. 74:423-434.

Burkinshaw, S.M. (2016) Physico-chemical Aspects of Textile Coloration. West Yorkshire: John Wiley & Sons. v. 53.

Busse-Wicher, M., Gomes, T.C.F., Tryfona, T., Nikolovski, N., Stott, K., Grantham, N.J., Bolam, D.N., Skaf, M.S., Dupree, P. (2014) The pattern of xylan acetylation suggests xylan may interact with cellulose microfibrils as a twofold helical screw in the secondary plant cell wall of *Arabidopsis thaliana*. Plant J. 79:492-506.

Busse-Wicher, M., Grantham, N.J., Lyczakowski, J.J., Nikolovski, N., Dupree, P. (2016a) Xylan decoration patterns and the plant secondary cell wall molecular architecture. Biochem. Soc. Trans. 44:74-78.

Busse-Wicher, M., Li, A., Silveira, R.L., Pereira, C.S., Tryfona, T., Gomes, T.C.F., Skaf, M.S., Dupree, P. (2016b) Evolution of xylan substitution patterns in gymnosperms and angiosperms: implications for xylan interaction with cellulose. Plant Physiol. 171:2418-243.

Chen, Q., Xu, S., Liu, Q., Masliyah, J., Xu, Z. (2016) QCM-D study of nanoparticle interactions. Adv. Colloid Interface Sci. 233:94-114.

Clayton, D.W., Phelps, G.R. (1965) The sorption of glucomannan and xylan on α-cellulose wood fibres. J. Polym. Sci. 11:197-220.

Cranston, E.D., Gray, D.G. (2006) Morphological and optical characterization of polyelectrolyte multilayers incorporating nanocrystalline cellulose. Biomacromolecules. 9:2522-2530.

Dahlman, O., Sjöberg, J., Jansson, U.B., Larsson, P.O. (2003) Effects of surface hardwood xylan on the quality of softwood pulps. Nordic Pulp Paper Res. J. 18:310-315.

Dahlman, O., Jacobs, A., Sjöberg, J. (2003) Molecular properties of hemicelluloses located in the surface and inner layers of hardwood and softwood pulps. Cellulose 10:325-334.

Dahlman, O., Jensen, A., Tormund, D., Östlund, J. (2008) Processing of xylan from hardwood spent cooking liquors. In: Conference proceedings from the Nordic Wood Biorefinery Conference, Sweden, pp 114-119.

Danielsson, S., Lindström, M.E. (2005) Influence of birch xylan adsorption during kraft cooking on softwood pulp strength. Nordic Pulp Paper Res. J. 20:436-441.

David, I., Viviana, K.P., Per Tomas, L., Anna-Stiina, J., Monica, E. (2010) Combination of alkaline and enzymatic treatments as a process for upgrading sisal paper- grade pulp to dissolving-grade pulp. Bioresour. Technol. 101:7416-7423.

Davis, M.F., Schroeder, H.R., Maciel, G.E. (1994) Solid-state ^{13}C nuclear magnetic resonance studies of wood decay. I. White rot decay of colorado blue spruce. Holzforschung. 48:99-105.

Ducker, W.A., Senden, T.J., Pashley, R.M. (1991) Direct measurement of colloidal forces using an atomic force microscope. Nature. 353:239-241.

Dupree, R., Simmons, T.J., Mortimer, J.C., Patel, D., Iuga, D., Brown, S.P., Dupree, P. (2015) Probing the molecular architecture of *Arabidopsis thaliana* secondary cell walls using two- and three-dimensional ^{13}C solid state nuclear magnetic resonance spectroscopy. Biochemistry. 54:2335-2345.

Dybowski, C., Bai, S. (2006) Solid-state nuclear magnetic resonance. Anal. Chem. 78:3853-3858.

Eriksson, E., Samuelson, O., Viale, A. (1963) Adsorption of hemicellulose isolated from sulfite cooking liquors by cellulose fibers. Svensk Papperstidning. 66:403-406.

Eriksson, E., Sjöström, E. (1968) Influence of acidic groups on the physical properties of high-yield pulps. Tappi. 51:56-59.

Fatisson, J., Domingos, R.F., Wilkinson, K.J., Tufenkji, N. (2009) Deposition of TiO_2 nanoparticles onto silica measured using a quartz crystal microbalance with dissipation monitoring. Langmuir. 25:6062-6069.

Gehmayr, V., Schild, G., Sixta, H. (2011) A precise study on the feasibility of enzyme treatments of a kraft pulp for viscose application. Cellulose 18:479-491.

Ghisalberti, E.L., Godfrey, I.M. (1998) Application of nuclear magnetic resonance spectroscopy to the analysis of organic archaeological materials. Stud. Conserv. 43:215-230.

Gil, A.M., Masui, K., Naito, A., Tatham, A.S., Belton, P.S., Saito, H. (1997) A ^{13}C-NMR study on the conformational and dynamical properties of a cereal seed storage protein, C-hordein, and its model peptides. Biopolymers. 41:289-300.

Gomes, V. J. Aperfeiçoamento de processos de produção de polpas para dissolução e para papel tissue a partir do eucalipto. Universidade Federal e Viçosa, Brasil, 2011.

Habibi, Y., Foulon, L., Aguié-Béghin, V., Molinari, M., Douillard, R. (2007) Langmuir-Blodgett films of cellulose nanocrystals: preparation and characterization. J. Colloid. Interface Sci. 316:388-397.

Hakala, T.K., Liitiä, T., Suurnäkki, A. (2013) Enzyme-aided alkaline extraction of oligosaccharides and polymeric xylan from hardwood kraft pulp. Carbohydr. Polym. 93:102-108.

Hansson, J-Å., Hartler, N. (1969) Sorption of hemicelluloses on cellulose fibres. Part 1. Sorption of xylans. Svensk Pappertidning. 72:521-530.

Hansson, J-Å. (1970) Sorption of hemicelluloses on cellulose fibres. Part 3. The temperature dependence on sorption of birch xylan and pine glucomannan at kraft pulping conditions. Svensk Papperstidning. 73:49-53.

Henriksson, A., Gatenholm, P. (2001) Controlled assembly of glucuronoxylans onto cellulose fibers. Holzforschung. 55:494-502.

Hult, E-L., Larsson, P.T., Iversen, T. (2000) A comparative CP/MAS ^{13}CNMR study of cellulose structure in spruce wood and kraft pulp. Cellulose. 7:35-55.

Ibarra, D., Köpcke V., Larsson P.T., Jääskeläinen A-S., Ek, M. (2010) Combination of alkaline and enzymatic treatments as a process for upgrading sisal paper-grade pulp to dissolving-grade pulp. Bioresour. Technol. 101:7416

Janzon, R., Puls, J., Saake, B. (2006) Upgrading of paper-grade pulps to dissolving pulps by nitren extraction: optimization of extraction parameters and application to different pulps. Holzforschung. 60:347-354.

Kleppe, P. (1970) Kraft pulping. Tappi. 53:35-47.

Köhnke, T., and Gatenholm, P. (2007) The effect of controlled glucuronoxylan adsorption on drying-induced strength loss of bleached softwood pulp. Nordic Pulp Paper Res. J. 22:508-515.

Kontturi, E., Johansson, L.-S., Kontturi, K.S., Ahonen, P., Thüne, P.C., Laine, J. (2007) Cellulose nanocrystal submonolayers by spin coating. Langmuir. 23:9674-9680.

Kontturi, E., Suchy, M., Penttilä, P., Jean, B., Pirkkalainen, K., Torkkeli, M., Serimaa, R. (2011) Amorphous characteristics of an ultrathin cellulose film. Biomacromolecules. 12:770-777.

Kontturi, E., Tammelin, T., Österberg, M. (2006) Cellulose-model films and the fundamental approach. Chem. Soc. Rev. 35:1287-1304.

Kontturi, E., Thune, P.C., Niemantsverdriet, J. W. (2003) Cellulose model surfaces: simplified preparation by spin coating and characterization by X-ray photoelectron spectroscopy, infrared spectroscopy, and atomic force microscopy. Langmuir. 19:5735-5741.

Kontturi, E., Thune, P.C., Niemantsverdriet, J.W. (2005) Trimethylsilylcellulose/polystyrene blends as a means to construct cellulose domains on cellulose. Macromolecules. 38:10712-10720.

Kontturi, K.S., Tammelin,T., Johansson, L.-S. Stenius, P. (2008) Adsorption of cationic starch on cellulose studied by QCM-D. Langmuir. 24:4743-4749.

Krogerus, B., Fuhrmann, A. (2009) Isolation of xylan and use as wet end- and binder chemical. In: Conference proceedings from the 15th International Symposium on Wood, Fibre and Pulping Chemistry, Norway. pp-110.

Kvarnlöf, N., Söderlund, C-A., Germgård, U. (2006) The effects of modifying the oxidative pre-aging conditions in the manufacture of viscose from wood pulp. Paper. ja Puu 88:175

Laine, J., Stenius, P. (1997) Effect of charge on the fibre and paper properties of bleached industrial kraft pulps. Pap. Puu-Pap. Tim. 70:257-266.

Lambert, J.B., Shawl, C.E., Stearns, J.A. Nuclear magnetic resonance in archaeology. Chem. Soc. Rev. 29:175-182.

Langmuir, I. (1920) The mechanism of the surface phenomena of flotation. Trans. Far. S. 15:62-74.

Langmuir, I., Schaefer, V. J. (1938) Activities of urease and pepsin monolayers. J. Am. Chem. Soc. 60:1351-1360.

Larsson, P.T., Hult, E-L., Wickholm, K., Pettersson, E., Iversen, T. (1999) CP/MAS ^{13}C-NMR spectroscopy applied to structure and interaction studies on cellulose I. Solid State Nucl. Magnet. Resonan. 15:31-40.

Larsson, P.T., Wickholm, K., Iversen, T. (1997) A CP/MAS ^{13}C NMR investigation of molecular ordering in celluloses. Carbohydr. Res. 302:19-25.

Li, J., Hu, H., Li, H., Huang, L., Chen, L., Ni, Y. (2017) Kinetics and mechanism of hemicelluloses removal from cellulosic fibers during the cold caustic extraction process. Bioresour. Technol. 234:61-66.

Li, J., Ma, X., Duan, C., Liu, Y., Zhang, H., Ni, Y. (2016) Enhanced removal of hemicelluloses from cellulosic fibers by poly (ethylene glycol) during alkali treatment. Cellulose 23:231-238.

Li, L., Perre, P., Frank, X., Mazeau, K. (2015a) A coarse-grain force-field for xylan and its interaction with cellulose. Carbohydr. Polym. 127:438-450.

Li, Y., Liu, Y., Chen, W., Wang, Q., Liu, Y., Li, J., Yu, P. (2015b) Facile extraction of cellulose nanocrystals from wood using ethanol and peroxide solvothermal pretreatment followed by ultrasonic nanofibrillation. Green Chem. 18:1010-1018.

Linder, A., Bergman, R., Bodin, A., Gatenholm, P. (2003) Mechanism of assembly of xylan onto cellulose surfaces. Langmuir. 19:5072-5077.

Lindgren, T., Edlund, U., Iversen, T. (1995) A multivariate characterization of crystal transformations of cellulose. Cellulose. 2:273-288.

Maunu, S., Liitiä, T., Kauliomäki, S., Hortling, B., Sundquist, J. (2000) ^{13}C CPMAS NMR investigations of cellulose polymorphs in different pulps. Cellulose. 7:147-159.

Mesquita, J.P., Donnici, C.L., Pereira, F.V. (2010) Biobased nanocomposites from layer-by-layer assembly of cellulose nanowhiskers with chitosan. Biomacromolecules. 11:473-480.

Mesquita, J.P., Patrício, P.S., Donnici, C.L., Petri, D.F.S., Oliveira, S.A., Pereira, F.V. (2011) Hybrid layer-by-layer assembly based on animal and vegetable structural materials: multilayered films of collagen and cellulose nanowhiskers. Soft Matter. 7:4405-4413.

Mikkelsen, D., Flanagan, B.M., Wilson, S.M., Bacic, A., Gidley, M.J. (2015) Interactions of arabinoxylan and (1,3)(1,4)-β-glucan with cellulose networks. Biomacromolecules. 16:1232-1239.

Mitikka-Eklund, M. Sorption of xylans on cellulose fibers. University of Jyväskylä, Finland, 1996.

Mobarak, F., El-Ashawy, A.E., Fahmy, Y. (1973) Hemicelluloses as additive in papermaking. Part 2. The role of added hemicellulose in situ on paper properties. Cellulose Chem. Technol. 7:325-335.

Mocchiuttia, P., Galvána, M.V., Peresinb, M.S., Schnella, C.N., Zanuttinia, M.A. (2015) Complexes of xylan and synthetic polyelectrolytes. Characterization and adsorption onto high quality unbleached fibres. Carbohydr. Polym. 116:131-139.

Mocchiuttia, P., Schnella, C.N., Rossia, G.D., Peresinb, M.S., Zanuttinia, M.A., Galvána, M.V. (2016) Cationic and anionic polyelectrolyte complexes of xylan and chitosan. Interaction with lignocellulosic surfaces. Carbohydr. Polym. 150:89-98.

Mora, F., Ruel, K., Comtat, J., Joseleau, J.P. (1986) Aspects of native and redeposited xylans at the surface of cellulose microfibrils. Holzforschung. 40:85-91.

Muguet, M.C.S., Pedrazzi, C., Jorge Luiz Colodette, J.L. (2011) Xylan deposition onto eucalypt pulp fibers during oxygen delignification. Holzforschung. 65:605-612.

Newman, R.H. (1992) Nuclear magnetic resonance study of spatial relationships between chemical components in wood cell walls. Holzforschung. 46:205-210.

Newman, R.H. (1998) Evidence for assignment of ^{13}C NMR signals to cellulose crystallite surfaces in wood, pulp and isolated celluloses. Holzforschung. 52:157-159.

Newman, R.H., Hemmingson, J.A. (1990) Determination of the degree of cellulose crystallinity in wood by carbon-13 nuclear magnetic resonance spectroscopy. Holzforschung. 44:351-355.

Newman, R.H., Hemmingson, J.A., Suckling, I.D. (1993) Carbon-13 nuclear magnetic resonance studies of kraft pulping. Holzforschung. 47:234-238.

Österberg, M., Valle-Delgado, J.J. (2017) Surface forces in lignocellulosic systems. Curr. Opin. Colloid. Interface Sci. 27:33-42.

Paananen, A., Österberg, M., Rutland, M., Tammelin, T., Saarinen, T., Tappura, K., Stenius, P. (2004) Interaction between cellulose and xylan: an atomic force microscope and quartz crystal microbalance study. In: Hemicelluloses: Science and technology. ACS Symposium Series 864. Eds. Gatenholm P., Tenkanen M. pp. 269-290.

Paci, M., Frederici, C., Capitani, D., Perenze, N., Segre, A.L. (1995) NMR study of paper. Carbohydr. Polym. 26:289-297.

Panthapulakkal, S., Kirk, D., Sain, M. (2015) Alkaline extraction of xylan from wood using microwave and conventional heating. J. Appl. Polym. Sci. 132. http://dx. doi.org/10.1002/app.41330.

Panthapulakkal, S., Pakharenko, V., Sain, M. (2013) Microwave assisted short-time alkaline extraction of birch xylan. J. Polym. Environ. 21:917-929.

Pedrazzi, C. Influência das xilanas na produçãoo e nas propriedades de polpas de eucalipto para papéis. Universidade Federal de Viçosa, Brazil, 2009.

Pinto, T.S., Alves, L.A., Cardozo, G.A., Munhoz, V.H.O., Verly, R.M., Pereira, F.V., Mesquita, J.P. (2017) Layer-by-layer self-assembly for carbon dots/chitosan-based multilayer: morphology, thickness and molecular interactions. Mater. Chem. Phys. 186:81-89.

Pournou, A. (2008) Deterioration assessment of waterlogged archaeological lignocellulosic material via ^{13}C CP/MAS NMR. Archaeometry. 50:129-141.

Ribe, E., Wernersson, F., Theliander, H. (2009) Optimal industrial birch black liquor for xylan sorption. In: Tappi Engineering, Pulping and Environmental Conference, USA. 19.3

Rydholm, S.A. (1965) Pulping Processes, New York, USA, Robert E. Krieger Publishing Company p.992. Reprinted in1985, ISBN 0-89874-856-9.

Santonia, I., Calloneb, E., Sandaka, A., Sandaka, J., Dirèb, S. (2015) Solid state NMR and IR characterization of wood polymer structure in relation to tree provenance. Carbohydr. Polym. 117:710-721.

Saric, S.P., Schofield, R.K. (1946) The dissociation constants of the carboxyl and hydroxyl groups in some insoluble and sol-forming polysaccharides. Proc. R. Soc. Lon. Ser-A. 1003:431-447.

Schömberg, C., Oksanem, T., Suurnäkki, A., Kettunem, H., Bucghert, J. (2001) The importance of xylan for the strength properties of spruce kraft fibres. Holzforscung. 55:639-644.

Sihtola, H., Blomberg, L. (1975) Hemicelluloses precipitated from steeping liquor in the viscose process as additives in papermaking. Cellul. Chem. and Technol. 9:555-560.

Simmons, T.J., Mortimer, J.C., Bernardinelli, O.D., Pöppler, A., Brown, S.P., Azevedo, E.R., Dupree, R., Dupree, P. (2016) Folding of xylan onto cellulose fibrils in plant cell walls revealed by solid-state NMR. Nat. Commun. 7:1-9.

Simonson, R. (1963) The hemicellulose in the sulphate pulping process. I. Isolation of hemicellulose fractions from sulphate cooking liquors. Svensk Papperstidning. 66:839-845.

Sjöström, E. Wood chemistry, fundamentals and applications. Academic Press, New York, 1981.

Sjöström, E., Enström, B. (1967) Characterization of acidic polysaccharides isolated from different pulps. Tappi. 50:32-36.

Soares, M.C.D.S.M. Métodos alternativos para deposição de xilanas em polpas de eucalipto. Universidade Federal de Viçosa, Brazil, 2009.

Srndovic, J.S. Interactions between wood polymers in wood cell walls and celulose/hemicellulose biocomposites. Chalmers University of Technology. Sweden, 2011.

Stigsson, V., Kloow, G., Germgård, U., Andersson,N. (2005) The influence of cobal (II) in carboxymethyl cellulose processing. Cellulose 12:395

Syed, H.U., Nebamoh, I.P., Germgård, U. (2013) A comparison of cold and hot caustic extraction of a spruce dissolving sulfite pulp prior to final bleaching. Appita J. 66:229-234.

Tammelin, T., Saarinen, T., Österberg, M., Laine, J. (2006) Preparation of Langmuir/Blodgett-cellulose surfaces by using horizontal dipping procedure. Application for polyelectrolyte adsorption studies performed with QCM-D. Cellulose. 13:519-535.

Taylor, M.G., Deslandes, Y., Bluhm, T., Marchessault, R.H., Vincendon, M., Saintgermain, J. (1983) Solid state ^{13}C NMR characterization of wood. Tappi J. 66:92-94.

Teleman, A., Harjunpää, V., Tenkanen, M., Buchert, J., Hausalo, T., Drakenberg, T., Vuorinen, T. (1995) Characterisation of 4-deoxy-β-L-enopyranosyluronic acid attached to xylan in pine Kraft pulp and pulping liquor by 1H and 13C NMR spectroscopy. Carbohydr. Res. 272:55-71.

Thio, B.J.R., Zhou, D., Keller, A.A. (2011) Influence of natural organic matter on the aggregation and deposition of titanium dioxide nanoparticles. J. Hazard. Mater. 189:556-563.

Timell, T.E. (1967) Recent progress in the chemistry of wood hemicelluloses. Wood Sci. Technol. 1:45-70.

Vaaler, D., Ljones, S., Ribe, E., Toven, K., Moe, S. (2002) Effects of hemicellulose stabilisation and raw material on the beatability of softwood kraft pulps. In: 7th EWLP, Finland. pp 147-150.

Van der Hart, D.L., Atalla, R.H. (1984) Studies of microstructures in native celluloses using solid-state ^{13}C NMR. Macromolecules. 17:1465-1472.

Vehviläinen M., Kamppuri T., Nousianen P., Kallioinen A., Siika-Aho., M., Elg-Christoffersson K., Rom M., Janicki J. (2010) Effect of acid and enzymatic treatments of TCF dissolving pulp on the properties of wet spun cellulosic fibres, Cellulose Chem. Technol. 44:147.

Wickholm, K., Larsson, P.T., Iversen, T. (1998) Assignment of noncrystalline forms in cellulose I by CP/MAS ^{13}C NMR spectroscopy. Carbohydr. Res. 312:123-129.

Winter, H.T., Cerclier, C., Delorme, N., Bizot, H., Quemener, B., Cathala, B. (2010) Improved colloidal stability of bacterial cellulose nanocrystal

suspensions for the elaboration of spin-coated cellulose-based model surfaces. Biomacromolecules. 11:3144-3151.

Wollboldt, R.P., Zuckerstätter, G., Weber, H.K., Larsson, P.T., Sixta, H. (2010) Accessibility, reactivity and supramolecular structure of E. globulus pulps with reduced xylan content. Wood Sci. Technol. 44:533-546.

Yllner, S., Enström, B. (1956) Studies of the adsorption of xylan on cellulose fibers during the sulphate cook. Part 1. Svensk Papperstidning. 59:229-232.

Winuprasitha, T., Suphantharik, M. (2013) Microfibrillated cellulose from mangosteen (Garcinia mangostana L.) rind: Preparation, characterization, and evaluation as an emulsion stabilizer. Food Hydrocoll. 32:383-394.

CONCLUSÕES GERAIS

A adsorção de xilana sobre celulose microcristalina foi observada quando realizada em pH13. Através das análises de RMN foi possível identificar duas regiões distintas das fibras de celulose onde a xilana é depositada. Isso sugere a existência de diferentes mecanismos de adsorção para cada região da fibra, cristalina e amorfa, provavelmente relacionados ao tamanho do fragmento de xilana.

Os experimentos de QCM-D demonstraram que a xilana foi irreversivelmente depositada sobre a superfície da celulose quando soluções mais concentradas de xilana foram utilizadas (1 mg mL^{-1}). As imagens de AFM mostraram que a xilana deposita sobre a celulose como aglomerados ovalados com diâmetros entre 0,01 e 0,1 μm enquanto a maior parte da superfície das fibras parece estar sem depósito de xilana.

A deposição de xilana no estágio de deslignificação em condições industriais mostrou-se tecnicamente viável. Entretanto, o uso do extrato de xilana em condições ácidas ocasionou a elevação do consumo de NaOH. Além disso, os experimentos de branqueamento indicam que a xilana continua acessível para reações de oxidação e hidrólise.

Os experimentos de deposição nos estágios do branqueamento demonstraram viabilidade principalmente no D1, apesar da elevação dos consumos de NaOH e ClO_2.

Os melhores resultados de deposição e evolução das propriedades da polpa foram obtidos no estágio de deslignificação. Foram observadas melhorias de rendimento e propriedades físicas da polpa e, principalmente, redução do consumo de energia no processo de refino em todos os estágios testados. Finalmente, foi possível observar os efeitos da deposição da xilana sobre a histerese, melhorando a reciclabilidade das fibras.

A carga de 240g de NaOH nos testes de extração alcalina atingiu as máximas eficiências. Cargas mais elevadas não mostraram diferenças significativas em relação ao teor de pentosanas. As extrações a 25 ºC mostraram melhores resultados. Entretanto, a extração a 60 ºC, que é uma condição mais adequada ao processo de produção de celulose, mostrou resultados muito próximos aos obtidos com temperaturas mais baixas.

As variações observadas nos resultados de deposição em condições industriais demonstram a necessidade de estudos de otimização dos processos para redução dos consumos de produtos químicos e custos de produção.

ANEXOS DO PAPER 1

Figura 1A. Espectro de RMN em estado sólido de ^{13}C CPMAS da referência de celulose microcristalina (MCC).

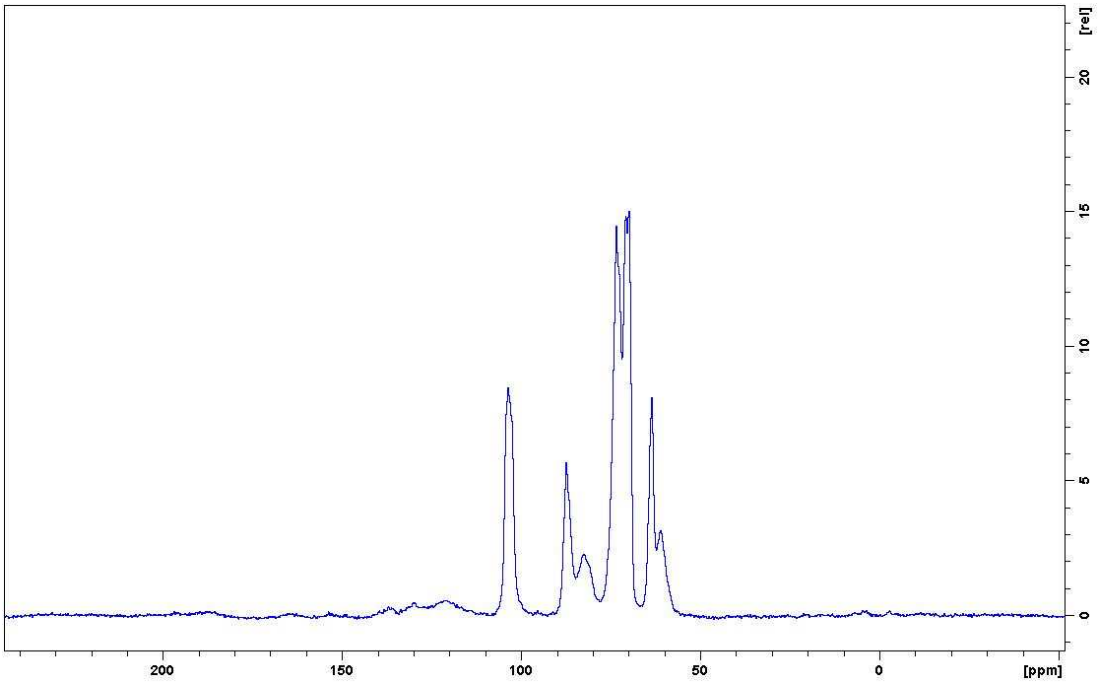

Figura 2A. Espectro de RMN em estado sólido de ^{13}C CPMAS da referência de xilana (Xyl).

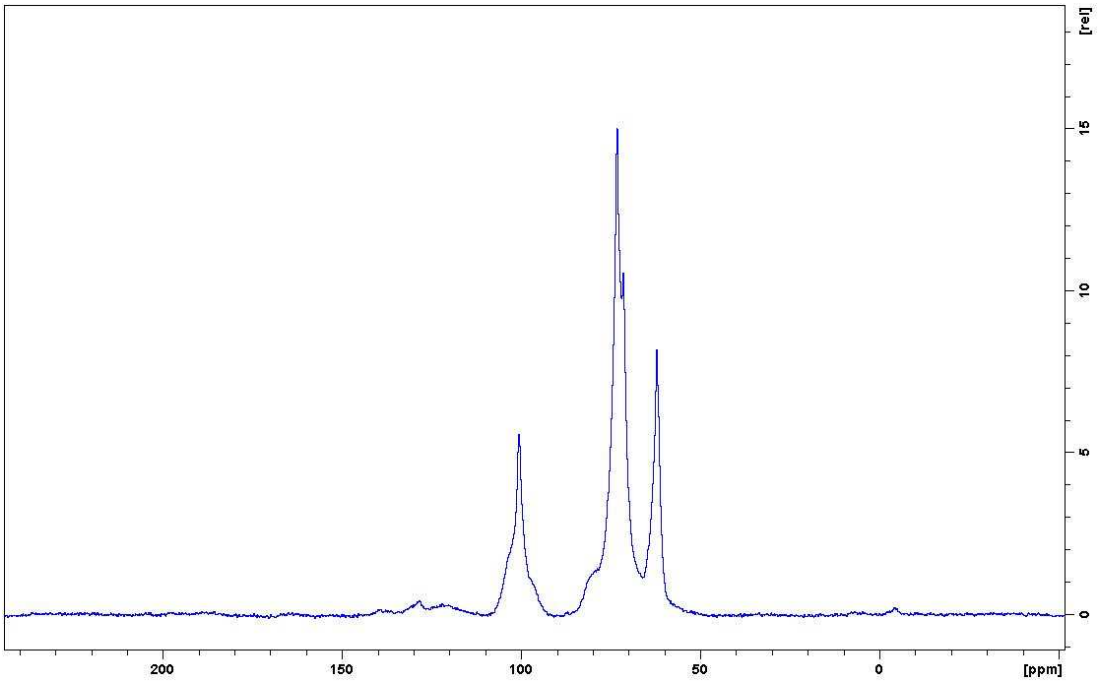

Figura 3A. Espectro de RMN em estado sólido de ^{13}C CPMAS da amostra MCC+Xyl sem lavar em pH10.

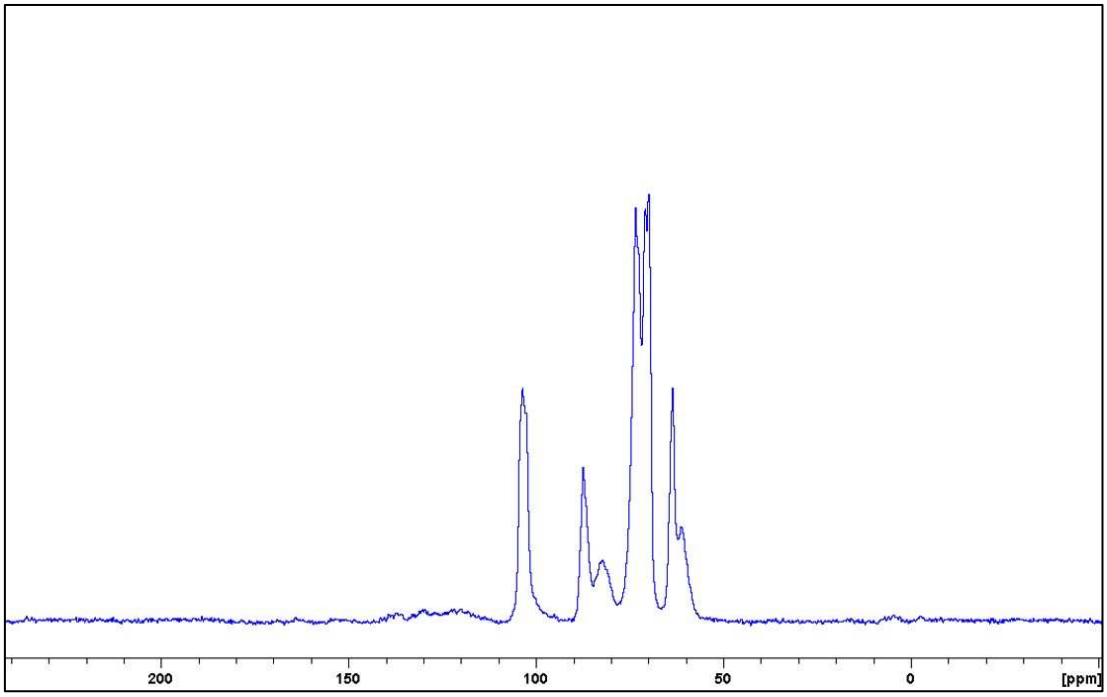

Figura 4A. Espectro de RMN em estado sólido de ^{13}C CPMAS da amostra MCC+Xyl lavada em pH10.

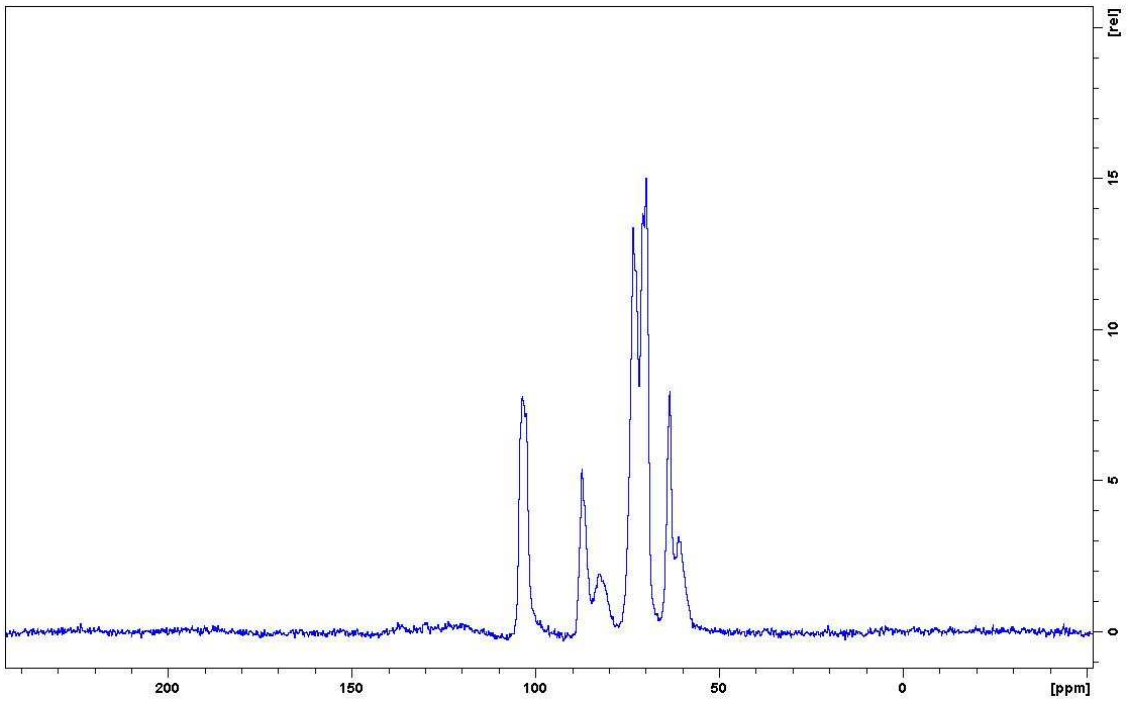

Figura 5A. Espectro de RMN em estado sólido de ^{13}C CPMAS da amostra MCC+Xyl sem lavar em pH13.

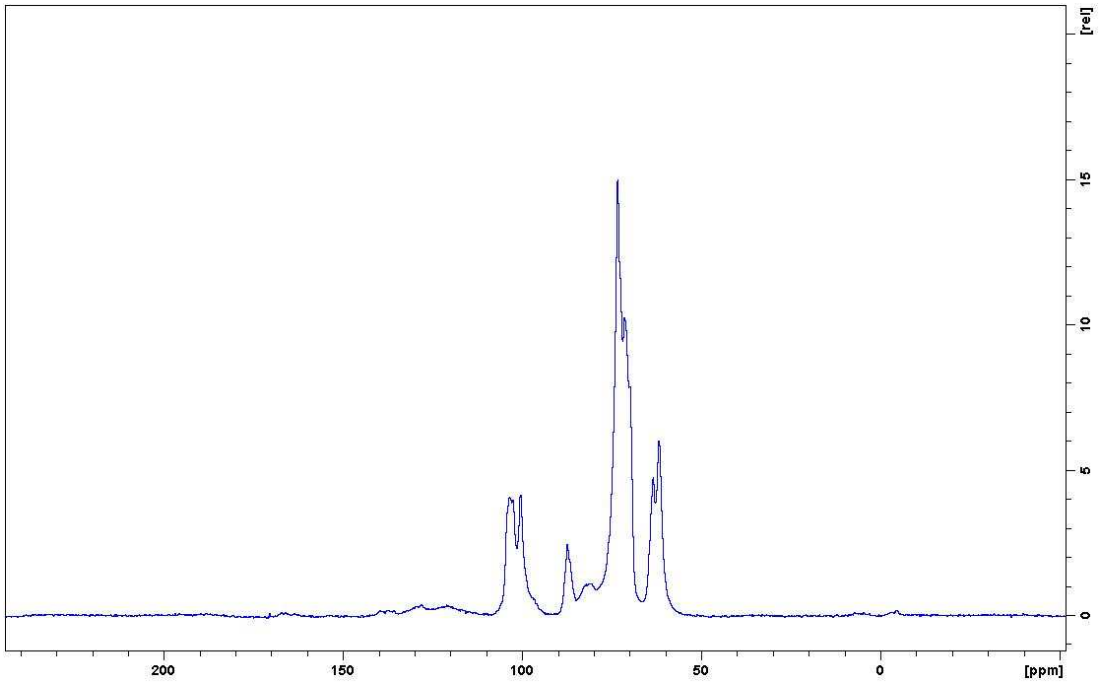

Figura 6A. Espectro de RMN em estado sólido de ^{13}C CPMAS da amostra MCC+Xyl lavada em pH13.

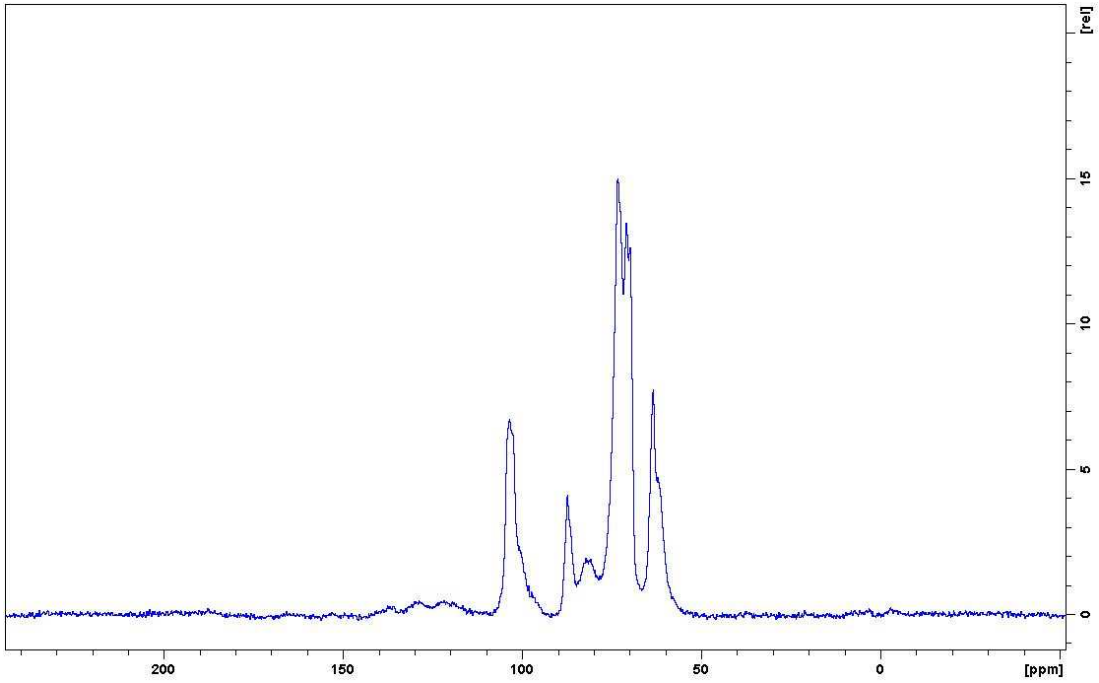

Figura 7A. Espectro de RMN em estado sólido de ^{13}C PSRE da amostra MCC+Xyl sem lavar em pH10.

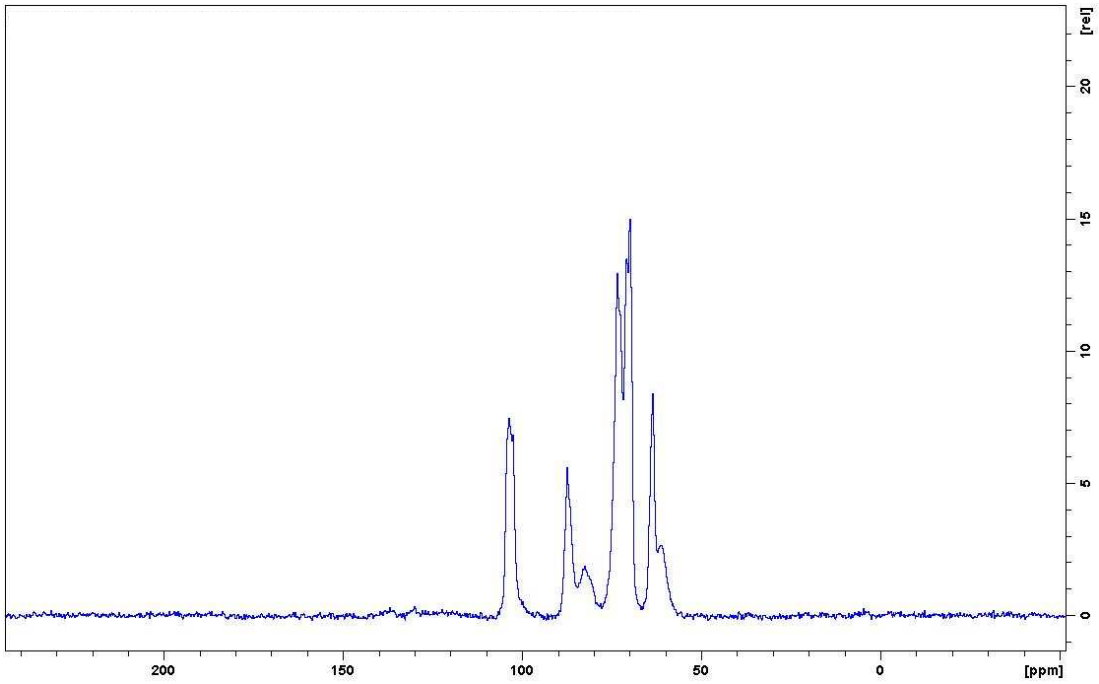

Figura 8A. Espectro de RMN em estado sólido de ^{13}C PSRE da amostra MCC+Xyl sem lavar em pH13.

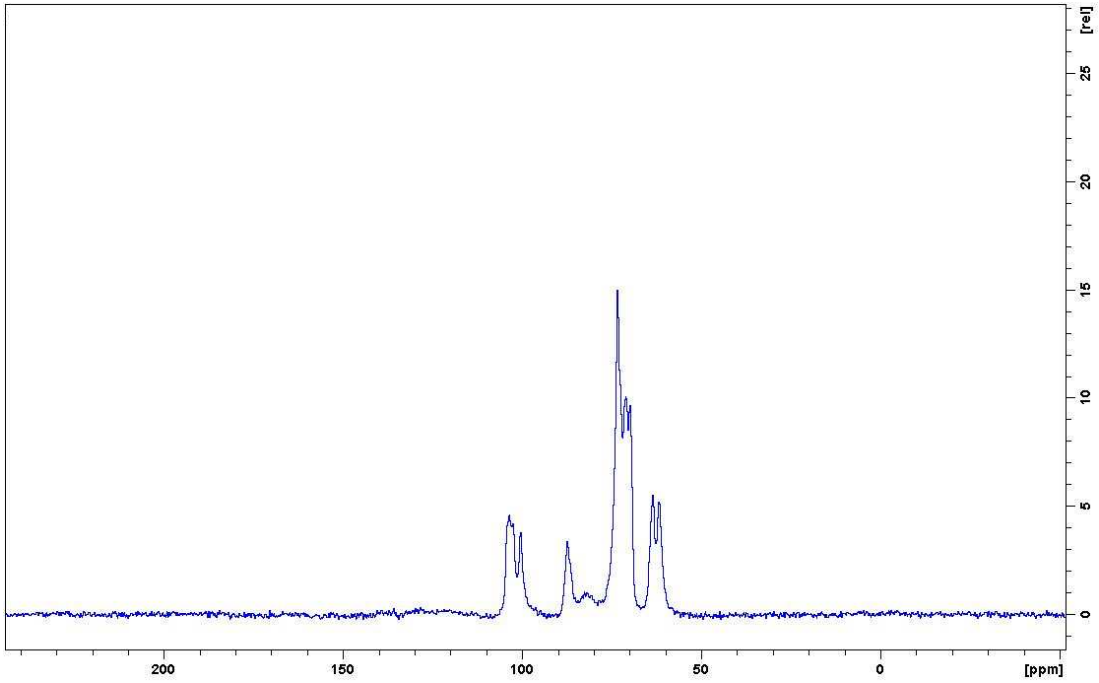

Figura 9A. Espectro de RMN em estado sólido de ^{13}C PSRE da amostra MCC+Xyl lavada em pH13.

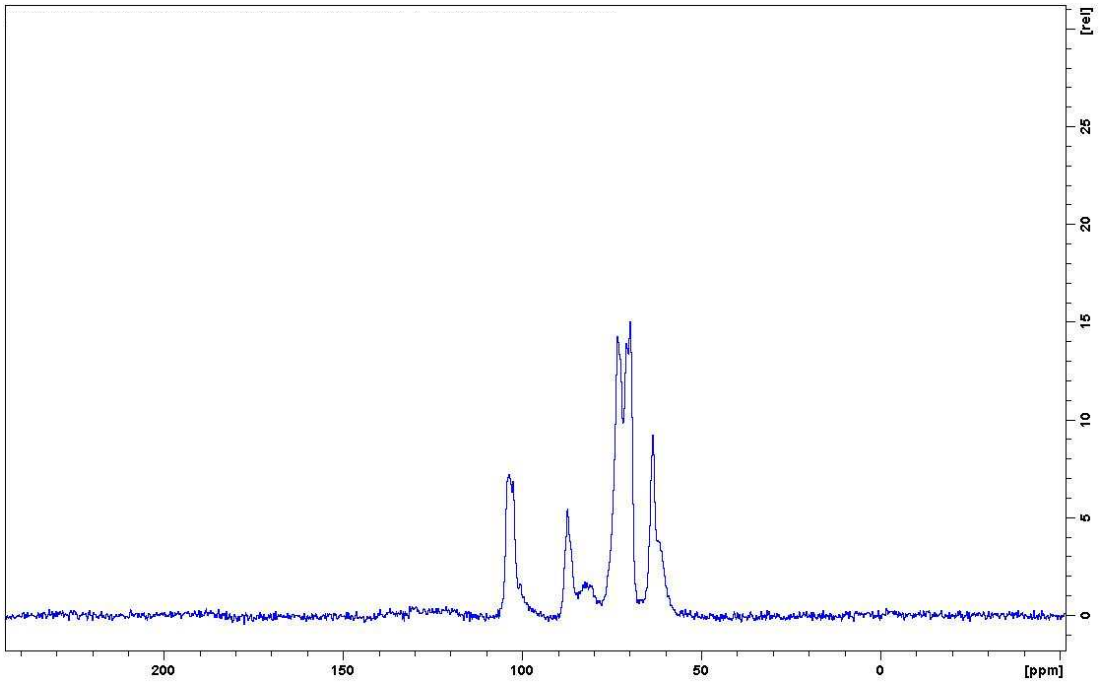

ANEXOS DO PAPER 2

Quadro 1B. Caracterização da madeira utilizada nos ensaios de cozimento.

Serragem									
Consistência					Consistência				
3,7263	50,4545	53,7235	87,7%	87,6%	1,7568	51,2525	52,8635	91,7%	91,7%
4,2238	50,3591	54,0565	87,5%		1,8089	50,3288	51,9893	91,8%	
Cinzas					Lignina insolúvel				
11,0332	43,6465	43,6718	0,26%	0,26%	0,3314	0,5535	0,6278	24,4%	24,7%
10,7322	41,7453	41,7703	0,27%		0,3316	0,5600	0,6357	24,9%	
Extrativos					Lignina solúvel				
5,5304	143,4566	143,5529	1,99%	1,89%	1,0075	0,7321	4,20	4,20	
5,4564	143,2776	143,3629	1,78%		1,0035	0,722	4,19		

Cavaco				
Consistência				
80,09	72,53	123,27	59,53%	60,23%
107,47	74	152,62	61,01%	
78,28	72,11	121,65	60,14%	
Densidade Básica				
107,15	90,52	150,78	481,99	481,96
79,96	90,7	123,67	481,92	
pH	4,42			

Quadro 2B. Curva de cozimento para determinação da carga alcalina.

Cozimento - Digestor de laboratório Haato

Condições:

Temperatura: 160°C

Relação licor/madeira: 3/1

Tempo de Cozimento: 170 min.

Sulfidez: 30%

Desenvolvimento de Curva

AE,%	#K
15,5	18,7
16,0	17,5
16,5	17,2
17,0	17,2
17,5	16,6
17,6	16,5
18,0	15,9
18,5	15,6
20,0	14,6
20,5	13,8

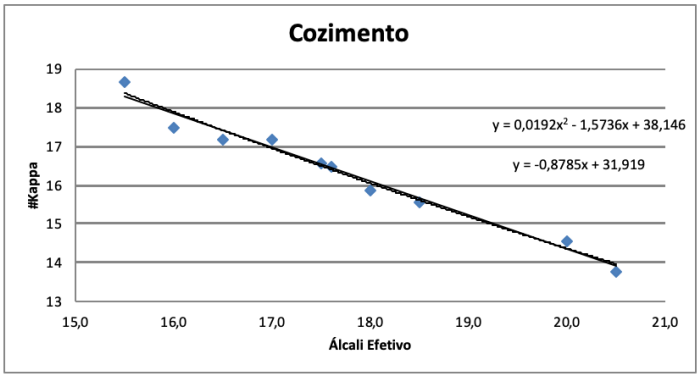

Definição de carga alcalina para o Kappa

K cal Pol	16,0
K cal Linear	16,0
AE, %	**18,0**
AE, %	**18,1**

K cal Pol	14,0
K cal Linear	14,0
AE, %	**20,4**
AE, %	**20,4**

K cal Pol	18,0
K cal Linear	18,0
AE, %	**15,9**
AE, %	**15,8**

Quadro 3B. Dados dos ensaios de Pré-branqueamento.

Pré Branqueamento	Polpa Referência												
	# Kappa	pH	Média	Alvura, % ISO	Média	Viscosidade, cP	Média	# Kappa	Média	Rendimento,%	Média	Pentosanas	Média
	#K14	10,7	10,7	55,8	55,8	21,0	21,03	8,7	8,7	98,83	98,83	15,37	15,37
		10,7		55,8		21,0		8,7		98,83			
	#K16	11,0	10,9	56,6	58,3	28,6	29,43	10,0	9,9	98,09	98,17	15,24	15,24
		10,7		59,9		30,3		9,9		98,25			
	#K18	11,0	10,9	58,3	58,6	33,8	33,12	10,8	10,8	97,63	97,50	15,58	15,58
		10,8		58,8		32,5		10,8		97,36			
	Polpa com redeposição de Xilana												
	# Kappa	pH	Média	Alvura, % ISO	Média	Viscosidade, cP	Média	# Kappa	Média	Rendimento,%	Média	Pentosanas	Média
	#K14	10,5	10,5	59,7	60,0	11,0	11,38	8,9	8,9	103,40	103,35	18,61	18,61
		10,4		60,2		11,7		8,9		103,30			
	#K16	10,48	10,8	59,7	59,8	15,3	14,72	10,2	10,2	102,60	102,50	17,86	17,86
		11,1		59,9		14,1		10,2		102,40			
	#K18	10,7	10,7	58,3	58,6	18,0	18,79	10,5	10,5	103,00	102,95	18,67	18,67
		10,7		58,8		19,6		10,5		102,90			
	*#K16	9,0	9,0	52,6	52,6	25,6	24,05	10,1	10,3	103,7	103,93	19,02	18,9
		8,9		52,5		22,5		10,4		104,1		18,77	

* Pré O2 realizada com mesma carga alcalina da referência

Quadro 4B. Análises de Pentosanas no Pré-branqueamento.

Identificação da amostra		CONSISTÊNCIA (%)				PENTOSANAS (%)				
		Peso úmido (g)	Peso Seco(g)	Consistência(%)	Média CST (%)	Peso úmido (g)	Peso Seco(g)	PB	Vol. Tit. (mL)	Pentosanas (%)
REFERÊNCIA	#14	1,7631	1,6201	91,89	92,15	1,0791	0,9944	40,75	20,735	14,10
	#14	1,5368	1,4203	92,42		1,0829	0,9979		20,570	14,17
	#16	1,8417	1,6898	91,75	91,96	1,0792	0,9924		19,495	15,06
	#16	1,2729	1,1732	92,17		1,0781	0,9914	39,915	19,110	14,74
	#18	1,7706	1,6374	92,48	92,13	1,0772	0,9925		19,105	14,73
	#18	1,0048	0,9223	91,79		1,0775	0,9927		18,900	14,88
XILANA	#14	2,0229	1,8529	91,60	91,99	1,0767	0,9905	39,915	14,140	18,52
	#14	1,294	1,1955	92,39		1,0833	0,9966		13,910	18,57
	#16	2,2705	2,0745	91,37	91,15	1,0766	0,9813		14,580	18,36
	#16	1,2363	1,1241	90,92		1,0740	0,9789	39,815	14,595	18,32
	#18	2,0757	1,8869	90,90	90,97	1,0889	0,9906		14,110	18,46
	#18	0,8481	0,7721	91,04		1,0846	0,9867		13,880	18,71

Quadro 5B. Análises de Pentosanas no D0.

Identificação da amostra		CONSISTÊNCIA (%)				PENTOSANAS (%)				
		Peso úmido (g)	Peso Seco(g)	Consistência(%)	Média CST (%)	Peso úmido (g)	Peso Seco(g)	PB	Vol. Tit. (mL)	Pentosanas (%)
REFERÊNCIA	#14A	1,6882	1,6405	97,17	97,15	1,083	1,0521	40,115	17,325	15,25
	#14B	1,6092	1,5629	97,12		1,0858	1,0548		17,370	15,17
	#16A	0,4676	0,4374	93,54	93,63	1,0697	1,0015		18,420	15,25
	#16B	0,6946	0,6509	93,71		1,0772	1,0085	39,96	18,500	15,07
	#18A	0,5824	0,5392	92,58	93,00	1,0716	0,9966		19,390	14,48
	#18B	0,7024	0,6562	93,42		1,0801	1,0045		19,015	14,64
XILANA	#14A	0,5952	0,559	93,92	93,64	1,0821	1,0133	39,865	15,715	16,95
	#14B	0,6068	0,5665	93,36		1,0883	1,0191		16,000	16,63
	#16A	0,6345	0,5937	93,57	93,86	1,0730	1,0071		15,285	17,30
	#16B	0,8734	0,8223	94,15		1,0900	1,0231	39,865	16,000	16,50
	#18A	0,4716	0,4391	93,11	93,42	1,0687	0,9983	40,075	13,950	18,63
	#18B	0,4572	0,4285	93,72		1,0961	1,0239		13,150	18,72
	#16P2	0,3623	0,3345	92,33	92,36	1,0723	0,9904	40,54	14,800	18,49
	#16P2	0,3983	0,368	92,39		1,074	0,9919		14,900	18,39

Quadro 6B. Análises de Pentosanas no EP.

Identificação da amostra		CONSISTÊNCIA (%)				PENTOSANAS (%)				
		Peso úmido (g)	Peso Seco(g)	Consistência(%)	Média CST (%)	Peso úmido (g)	Peso Seco(g)	PB	Vol. Tit. (mL)	Pentosanas (%)
REFERÊNCIA	#14A	0,3961	0,3658	92,35	92,36	1,0744	0,9923	40,075	19,900	14,25
	#14B	0,4298	0,397	92,37		1,0962	1,0124		20,100	13,80
	#16A	0,5959	0,5455	91,54	91,52	1,0722	0,9813		19,580	14,53
	#16B	0,8745	0,8002	91,50		1,0828	0,9910	39,895	19,145	14,70
	#18A	0,6022	0,5514	91,56	91,50	1,0801	0,9883		18,990	14,86
	#18B	0,7714	0,7053	91,43		1,0748	0,9834		19,915	14,24
XILANA	#14A	0,3851	0,3526	91,56	91,71	1,0796	0,9901	40,205	16,315	17,10
	#14B	0,4006	0,368	91,86		1,0756	0,9864		17,100	16,57
	#16A	0,4706	0,4313	91,65	91,56	1,0869	0,9952		16,520	16,85
	#16B	0,5755	0,5264	91,47		1,0745	0,9838	40,54	16,765	16,87
	#18A	0,46	0,4202	91,35	91,48	1,0863	0,9937		15,590	17,83
	#18B	0,3696	0,3386	91,61		1,0845	0,9921		15,245	18,12
	#16P2	0,8819	0,8113	91,99	91,97	1,0844	0,9973	40,48	15,985	17,42
	#16P2	0,5161	0,4745	91,94		1,0747	0,9884		16,815	16,96

Quadro 7B. Análises de Pentosanas no D1.

Identificação da amostra		CONSISTÊNCIA (%)				PENTOSANAS (%)				
		Peso úmido (g)	Peso Seco(g)	Consistência(%)	Média CST (%)	Peso úmido (g)	Peso Seco(g)	PB	Vol. Tit. (mL)	Pentosanas (%)
XILANA	#16A D4	0,8132	0,7609	93,57	93,48	1,0795	1,0091	40,595	17,850	15,90
	#16B D4	0,7554	0,7055	93,39		1,0764	1,0062	40585	17,500	16,21
	#18A D4	0,6726	0,6275	93,29	93,34	1,0788	1,0069		15,945	17,36
	#18B D4	0,533	0,4977	93,38		1,0734	1,0019		16,865	16,76
	#16P2 D14	0,3665	0,3382	92,28	92,67	1,0702	0,9918	40,48	16,480	17,15
	#16P2 D14	0,4313	0,4014	93,07		1,0799	1,0008		16,510	16,96

Quadro 8B. Análises de Pentosanas no P.

Identificação da amostra		CONSISTÊNCIA (%)			PENTOSANAS (%)				
		Peso úmido (g)	Peso Seco(g)	Consistência(%)	Peso úmido (g)	Peso Seco(g)	PB	Vol. Tit. (mL)	Pentosanas (%)
REFERÊNCIA	#14A	0,6602	0,6205	93,99	1,0658	1,0017		21,630	13,54
	#14B	0,7324	0,6909	94,33	1,0605	1,0004	41,055	21,285	13,82
	#16A	0,7043	0,6615	93,92	1,0652	1,0005		19,640	15,05
	#16B	0,8722	0,8218	94,22	1,0614	1,0001		19,150	15,03
	#18A	0,7032	0,6594	93,77	1,0665	1,0001	40,52	19,625	14,67
	#18B	0,8336	0,7821	93,82	1,0669	1,0010		19,590	14,68
XILANA	#14A	0,4017	0,3834	95,44	1,0699	1,0212		16,655	16,85
	#14B	0,5014	0,4749	94,71	1,0726	1,0159	40,96	16,315	17,05
	#16A	0,6018	0,575	95,55	1,0708	1,0231		17,085	16,50
	#16B	0,6828	0,6534	95,69	1,0730	1,0268		16,870	16,46
	#18A	0,5306	0,5059	95,34	1,0705	1,0207	40,77	17,100	16,53
	#18B	0,5673	0,5389	94,99	1,0728	1,0191		16,925	16,55

Quadro 9B. Análises de carboidratos.

Amostras	Rep.	Carboidratos, %				
		Arabinanas	Galactanas	Glicanas	Xilanas	Mananas
14 UKP - Origem	A	0,0	0,1	77,8	14,4	0,1
	B	0,0	0,1	77,4	14,6	0,1
	Média	0,0	0,1	77,6	14,5	0,1
14 PreO2 - Ref	A	0,0	0,1	78,6	13,8	0,1
	B	0,0	0,1	78,5	13,7	0,1
	Média	0,0	0,1	78,6	13,8	0,1
14 Do - Ref	A	0,0	0,1	81,2	14,4	0,1
	B	0,0	0,1	80,8	14,5	0,1
	Média	0,0	0,1	81,0	14,5	0,1
14 D1 - Ref	A	0,0	0,1	79,6	14,1	0,1
	B	0,0	0,1	79,3	13,9	0,1
	Média	0,0	0,1	79,5	14,0	0,1
14 EP - Ref	A	0,0	0,1	79,6	14,0	0,1
	B	0,0	0,1	79,4	14,0	0,1
	Média	0,0	0,1	79,5	14,0	0,1
14 PF - Ref	A	0,0	0,1	81,1	14,4	0,2
	B	0,0	0,1	82,1	14,6	0,1
	Média	0,0	0,1	81,6	14,5	0,2
14 PreO2 - Xilana	A	0,0	0,1	74,6	17,3	0,1
	B	0,0	0,1	75,7	16,9	0,1
	Média	0,0	0,1	75,2	17,1	0,1
14 Do - Xilana	A	0,0	0,1	74,2	16,6	0,1
	B	0,0	0,1	74,5	16,5	0,1
	Média	0,0	0,1	74,4	16,6	0,1
14 D1 - Xilana	A	0,0	0,1	75,8	16,1	0,1
	B	0,0	0,1	75,1	15,9	0,1
	Média	0,0	0,1	75,5	16,0	0,1
14 EP - Xilana	A	0,0	0,1	73,0	15,8	0,1
	B	0,0	0,1	72,8	15,6	0,1
	Média	0,0	0,1	72,9	15,7	0,1
14 PF - Xilana	A	0,0	0,1	74,7	15,2	0,1
	B	0,0	0,1	75,0	15,4	0,1
	Média	0,0	0,1	74,9	15,3	0,1
16 UKP - Origem	A	0,0	0,1	79,1	15,1	0,2
	B	0,0	0,2	79,6	15,1	0,2
	Média	0,0	0,2	79,4	15,1	0,2
16 PreO2 - Ref	A	0,0	0,1	82,2	14,8	0,2
	B	0,0	0,1	81,3	14,7	0,2
	Média	0,0	0,1	81,8	14,8	0,2
16 Do - Ref	A	0,0	0,1	80,7	14,5	0,2
	B	0,0	0,1	79,6	14,4	0,2

	Média	0,0	0,1	80,2	14,5	0,2
16 D1 - Ref	A	0,0	0,1	72,9	12,7	0,1
	B	0,0	0,1	73,3	12,7	0,1
	Média	0,0	0,1	73,1	12,7	0,1
16 EP - Ref	A	0,0	0,1	72,5	12,8	0,1
	B	0,0	0,1	73,2	12,9	0,2
	Média	0,0	0,1	72,9	12,9	0,2
16 PF - Ref	A	0,0	0,1	76,6	13,4	0,1
	B	0,0	0,1	76,0	13,0	0,1
	Média	0,0	0,1	76,3	13,2	0,1
16 PreO2 - Xilana	A	0,0	0,1	71,1	15,9	0,1
	B	0,0	0,1	71,4	15,9	0,1
	Média	0,0	0,1	71,3	15,9	0,1
16 Do - Xilana	A	0,0	0,1	71,0	15,9	0,1
	B	0,0	0,1	71,0	15,9	0,1
	Média	0,0	0,1	71,0	15,9	0,1
16 D1 - Xilana	A	0,0	0,0	72,6	15,3	0,1
	B	0,0	0,1	72,7	15,3	0,1
	Média	0,0	0,1	72,7	15,3	0,1
16 EP - Xilana	A	0,0	0,1	71,2	15,3	0,1
	B	0,0	0,1	71,5	15,3	0,1
	Média	0,0	0,1	71,4	15,3	0,1
16 PF - Xilana	A	0,0	0,1	73,7	14,9	0,1
	B	0,0	0,1	73,4	14,9	0,1
	Média	0,0	0,1	73,6	14,9	0,1
16 (P2) O2 - Xilana	A	0,1	0,1	77,1	18,1	0,2
	B	0,1	0,0	77,0	17,8	0,1
	Média	0,1	0,1	77,1	18,0	0,2
16 (P2) Do - Xilana	A	0,0	0,1	75,5	17,9	0,2
	B	0,0	0,1	76,0	17,9	0,2
	Média	0,0	0,1	75,8	17,9	0,2
16 (P2) D1	A	0,0	0,0	77,0	16,4	0,1
	B	0,0	0,1	76,2	17,0	0,1
	Média	0,0	0,1	76,6	16,7	0,1
16 (P2) EP - Xilana	A	0,1	0,1	77,1	17,3	0,2
	B	0,0	0,1	76,3	16,7	0,2
	Média	0,1	0,1	76,7	17,0	0,2
16 P2 - PF	A	0,0	0,1	77,0	16,7	0,2
	B	0,0	0,1	77,7	16,9	0,2
	Média	0,0	0,1	77,4	16,8	0,2
18 UKP - Origem	A	0,0	0,2	74,0	13,4	0,1
	B	0,0	0,2	74,5	13,5	0,1
	Média	0,0	0,2	74,3	13,5	0,1
18 B PreO2	A	0,0	0,2	75,2	13,9	0,1
	B	0,0	0,2	76,0	14,1	0,1

	Média	0,0	0,2	75,6	14,0	0,1
18 Do - Ref	A	0,0	0,1	74,2	12,9	0,1
	B	0,0	0,1	74,5	13,5	0,1
	Média	0,0	0,1	74,4	13,2	0,1
18 D1 - Ref	A	0,0	0,1	73,7	12,6	0,1
	B	0,0	0,1	73,7	12,7	0,1
	Média	0,0	0,1	73,7	12,7	0,1
18 EP - Ref	A	0,0	0,1	74,6	12,9	0,1
	B	0,0	0,1	75,4	13,0	0,1
	Média	0,0	0,1	75,0	13,0	0,1
18 PF - Ref	A	0,0	0,1	75,6	13,0	0,1
	B	0,0	0,1	75,7	12,9	0,1
	Média	0,0	0,1	75,7	13,0	0,1
18 PreO2 - Xilana	A	0,0	0,2	67,5	15,1	0,1
	B	0,0	0,2	67,4	15,2	0,1
	Média	0,0	0,2	67,5	15,2	0,1
18 Do - Xilana	A	0,1	0,2	74,4	18,7	0,2
	B	0,1	0,0	74,3	17,5	0,2
	Média	0,1	0,1	74,4	18,1	0,2
18 D1 - Xilana	A	0,1	0,0	76,7	16,9	0,2
	B	0,0	0,1	75,8	16,8	0,1
	Média	0,1	0,1	76,3	16,9	0,2
18 EP - Xilana	A	0,0	0,1	70,1	14,8	0,1
	B	0,0	0,1	69,3	14,7	0,1
	Média	0,0	0,1	69,7	14,8	0,1
18 PF - Xilana	A	0,0	0,1	75,4	16,2	0,2
	B	0,0	0,1	75,3	16,1	0,1
	Média	0,0	0,1	75,4	16,2	0,2
Filtrado	A	0,0	0,1	0,1	7,7	0,0
	B	0,0	0,1	0,2	8,0	0,0
	Média	0,0	0,1	0,2	7,9	0,0

Quadro 10B. Dados de branqueamento, polpa de referência, kappa 14 (A).

Identificação:	**Nº KAPPA 14,0 - REFERENCIA (A)**							**Número:**	
Produção tsa.h^{-1}	**88**	**CARGA DE OXIGÊNIO FIXA ? (S/N)**		**N**				**Data:**	
Dados Polpa Origem									
Viscosidade	**Kappa**		**Alvura**		**HexA's**		**DQO**	**Metais, kg/t**	
mPa.s	Nº		% ISO		mmol/kg		kg/tsa	Ca Mg Fe Mn Cu	
	14,02		38,56						

Estágios	**OO**		**Do**	**EP**	**D_1**	**D_1**	**D_1**	**P**	**P**	**P**
Determinação	**R1**	**R2**								
Peso Úmido total, g	828,1		713,9	624,0	175,3	175,3	175,3	153,4	155,6	151,3
Peso seco, g	250,0		221,85	196,68	55	55	55	46	46	46
CST inicial, %	30,19		31,1	31,5	31,4	31,4	31,4	30,0	29,6	30,4
Reagente de ajuste	**NaOH**		**NaOH**	**NaOH**	**NaOH**	**NaOH**	**NaOH**	**NaOH**	**NaOH**	**NaOH**
Kg/tsa	10,0		2,6	11,2	0,51	1,2	2,1	2,05	2,1	2,1
Conc. solução, g L^{-1}	174,80		20	20	20	20	20	20	20	20
Vol. solução, mL	**15,89**		**32,0**	**122,4**	**1,6**	**3,7**	**6,4**	**5,2**	**5,4**	**5,4**
Reagente oxidante	**O_2**		**ClO_2**	**H_2O_2**	**ClO_2**	**ClO_2**	**ClO_2**	**H_2O_2**	**H_2O_2**	**H_2O_2**
Kg/tsa	**15,4**		17,23	3	2	4	6	3	3	3
Conc. solução, g L^{-1}	-		23,72	28,92	22,76	22,76	22,76	28,49	28,49	28,49
Vol, mL/Press.O_2, kgf cm^{-2}	**3,5**		**179,0**	**22,7**	**5,37**	**10,74**	**16,11**	**5,38**	**5,38**	**5,38**
Reagente	**$MgSO_4$**									
Kg/tsa										
Conc. solução, g/L										
Vol. solução, mL	0,0		0	0	0	0	0	0	0	0
Filtrado a adicionar, mL	1500		0,0	0,0	0,0	0,0	0,0	0,0	0,0	0,0
H_2O a adicionar, mL	156,0		1293,5	1197,8	367,7	360,3	352,1	295,9	293,6	297,9
CST. do branqto, %	**10**		**10**	**10**	**10**	**10**	**10**	**10**	**10**	**10**
Tempo retenção, min	25	35	113	105	222	222	222	120	120	120
Temperatura, °C	95	100	75	80	80	80	80	80	80	80
pH inicial	-		**11,4**	**12,1/11,4**	**9,0**	**11,0**	**11,6**	**11,4/10,5**	**11,2/10,5**	**11,2/10,7**
pH final	**10,7**		**3,4**	**11,0**	**5,0**	**5,0**	**5,3**	**10,1**	**9,6**	**10,3**
H_2O de lavag. m^3 tsa^{-1}								-	-	-
Rendimento,%	98,83		99,0	99,2	99,7	99,5	98,7	98,9	100,0	98,6
Vol. alíq. p/ res., mL			100	100	100	100	100	100	100	100
Vol.Cons. $Na_2S_2O_3$, mL	-		0	0,14	0,44	0	1,88	1,655	0,15	0,56
Consumo, %	-		100,00	99,36	93,67	100,00	90,99	92,40	99,31	97,43
Peso Úmido pós, g	791		703,70	603,43	182,94	185,06	178,65	147,0	149,9	154,1
Kappa / µKappa / NP, Nº	**8,7**		**3,94**	**3,19**	**2,07**	**1,64**	**1,56**	**2,05**	**1,71**	**1,51**
Viscosidade, mPa.s	**21,02**		**17,19**	**13,08**	**13,73**	**18,36**	**12,57**	12,98	12,55	12,43
Alvura A.D., % ISO	**55,82**		**75,4**	**82,8**	**86,2**	**87,5**	**88,1**	87,8	88,9	89,1
Alvura O.D., % ISO	-		-	-	-	-	-	84,3	85,4	85,4

Observações:

Fator Kappa = **0,22**

Quadro 11B. Dados de branqueamento, polpa de referência, kappa 14 (B).

Identificação:	**Nº KAPPA 14,0 - REFERENCIA (B)**							**Número:**	
Produção tsa.h^{-1}	**88**	**CARGA DE OXIGÊNIO FIXA ? (S/N)**		**N**				**Data:**	
Dados Polpa Origem									
Viscosidade	**Kappa**	**Alvura**		**HexA's**		**DQO**		**Metais, kg/t**	
mPa.s	Nº	% ISO		mmol/kg		kg/tsa		Ca Mg Fe Mn Cu	
	14,02	38,56							

Estágios	**OO**		**Do**	**EP**	**D_1**	**D_1**	**D_1**	**P**	**P**	**P**
Determinação	**R1**	**R2**								
Peso Úmido total, g	828,1		713,9	624,0	175,3	175,3	175,3	155,6	155,8	158,2
Peso seco, g	250,0		221,85	196,68	55	55	55	46	46	46
CST inicial, %	30,19		31,1	31,5	31,4	31,4	31,4	29,6	29,5	29,1
Reagente de ajuste	**NaOH**		**NaOH**	**NaOH**	**NaOH**	**NaOH**	**NaOH**	**NaOH**	**NaOH**	**NaOH**
Kg/tsa	10,1		3	11	0,51	1,36	2,15	2,1	2,25	2,1
Conc. solução, g L^{-1}	174,80		20	20	20	20	20	20	20	20
Vol. solução, mL	**16,05**		**37,0**	**120,2**	**1,6**	**4,2**	**6,6**	**5,4**	**5,8**	**5,4**
Reagente oxidante	**O_2**		**ClO_2**	**H_2O_2**	**ClO_2**	**ClO_2**	**ClO_2**	**H_2O_2**	**H_2O_2**	**H_2O_2**
Kg/tsa	**15,4**		17,23	3	2	4	6	3	3	3
Conc. solução, g L^{-1}	-		23,14	29,02	22,63	22,63	22,63	28,08	28,08	28,08
Vol, mL/Press.O_2, kgf cm^{-2}	**3,5**		**183,5**	**22,6**	**5,40**	**10,80**	**16,20**	**5,46**	**5,46**	**5,46**
Reagente	**$MgSO_4$**									
Kg/tsa										
Conc. solução, g/L										
Vol. solução, mL	0,0		0	0	0	0	0	0	0	0
Filtrado a adicionar, mL	-		0,0	0,0	0,0	0,0	0,0	0,0	0,0	0,0
H_2O a adicionar, mL	1655,9		1284,1	1200,0	367,7	359,7	351,9	293,6	293,0	291,0
CST. do branqto, %	**10**		**10**	**10**	**10**	**10**	**10**	**10**	**10**	**10**
Tempo retenção, min	25	35	113	105	222	222	222	120	120	120
Temperatura, °C	95	100	75	80	80	80	80	80	80	80
pH inicial	-		**11,6**	**12/11,3**	**8,7**	**11,2**	**11,6**	**11,5/10,8**	**11,2/10,7**	**11,3/10,7**
pH final	**10,7**		**3,7**	**10,9**	**5,8**	**6,0**	**5,6**	**10,6**	**9,8**	**10**
H_2O de lavag. m^3 tsa^{-1}								-	-	-
Rendimento,%	0		0	0	0	0	0	-	-	-
Vol. alíq. p/ res., mL	98,83		99,2	99,6	99,6	100,0	99,9	100,0	99,7	99,0
Vol.Cons. $Na_2S_2O_3$, mL	-		100	100	100	100	100	100	100	100
Consumo, %	-		0	0	0,71	3,44	2,98	0,08	1,21	1,51
Peso Úmido pós, g	-		100,00	100,00	89,79	75,27	85,72	99,63	94,45	93,07
Kappa / µKappa / NP, Nº	797,26		691,70	643,74	185,52	186,33	188,87	144,7	140,6	153,6
Viscosidade, mPa.s	**8,7**		**3,76**	**3,42**	**1,92**	**2,01**	**1,7**	**2,1**	**2,06**	**1,63**
Alvura A.D., % ISO	**21,04**		**18,21**	**13,91**				12,91	11,89	13,56
Alvura O.D., % ISO	**55,82**		**75,6**	**80,8**	**86,7**	**87,5**	**88,3**	**87,7**	**88,9**	**89,1**
Alvura O.D., % ISO	-		-	-	-	-	-	83,55	84,09	86,01

Observações:

Fator Kappa = **0,22**

Quadro 12B. Dados de branqueamento, polpa de referência, kappa 16 (A).

Identificação:	**Nº KAPPA 16,0 - REFERENCIA (A)**							**Número:**	
Produção tsa.h^{-1}	**88**	**CARGA DE OXIGÊNIO FIXA ? (S/N)**		**N**				**Data:**	
Dados Polpa Origem									
Viscosidade	**Kappa**	**Alvura**		**HexA's**		**DQO**		**Metais, kg/t**	
mPa.s	Nº	% ISO		mmol/kg		kg/tsa		Ca Mg Fe Mn Cu	
	16,05	37,18							

Estágios	**OO**		**Do**	**EP**	**D_1**	**D_1**	**D_1**	**P**	**P**	**P**
Determinação	**R1**	**R2**								
Peso Úmido total, g	866,3		730,5	650,0	184,7	184,7	184,7	164,8	163,1	171,6
Peso seco, g	250,0		220,95	195,9	55	55	55	46	46	46
CST inicial, %	28,86		30,2	30,1	29,8	29,8	29,8	27,9	28,2	26,8
Reagente de ajuste	**NaOH**		**NaOH**	**NaOH**	**NaOH**	**NaOH**	**NaOH**	**NaOH**	**NaOH**	**NaOH**
Kg/tsa	11,1		2,6	11,6	0,54	1,3	2,1	2,25	2,08	2,25
Conc. solução, g L^{-1}	174,80		20	20	20	20	20	20	20	20
Vol. solução, mL	**17,64**		**31,9**	**126,2**	**1,7**	**4,0**	**6,4**	**5,8**	**5,3**	**5,8**
Reagente oxidante	**O_2**		**ClO_2**	**H_2O_2**	**ClO_2**	**ClO_2**	**ClO_2**	**H_2O_2**	**H_2O_2**	**H_2O_2**
Kg/tsa	**17,7**		19,72	3	2	4	6	3	3	3
Conc. solução, g L^{-1}	-		23,72	28,92	22,76	22,76	22,76	28,49	28,49	28,49
Vol, mL/Press.O_2, kgf cm^{-2}	**4,1**		**204,1**	**22,6**	**5,37**	**10,74**	**16,11**	**5,38**	**5,38**	**5,38**
Reagente	**$MgSO_4$**									
Kg/tsa										
Conc. solução, g/L										
Vol. solução, mL	0,0		0	0	0	0	0	0	0	0
Filtrado a adicionar, mL	-		0,0	0,0	0,0	0,0	0,0	0,0	0,0	0,0
H_2O a adicionar, mL	1616,1		1242,9	1160,2	358,2	350,5	342,7	284,1	286,2	277,2
CST. do branqto, %	**10**		**10**	**10**	**10**	**10**	**10**	**10**	**10**	**10**
Tempo retenção, min	25	35	113	105	222	222	222	120	120	120
Temperatura, °C	95	100	75	80	80	80	80	80	80	80
pH inicial	-		**11,4**	**12,1/11,2**	**9**	**11,1**	**11,6**	**11,3/10,6**	**11,2/10,4**	**11,3/10,7**
pH final	**11,0**		**3,5**	**11,0**	**6**	**5,2**	**5,7**	**10**	**9,7**	**10,3**
H_2O de lavag. m^3 tsa^{-1}								**-**	**-**	**-**
Rendimento,%	0		0	0	0	0	0	**-**	**-**	**-**
Vol. alíq. p/ res., mL	98,09		99,1	99,0	99,9	99,7	99,3	98,5	100,0	97,5
Vol.Cons. $Na_2S_2O_3$, mL			100	100	100	100	100	100	100	100
Consumo, %	**-**		0	0,13	0,57	0,24	3,66	0,66	4,18	0,09
Peso Úmido pós, g	**-**		100,00	99,40	91,80	98,27	82,46	96,97	80,81	99,59
Kappa / µKappa / NP, Nº	809,77		729,30	634,96	196,70	194,47	203,72	153,2	157,1	166,4
Viscosidade, mPa.s	**9,96**		**4,29**	**3,51**	**2,26**	**1,45**	**1,74**	**2,14**	**1,68**	**1,54**
Alvura A.D., % ISO	**28,59**		**18,47**	**19,83**	**22,3**	**13,63**	**18,31**			
Alvura O.D., % ISO	**56,32**		**76,0**	**82,7**	**86,3**	**87,6**	**88,0**	**87,8**	**88,7**	**89,4**
Alvura O.D., % ISO	**-**		**-**	**-**	**-**	**-**	**-**	83,19	85,75	85,2

Observações:

Fator Kappa = **0,22**

Quadro 13B. Dados de branqueamento, polpa de referência, kappa 16 (B).

Identificação:	**Nº KAPPA 16,0 - REFERENCIA (B)**							**Número:**	
Produção tsa.h^{-1}	**88**	**CARGA DE OXIGÊNIO FIXA ? (S/N)**		**N**				**Data:**	
Dados Polpa Origem									
Viscosidade	**Kappa**	**Alvura**		**HexA's**		**DQO**		**Metais, kg/t**	
mPa.s	Nº	% ISO		mmol/kg		kg/tsa		Ca Mg Fe Mn Cu	
	16,05	37,18							

Estágios	**OO**		**Do**	**EP**	**D_1**	**D_1**	**D_1**	**P**	**P**	**P**
Determinação	**R1**	**R2**								
Peso Úmido total, g	866,3		730,5	650,0	184,7	184,7	184,7	160,4	158,6	163,9
Peso seco, g	250,0		220,95	195,9	55	55	55	46	46	46
CST inicial, %	28,86		30,2	30,1	29,8	29,8	29,8	28,7	29,0	28,1
Reagente de ajuste	**NaOH**		**NaOH**	**NaOH**	**NaOH**	**NaOH**	**NaOH**	**NaOH**	**NaOH**	**NaOH**
Kg/tsa	10,9		3	11,4	0,51	1,3	2,1	2,25	2,5	2,25
Conc. solução, g L^{-1}	174,80		20	20	20	20	20	20	20	20
Vol. solução, mL	**17,32**		**36,8**	**124,1**	**1,6**	**4,0**	**6,4**	**5,8**	**6,4**	**5,8**
Reagente oxidante	**O_2**		**ClO_2**	**H_2O_2**	**ClO_2**	**ClO_2**	**ClO_2**	**H_2O_2**	**H_2O_2**	**H_2O_2**
Kg/tsa	**17,7**		19,64	3	2	4	6	3	3	3
Conc. solução, g L^{-1}	-		23,14	29,02	22,63	22,63	22,63	28,08	28,08	28,08
Vol, mL/Press.O_2, kgf cm^{-2}	**4,1**		**208,4**	**22,5**	**5,40**	**10,80**	**16,20**	**5,46**	**5,46**	**5,46**
Reagente	**$MgSO_4$**									
Kg/tsa										
Conc. solução, g/L										
Vol. solução, mL	0,0		0	0	0	0	0	0	0	0
Filtrado a adicionar, mL	-		0,0	0,0	0,0	0,0	0,0	0,0	0,0	0,0
H_2O a adicionar, mL	1616,4		1233,8	1162,5	358,3	350,5	342,6	288,3	289,6	284,9
CST. do branqto, %	**10**		**10**	**10**	**10**	**10**	**10**	**10**	**10**	**10**
Tempo retenção, min	25	35	113	105	222	222	222	120	120	120
Temperatura, °C	95	100	75	80	80	80	80	80	80	80
pH inicial	-		**11,6**	**12/11,1**	**8,8**	**11,2**	**11,5**	**11,4/10,6**	**11/10,5**	**11,5/10,6**
pH final	**10,7**		**3,7**	**10,9**	**6**	**5,5**	**5,7**	**10,2**	**9,8**	**10,2**
H_2O de lavag. m^3 tsa^{-1}								**-**	**-**	**-**
Rendimento,%	0		0	0	0	0	0	**-**	**-**	**-**
Vol. alíq. p/ res., mL	98,25		99,40	99,10	99,90	100,00	100,00	97,42	100,00	97,47
Vol.Cons. $Na_2S_2O_3$, mL			100		100	100	100	100	100	100
Consumo, %	**-**		0		1,12	1,76	3,35	0,93	2,86	0,09
Peso Úmido pós, g	**-**		100,00		83,90	87,35	83,95	95,73	86,87	99,59
Kappa / µKappa / NP, Nº	813,12		874,96	669,16	191,59	189,53	195,88	158,6	151,2	152,3
Viscosidade, mPa.s	**9,92**		**4,08**	**3,38**	**2,24**	**1,79**	**1,97**	**2,15**	**1,66**	**1,86**
Alvura A.D., % ISO	**30,26**		**18,67**	**20,26**						
Alvura O.D., % ISO	**56,6**		**76,4**	**82,6**	**86,4**	**87,6**	**88,2**	**88,1**	**89,0**	**89,2**
Alvura O.D., % ISO	**-**		**-**	**-**	**-**	**-**	**-**	82,77	84,25	84,68

Observações:

Fator Kappa = **0,22**

Quadro 14B. Dados de branqueamento, polpa de referência, kappa 18 (A).

Identificação:	**Nº KAPPA 18,0 - REFERENCIA (B)**								**Número:**	
Produção tsa.h^{-1}	**88**	**CARGA DE OXIGÊNIO FIXA ? (S/N)**		**N**					**Data:**	
Dados Polpa Origem										
Viscosidade	**Kappa**		**Alvura**		**HexA's**		**DQO**		**Metais, kg/t**	
mPa.s	Nº		% ISO		mmol/kg		kg/tsa		Ca Mg Fe Mn Cu	
	17,91		36,03							
Estágios	**OO**		**Do**	**EP**	**D_1**	**D_1**	**D_1**	**P**	**P**	**P**
Determinação	**R1**	**R2**								
Peso Úmido total, g	890,9		752,6	668,0	180,6	180,6	180,6	174,2	164,6	166,4
Peso seco, g	250,0		219,58	196,6	55	55	55	46	46	46
CST inicial, %	28,06		29,2	29,4	30,5	30,5	30,5	26,4	28,0	27,7
Reagente de ajuste	**NaOH**		**NaOH**	**NaOH**	**NaOH**	**NaOH**	**NaOH**	**NaOH**	**NaOH**	**NaOH**
Kg/tsa	12,0		2,6	11,6	0,51	1,2	2,1	2,4	2,25	2,1
Conc. solução, g L^{-1}	174,80		20	20	20	20	20	20	20	20
Vol. solução, mL	**19,07**		**31,7**	**126,7**	**1,6**	**3,7**	**6,4**	**6,1**	**5,8**	**5,4**
Reagente oxidante	**O_2**		**ClO_2**	**H_2O_2**	**ClO_2**	**ClO_2**	**ClO_2**	**H_2O_2**	**H_2O_2**	**H_2O_2**
Kg/tsa	**19,7**		21,32	3	2	4	6	3	3	3
Conc. solução, g L^{-1}	-		23,72	28,92	22,76	22,76	22,76	28,49	28,49	28,49
Vol, mL/Press.O_2, kgf cm^{-2}	**4,5**		**219,3**	**22,7**	**5,37**	**10,74**	**16,11**	**5,38**	**5,38**	**5,38**
Reagente	**$MgSO_4$**									
Kg/tsa										
Conc. solução, g/L										
Vol. solução, mL	0,0		0	0	0	0	0	0	0	0
Filtrado a adicionar, mL	-		0,0	0,0	0,0	0,0	0,0	0,0	0,0	0,0
H_2O a adicionar, mL	1590,0		1192,1	1148,6	362,4	355,0	346,8	274,2	284,3	282,9
CST. do branqto, %	**10**		**10**	**10**	**10**	**10**	**10**	**10**	**10**	**10**
Tempo retenção, min	25	35	113	105	222	222	222	120	120	120
Temperatura, °C	95	100	75	80	80	80	80	80	80	80
pH inicial	-		**11,3**	**12,2/11,3**	**8,9**	**11,1**	**11,6**	**11,3/10,8**	**11,3/10,7**	**11,1/10,5**
pH final	**11,0**		**3,5**	**11,0**	**5,8**	**5,2**	**5,5**	**10,6**	**10,4**	**9,8**
H_2O de lavag. m^3 tsa^{-1}								**-**	**-**	**-**
Rendimento,%	0		0	0	0	0	0	**-**	**-**	**-**
Vol. alíq. p/ res., mL	97,63		99,90	98,50	100,00	99,40	99,90	98,90	96,20	100,00
Vol.Cons. $Na_2S_2O_3$, mL			100	100	100	100	100	100	100	100
Consumo, %	**-**		0	0,105	0,7	0,8	3,29	1,59	0,11	2,88
Peso Úmido pós, g	**-**		100,00	99,52	89,94	94,25	84,23	92,70	99,50	86,78
Kappa / µKappa / NP, Nº	825,05		743,60	641,84	208,36	203,20	198,80	169,5	161,5	156,5
Viscosidade, mPa.s	**10,77**		**4,06**	**3,24**	**2,2**	**1,71**	**1,64**	**2,2**	**1,51**	**1,52**
Alvura A.D., % ISO	**33,78**		**21,16**	**18,71**	**18,79**	**19,16**	**19,4**			
Alvura O.D., % ISO	**54,51**		**74,0**	**80,7**	**86,5**	**87,9**	**88,4**	**87,8**	**88,7**	**89,2**
Alvura O.D., % ISO	**-**		**-**	**-**	**-**	**-**	**-**	82,63	84,73	85,41

Observações:

Fator Kappa = **0,22**

Quadro 15B. Dados de branqueamento, polpa de referência, kappa 18 (B).

Identificação:	**Nº KAPPA 18,0 - REFERENCIA (B)**							**Número:**	
Produção tsa.h^{-1}	**88**	**CARGA DE OXIGÊNIO FIXA ? (S/N)**		**N**				**Data:**	
Dados Polpa Origem									
Viscosidade	**Kappa**		**Alvura**		**HexA's**		**DQO**	**Metais, kg/t**	
mPa.s	Nº		% ISO		mmol/kg		kg/tsa	Ca Mg Fe Mn Cu	
	17,91		36,03						

Estágios	**OO**		**Do**	**EP**	**D_1**	**D_1**	**D_1**	**P**	**P**	**P**
Determinação	**R1**	**R2**								
Peso Úmido total, g	890,9		752,6	668,0	180,6	180,6	180,6	159,9	164,6	156,0
Peso seco, g	250,0		219,58	196,6	55	55	55	46	46	46
CST inicial, %	28,06		29,2	29,4	30,5	30,5	30,5	28,8	28,0	29,5
Reagente de ajuste	**NaOH**		**NaOH**	**NaOH**	**NaOH**	**NaOH**	**NaOH**	**NaOH**	**NaOH**	**NaOH**
Kg/tsa	11,9		3	11,4	0,51	1,3	2,1	2,25	2,25	2,25
Conc. solução, g L^{-1}	174,80		20	20	20	20	20	20	20	20
Vol. solução, mL	**18,91**		**36,6**	**124,5**	**1,6**	**4,0**	**6,4**	**5,8**	**5,8**	**5,8**
Reagente oxidante	**O_2**		**ClO_2**	**H_2O_2**	**ClO_2**	**ClO_2**	**ClO_2**	**H_2O_2**	**H_2O_2**	**H_2O_2**
Kg/tsa	**19,7**		21,32	3	2	4	6	3	3	3
Conc. solução, g L^{-1}	-		23,14	29,02	22,63	22,63	22,63	28,08	28,08	28,08
Vol, mL/Press.O_2, kgf cm^{-2}	**4,5**		**224,8**	**22,6**	**5,40**	**10,80**	**16,20**	**5,46**	**5,46**	**5,46**
Reagente	**$MgSO_4$**									
Kg/tsa										
Conc. solução, g/L										
Vol. solução, mL	0,0		0	0	0	0	0	0	0	0
Filtrado a adicionar, mL	-		0,0	0,0	0,0	0,0	0,0	0,0	0,0	0,0
H_2O a adicionar, mL	1590,1		1181,7	1150,9	362,4	354,6	346,8	288,8	284,2	292,8
CST. do branqto, %	**10**		**10**	**10**	**10**	**10**	**10**	**10**	**10**	**10**
Tempo retenção, min	25	35	113	105	222	222	222	120	120	120
Temperatura, °C	95	100	75	80	80	80	80	80	80	80
pH inicial	-		**11,5**	**12,1/11,1**	**8,9**	**11,1**	**11,5**	**11,3/10,7**	**11,3/10,5**	**11,3/10,7**
pH final	**10,8**		**3,6**	**10,8**	**6,0**	**5,5**	**5,5**	**10,1**	**10,2**	**10,2**
H_2O de lavag. m^3 tsa^{-1}								-	-	-
Rendimento,%	0		0	0	0	0	0	-	-	-
Vol. alíq. p/ res., mL	97,36		99,40	98,60	100,00	98,40	98,80	100,00	96,20	98,40
Vol.Cons. $Na_2S_2O_3$, mL			100	100	100	100	100	100	100	100
Consumo, %	-		0	0	1,27	0,98	2,29	2,12	1,64	0,66
Peso Úmido pós, g	-		100,00	100,00	81,74	92,96	89,03	90,27	92,47	96,97
Kappa / µKappa / NP, Nº	845,97		743,32	630,63	191,32	193,67	184,41	151,5	163,0	157,6
Viscosidade, mPa.s	**10,77**		**3,91**	**3,61**	**2,18**	**1,71**	**1,5**	**2,11**	**1,63**	**1,6**
Alvura A.D., % ISO	**32,46**		**21,55**	**18,96**						
Alvura O.D., % ISO	**54,51**		**73,4**	**80,9**	**86,7**	**87,7**	**88,1**	**88,3**	**89,2**	**89,3**
Alvura O.D., % ISO	-		-	-	-	-	-	83,26	85,35	84,51

Observações:

Fator Kappa = **0,22**

Quadro 16B. Testes físicos.

Amostra	Revolução	Consumo Energia Wh	Schopper Riegler	Freeness mL	WRV g g^{-1}	Peso Esp. Aparente g m^{-3}	Vol.Esp. Aparente cm^3 g^{-1}	Índice Tração N m g^{-1}	Índice Arrebentamento kPa m^2 g^{-1}	Índice Rasgo mN m^2 g^{-1}	Alongamento %	Opacidade %	Coef. Disp. Luz m^2 kg^{-1}	Resistência Passagem de Ar s $100cm^{-3}$
REF.#K14	0	0	18	507	1,35	0,471	2,124	25,9	1,28	3,5	1,9	79,0	438	1,4
	750	9	24	431	-	0,569	1,757	52,1	2,92	7,8	3,3	76,7	386	2,4
	1500	20	28	366	-	0,629	1,590	72,3	4,25	9,0	3,7	74,5	350	5,2
	2250	30	36	273	-	0,671	1,490	85,6	5,28	9,6	4,6	72,9	317	15,4
REF.#K16	0	0	20	497	1,49	0,494	2,025	33,4	1,57	4,8	2,7	77,7	413	1,5
	750	9	27	387	-	0,603	1,658	67,5	4,08	9,4	4,3	75,1	355	4,2
	1500	19	36	283	-	0,660	1,515	90,9	5,16	10,3	4,9	72,2	311	13,7
	2250	28	49	183	-	0,708	1,412	105	6,91	10,5	5,2	69,4	271	64,0
REF.#K18	0	0	19	504	1,53	0,511	1,956	34,4	1,72	4,4	2,8	77,4	405	1,6
	750	9	27	323	-	0,584	1,712	62,8	3,61	9,9	4,6	74,8	353	3,4
	1500	19	34	295	-	0,664	1,506	90,3	5,76	10,4	5,2	72,5	306	13,1
	2250	26	47	194	-	0,705	1,418	102	7,34	10,2	5,5	69,4	273	57,9
XIL.#K14	0	0	24	429	1,41	0,476	2,101	35,8	1,95	5,1	2,9	78,7	435	1,7
	750	9	34	311	-	0,581	1,720	62,9	3,95	8,0	4,2	76,2	375	4,3
	1500	19	41	231	-	0,666	1,501	85,6	5,36	8,4	4,7	73,3	324	16,6
	2250	27	55	161	-	0,681	1,469	94,6	6,22	8,8	4,9	71,6	308	46,7
XIL.#K16	0	0	27	379	1,56	0,513	1,949	43,2	2,54	5,9	3,7	77,8	409	2,0
	750	9	41	245	-	0,635	1,576	77,2	5,02	9,7	5,0	73,8	333	11,9
	1500	17	53	159	-	0,694	1,440	94,7	6,42	8,9	5,3	71,4	290	55,9
	2250	26	67	105	-	0,718	1,392	108	7,32	8,8	5,7	69,4	272	176
XIL.#K18	0	0	28	356	1,63	0,556	1,797	49,8	2,86	7,0	4,2	76,9	395	3,4
	750	8	45	209	-	0,646	1,548	82,1	5,43	9,5	5,3	73,1	324	17,5
	1500	17	59	136	-	0,699	1,431	103	6,99	9,4	5,7	70,1	279	92,6
	2250	25	73	79	-	0,771	1,297	111	8,05	9,2	5,8	67,0	238	463
XIL.#K16(P2)	0	0	33	305	1,58	0,570	1,756	52,5	2,98	6,4	4,1	77,7	405	4,3
	750	9	44	202	-	0,631	1,586	77,1	4,83	9,0	5,3	74,8	351	15,5
	1500	19	55	145	-	0,693	1,442	98,2	6,26	8,9	5,5	72,3	305	56,9
	2250	26	67	99	-	0,739	1,353	109	7,34	8,5	5,5	69,6	273	196

Quadro 17B. Resultados dos testes de histerese.

Amostra	Ciclos	Teor de Xilanas	Freeness mL	WRV g g^{-1}	Peso Esp. Aparente g m^{-3}	Vol.Esp. Aparente cm^3 g^{-1}	Índice Tração N m g^{-1}	Índice Arrebentamento kPa m^2 g^{-1}	Índice Rasgo mN m^2 g^{-1}	Alongamento %	Opacidade %	Coef. Disp. Luz m^2 kg^{-1}	Resistência Passagem de Ar s $100cm^{-3}$	Alvura %ISO	Alvura Revertida %ISO
REF.A	Ciclo 0	15,5	430	1,36	0,504	1,984	31,0	1,49	4,8	2,1	78,6	43	2,0	86,5	85,5
	Ciclo 1		423	1,08	0,488	2,051	23,9	0,93	3,4	1,6	79,6	47	2,0	86,1	85,6
	Ciclo 2		441	0,98	0,468	2,135	20,0	0,78	2,6	1,4	78,4	47	1,6	88,6	85,7
	Ciclo 3		449	0,92	0,450	2,223	18,1	-	3,2	1,5	-	-	-	88,4	85,6
	Ciclo 4		476	0,82	0,409	2,443	15,1	-	1,9	1,3	-	-	-		
	Ciclo 5														
REF.B	Ciclo 0	15,5	435	1,37	0,525	1,904	29,7	1,30	4,7	2,2	78,2	42	2,3	87,0	85,3
	Ciclo 1		410	1,21	0,460	2,174	24,4	1,00	3,7	1,8	80,0	46	1,6	86,9	85,2
	Ciclo 2		435	0,90	0,460	2,174	25,9	1,11	3,5	1,9	78,8	45	1,5	88,6	85,5
	Ciclo 3		445	0,97	0,450	2,220	20,2	-	2,6	1,6	-	-	-	88,7	85,6
	Ciclo 4		456	0,84	0,446	2,244	14,3	-	3,4	1,1	-	-	-		
	Ciclo 5														
XIL.A	Ciclo 0	17,1	378	1,45	0,514	1,946	32,9	1,37	5,9	2,7	78,3	43	1,9	87,7	83,6
	Ciclo 1		367	1,12	0,491	2,038	25,2	7,56	4,0	2,1	-	-	-	87,6	84,0
	Ciclo 2		420	1,01	0,439	2,277	19,7	-	4,0	1,6	-	-	-	87,6	84,0
	Ciclo 3		465	0,90	0,450	2,225	17,8	-	2,5	1,6	-	-	-	87,5	83,9
	Ciclo 4		455	0,86	0,456	2,191	18,9	-	2,4	1,4	-	-	-	87,1	84,3
	Ciclo 5		463	0,83	0,432	2,317	15,2	-	1,9	1,2	-	-	-		
XIL.B	Ciclo 0	17,1	389	1,45	0,521	1,920	32,7	1,74	5,5	2,5	78,1	42	2,1	87,7	82,9
	Ciclo 1		371	1,11	0,493	2,028	25,5	7,52	4,2	1,9	-	-	-	88,0	83,5
	Ciclo 2		429	0,99	0,450	2,224	17,7	-	3,5	1,6	-	-	-	87,6	83,5
	Ciclo 3		463	1,09	0,452	2,212	18,7	-	2,6	1,5	-	-	-	87,6	84,0
	Ciclo 4		471	0,79	0,445	2,250	16,8	-	2,4	1,3	-	-	-	87,2	84,1
	Ciclo 5		459	0,80	0,434	2,306	15,6	-	2,1	1,3	-	-	-		
PE.A	0	4,6	610	1,19	0,407	2,460	-	-	1,6	-	-	-	-	89,1	87,2
	Ciclo 1		614	0,74	0,339	2,950	-	-	0,9	-	-	-	-	90,3	88,4
	Ciclo 2		622	0,69	0,333	3,006	-	-	0,9	-	-	-	-	89,8	87,9
	Ciclo 3		623	0,68	0,320	3,128	-	-	0,8	-	-	-	-	90,6	88,6
	Ciclo 4		631	0,62	0,308	3,249	-	-	0,8	-	-	-	-	90,9	89,0
	Ciclo 5		623	0,60	0,306	3,265	-	-	0,8	-	-	-	-	90,5	88,6
PE.B	0	4,6	620	1,18	0,386	2,590	-	-	1,4	-	-	-	-	89,1	87,3
	Ciclo 1		614	0,74	0,341	2,936	-	-	0,9	-	-	-	-	90,9	88,9
	Ciclo 2		621	0,68	0,324	3,087	-	-	1,0	-	-	-	-	90,8	88,8
	Ciclo 3		624	0,67	0,306	3,271	-	-	0,8	-	-	-	-	90,9	89,0
	Ciclo 4		634	0,62	0,309	3,234	-	-	0,9	-	-	-	-	91,0	89,1
	Ciclo 5		633	0,56	0,296	3,381	-	-	0,8	-	-	-	-	90,8	89,0

Para simular o fenômeno de histerese, as polpas referência, com xilanas e polpa extraída, da qual removeu-se as xilanas, foram secadas em estufa a 60 ºC por 60 minutos, em vários ciclos, sendo ao termino de cada um, umedecidas, desintegradas e avaliadas.

PE - Polpa extraída, ou seja, com baixo teor de xilanas
XIL - Polpa com redeposição de xilanas

ANEXOS DO PAPER 3

Quadro 1C. Dados do Branqueamento.

Amostra	EPO						
	H_2O_2 kg/tsa	NaOH kg/tsa	# Kappa/NP	Viscosidade mP.s	Pentosanas %	Rendimento %	Alvura % ISO
REF A	3,0	5,7	3,85	14,9	15,46	98,95	79,9
REF B	3,0	5,7	3,89	14,5	15,69	98,84	80,3
XIL A	3,0	12,3	4,04	13,0	15,83	99,69	77,7
XIL B	3,0	12,5	4,02	12,9	15,95	99,68	76,8

Amostra	D1						
	ClO_2 c/ Cl_2 kg/tsa	NaOH kg/tsa	# Kappa/NP	Viscosidade mP.s	Pentosanas %	Rendimento %	Alvura % ISO
REF A	18,0	6,2	1,22	11,0	15,71	98,64	89,3
REF B	18,0	6,2	1,00	10,8	15,21	98,37	89,5
XIL A	18,0	5,8	1,49	10,1	15,63	98,34	89,3
XIL B	18,0	5,8	1,47	10,0	15,68	97,94	89,2

Quadro 2C. Resultados dos testes físicos.

AMOSTRA: REF.A

NÍVEIS DE REFINO	UNIDADE	0	750	1500	2250
CONSUMO DE ENERGIA	Wh	0	9	18	26
FREENESS	mL	380	306	215	135
SCHOPPER RIEGLER	ºSR	27	33	44	58
ÍNDICE DE TRAÇÃO	N m g^{-1}	39,5	69,2	86,3	98,4
ALONGAMENTO	%	2,9	3,8	4,6	5,1
ÍNDICE DE ESTOURO	Kpa.m^2 g^{-1}				
ÍNDICE DE RASGO	mN.m^2 g^{-1}	6,5	7,7	7,9	8,2
DENSIDADE	g cm^{-3}	0,540	0,636	0,683	0,723
VOLUME ESPECÍFICO	cm^3 g^{-1}	1,85	1,57	1,46	1,38
RESISTÊNCIA AO AR	s 100 mL^{-1}	2,4	7,9	30,3	15,4
COEFICIENTE DISP. LUZ	cm^2 g^{-1}	40	34	31	28
OPACIDADE	%	76,8	73,7	71,6	70,8

Para :	IT 70	°SR 35
C.En.	10	11
CSF	294	289
°SR	34	35
I.T.	70	71
Al.	3,9	4,0
I.E.	0,00	0,00
I.R.	7,61	7,66
Dens.	0,639	0,644
V.Esp.	1,564	1,552
R. Ar	9,42	10,27
C. D. L	34,2	33,9
Opac.	73,4	73,2

AMOSTRA: REF.B

NÍVEIS DE REFINO	UNIDADE	0	750	1500	2250
CONSUMO DE ENERGIA	Wh	0	9	18	27
FREENESS	mL	381	310	220	140
SCHOPPER RIEGLER	ºSR	26	33	43	58
ÍNDICE DE TRAÇÃO	N m g^{-1}	37	69	83	97
ALONGAMENTO	%	3	4	5	5
ÍNDICE DE ESTOURO	Kpa.m^2 g^{-1}				
ÍNDICE DE RASGO	mN.m^2 g^{-1}	6	8	8	8
DENSIDADE	g cm^{-3}	0,552	0,629	0,685	0,746
VOLUME ESPECÍFICO	cm^3 g^{-1}	1,81	1,59	1,46	1,34
RESISTÊNCIA AO AR	s 100 mL^{-1}	2,2	8,2	30,9	155,0
COEFICIENTE DISP. LUZ	cm^2 g^{-1}	40	35	31	27
OPACIDADE	%	76,8	74,2	71,8	68,7

Para :	IT 70	°SR 35
C.En.	10	11
CSF	293,7	289,0
°SR	34	35
I.T.	70	71
Al.	4,3	4,4
I.E.	0,00	0,00
I.R.	8,15	8,20
Dens.	0,634	0,637
V.Esp.	1,578	1,569
R. Ar	10,79	11,76
C. D. L	34,6	34,3
Opac.	73,9	73,7

AMOSTRA: XIL.A

NÍVEIS DE REFINO	UNIDADE	0	750	1500	2250
CONSUMO DE ENERGIA	Wh	0	9	18	26
FREENESS	mL	360	270	180	110
SCHOPPER RIEGLER	ºSR	27	36	48	64
ÍNDICE DE TRAÇÃO	N m g^{-1}	36,5	75,0	92,2	98,3
ALONGAMENTO	%	2,8	4,3	4,7	4,8
ÍNDICE DE ESTOURO	Kpa.m^2 g^{-1}				
ÍNDICE DE RASGO	mN.m^2 g^{-1}	6,9	7,8	7,9	7,6
DENSIDADE	g cm^{-3}	0,535	0,638	0,698	0,756
VOLUME ESPECÍFICO	cm^3 g^{-1}	1,87	1,57	1,43	1,32
RESISTÊNCIA AO AR	s 100 mL^{-1}	1,6	10,4	52,7	205,0
COEFICIENTE DISP. LUZ	cm^2 g^{-1}	42	34	30	26
OPACIDADE	%	77,2	73,1	70,1	66,8

Para :	IT 70	°SR 35
C.En.	8	8
CSF	283,0	274,4
°SR	34	35
I.T.	70	73
Al.	4,0	4,1
I.E.	0,00	0,00
I.R.	7,63	7,68
Dens.	0,606	0,617
V.Esp.	1,650	1,621
R. Ar	6,97	8,16
C. D. L	75,1	74,7
Opac.	35,1	34,5

AMOSTRA: XIL.B

NÍVEIS DE REFINO	UNIDADE	0	750	1500	2250
CONSUMO DE ENERGIA	Wh	0	9	18	26
FREENESS	mL	361	280	190	115
SCHOPPER RIEGLER	ºSR	27	35	49	64
ÍNDICE DE TRAÇÃO	N m g^{-1}	38,3	69,1	90,3	92,5
ALONGAMENTO	%	2,7	4,0	4,3	4,8
ÍNDICE DE ESTOURO	Kpa.m^2 g^{-1}				
ÍNDICE DE RASGO	mN.m^2 g^{-1}	6,4	8,1	7,9	8,2
DENSIDADE	g cm^{-3}	0,542	0,626	0,685	0,730
VOLUME ESPECÍFICO	cm^3 g^{-1}	1,85	1,60	1,46	1,37
RESISTÊNCIA AO AR	s 100 mL^{-1}	2,2	8,1	42,7	218,0
COEFICIENTE DISP. LUZ	cm^2 g^{-1}	41	34	30	27
OPACIDADE	%	76,7	73,1	70,5	68,0

Para :	IT 70	°SR 35
C.En.	9	9
CSF	282,0	281,8
°SR	35	35
I.T.	70	70
Al.	3,7	3,7
I.E.	0,00	0,00
I.R.	7,68	7,69
Dens.	0,618	0,618
V.Esp.	1,619	1,618
R. Ar	8,71	8,74
C. D. L	74,3	74,3
Opac.	34,4	34,4